

POLITECNICO DI TORINO

Master of Science in Civil Engineering

Master Degree thesis

HPFRCC made with recycled steel fibers
from end-of-life tires



Professor

Student

Prof. Alessandro Pasquale Fantilli

Farmehr MohammadpourDehkordi

Contents

1 Thesis Abstraction	5
2 Introduction & literature review	6
2.1 Introductory remarks	6
2.2 Materials characterization	7
2.3 HPFRCC: High Performance Fiber-Reinforced Cementitious Composites	9
2.4 Modeling of steel reinforced cementitious composites elements in tension	14
2.5 fundamental features and recent application of HPFRCC	16
2.6 Use of selected waste materials in concrete mixes	20
2.7 Eco-Mechanical Analysis	21
2.8 Evaluation of Ecological and mechanical indexes	24
2.9 Research significance	26
2.10 Industrial fibers VS ELTs (End Life Tires)	27
3 Materials Review	28
3.1 Waste-Tire management and recycling techniques	28
3.2 Tire constituents	29
3.3 Tire recycling techniques	27
3.4 Properties of concrete	34
3.5 Properties and application of HPFRCC	36
4 Experimental program	40
4.1 Introductory remarks And Work Methodology	40
4.2 Molds, casting and curing	42
4.3 Flexural tests	48
4.4 Compressive tests	44

4.5 Mixes and fiber used	52
4.5.1 1° series: Test on 23_9	53
4.5.2 2° series of tests: not tested.....	53
4.5.3 3° series of tests: 15_10	54
4.5.4 4° series of tests: 29_10	55
4.5.5 5° series of tests: 6_11	56
4.5.6 6° series of tests: not tested	57
4.5.7 7° series of tests: 21_11	57
4.5.8 8° series of tests: 10_12	58
4.5.9 9° series of tests: 18_02	58
4.5.10 10° series of tests: 25-06	59
4.5.11 11° series of tests: 25-06	59
4.6 Fly-Ash and Silica Fume	60
 5 Experimental results and behavior	 62
5.1 General overview	62
5.2 3PB Test Result	66
5.2.1 1° series: Test on 23_9	66
5.2.2 2° series of tests: 15_10	67
5.2.3 3° series of tests: 29_10	67
5.2.4 4° series of tests: 6_11	68
5.2.5 5° series of tests: 21_11	68
5.2.6 6° series of tests: 10_12	68
5.2.7 7° series of tests: 18_2	69
5.2.8 8° series of tests: 25_06	69
5.2.9 9° series of tests: 25_06	70
5.2.10 Comparison of test results	71
5.3 Compressive Test Result	73

5.4 Advantageous of Adding Fiber	78
5.5 Substitution Strategy	79
6 Analysis of Results	83
6.1 Mechanical Parameters	83
6.2 Ductility of HPFRCC	88
6.3 Practical assessment of the Ecological performances	90
6.4 Eco-mechanical Analysis	102
6.5 Eco-mechanical chart	104
7 Conclusion and Recommendations	106
7.1 Conclusions	106
7.2 Recommendation for Further study	107
8 REFERENCES	108

Thesis Abstraction:

Fast-growing demand for more sustainable and longer life-structures has generated new challenges in the field of construction and civil engineering, particularly regarding the usage of recycled materials. Considering this aspect, concrete has played a crucial role in the development of structural and infrastructural projects and it is also one of the main building materials.

On the other hand, the disposal of waste tires is a serious worldwide environmental problem. Every year an estimated 1 billion tires are discarded. The indiscriminate dumping of large quantities of Waste Tires (WT) into landfills has caused significant damage to the environment. Additionally, tires consist of high-quality, high-strength raw materials, including steel fibers that have inherent properties worthy of being reused which can be especially useful in civil engineering applications.

The thesis discussed the high quantity application of the Recycled Tire Steel Fibers (RTSF) in concrete in order to investigate different HPFRCC mixes and specify the optimal ones based on both mechanical behavior and environmental impact.

The first part consists of general definitions and basic knowledge that applied for developing the work. After that we provided the experimental steps which we performed, starting from specimen preparation, followed by test procedures, and finally analysis of results.

The tests were performed according to EN 196-1, for each mix, we made 3 samples and performed 3PB and compressive tests based on the code rules. The main aim of the experimental work was to assess the contribution of RTSF on the overall structural performance and determine the optimal fiber blend. The environmental impact and the mechanical behavior of the different HPFRCC mixes were also assessed through the evaluation of their Eco-Mechanical index (EMI), implementing a technique developed at the Politecnico Di Torino. The specimens have been compared using an eco-mechanical chart that allows to simultaneously displaying both ecological and mechanical properties, with the purpose to select those ones with a combination of high mechanical and ecological features.

Different HPFRCC mixtures have been designed and investigated in order to reach the best mechanical and ecological solutions comparing to industrial fibers. As we know, large amount of CO₂ is released during the manufacturing of cement, particularly in the calcination of limestone, transportation, manufacturing and construction procedures. To tackle this problem, industrial by-products, such as fly ash, are used in this experimental study to reduce the environmental impact.

Finally, the last chapter contains a summary of the main findings of the research and subjects which are remained for future studies. In this part, we concluded that using RTSF can lead to some advantageous due to providing a compensating method but there are still critical technological issues, especially when dealing with concrete mix preparation and testing procedures.

Chapter 2 Introduction & literature review

2.1: Introductory remarks

Steel waste is a substance that is durable, and is extremely resistant to most natural conditions. The disposal of these used tires is therefore a major concern because improper disposal can lead to considerable environmental and aesthetic problems. This is especially true in developing countries, where environmental regulation is generally the only driving force behind sound tire management.

Every year an estimated 1 billion tires are discarded. The indiscriminate dumping of large quantities of Waste Tires (WT) into landfills has caused significant damage to the environment in many European states due to their infamous biodegradable function. Since July 2006 it was illegal to dispose of whole or broken tires into landfill.

As a result, almost all European Governments transposed this directive into national legislation and codes, encouraging the production of sustainable tire disposal, recovery and reuse options. Italy has been very vigilant and farsighted in this regard: the European Directive 2008/98/Ce extends the definition of "end of waste" in Europe, already adopted by the Italian legislature. In particular, the prospect of selling rubber granules and dusts as well as steel fiber without being subject to the strict requirements of waste legislation, resulting from the provisions of the Codes, may significantly promote the diffusion and use of materials obtained by treating waste tires.

Indeed, waste tires pose a health hazard because of the shape and impermeability of the tires, they can hold water for long periods, providing sites for the development of mosquito larvae. Waste tires also pose a serious fire hazard, since it is difficult to ignite waste tires and waste tire stocks.

Furthermore, tires burn very hot once ignited and are very difficult to extinguish. This is due to the 75% void space in an entire waste tire, making it impossible to quench the tires with water or remove the supply of oxygen. However, the doughnut-shaped tire casings allow air drafts to stoke the fire. A large tire fire will smolder on the surrounding landscape for several weeks or even months, often with dramatic effect. In 1983, almost nine months of a 7-million-tyre fire burned in Virginia, polluting local water bodies.

The peculiar properties of the waste tires have made it impossible to eradicate waste tire stockpiles. Several of these issues are related to their hardness (difficult to break down and decompose), durability (difficult to process), shape (large void room, low storage and transport room efficiency) and volume (large volume occupies).

The use of recycled tire steel in cement concrete will provide an effective means of steel utilization. In addition to the environmental benefits, the use of waste particles from tire steel may provide a new form of concrete with special mechanical and fracture properties.

For concrete structures, 90 per cent of total life-energy is required to produce the material (i.e., typically clinker), while only 10 per cent is connected to the manufacture, transport and use of the product. Thus, an approach to eco-design should be focused on choosing concrete components with low embodied energy and low carbon footprint, and reducing the concrete mass.

2.2: Materials characterization

Increasing the amount of waste tires worldwide makes tire disposal a important issue that needs to be solved. Over Three million tons of waste tires were produced in the EU states during those years. To comply with the two EU laws on recycling, all European countries are forced to develop markets (which will use used tires as secondary raw material) to compensate for this.

The need to build new markets is also motivated by increasing environmental concerns about the more prominent alternative of energy recovery in cement kilns, as contaminants are released into the atmosphere. If landfill disposal of waste tires is to be drastically reduced, the creation of new markets for the tires becomes crucial.

Given the highly inhomogeneous and disproportionate scale of the composition of these recycled fibers, it became clear that the final properties of the proposed concrete had to be strengthened, taking into account the potential of an industrial application. In fact, it is well accepted that the key parameter to be managed during the production of the most suitable mixture is its workability, which is significantly influenced by the particular type of used fiber.

As we know, adding fibers to a concrete matrix may diminish their rheological properties. This point is much more meaningful with the use of steel fibers derived from ELTs, as the high dimensional volatility characteristic of these fibers is the main cause of their balling tendency within the mixture, which ultimately decreases the mix's workability.

Reinforcing concrete matrix with discontinuous steel fibers is a commonly known technique used in many applications to improve these concrete's mechanical properties. As well-known, the most important effect of this kind of reinforcement, in particular, affects the material's post-cracking behavior. As crack starts to form underneath loads,



Figure 2.1: Recycled steel fibers

We need to note the pro and con points of various parts of that about the characteristic of these ELTs. We have a high quality material, low cost, starting from steels. But that material, on the other hand, is difficult to isolate. This fiber is assumed to have poorer efficiency compared with industrial fibers.

The positive aspects of the rubber component are the light weight of this material, and its low cost. But, particularly in compression, using this material as aggregates we would have a concrete with a lower strength.



Figure 2.2: Rubber waste of tires

2.3: HPFRCC: High Performance Fiber-Reinforced Cementitious Composites

Concrete is one of the most commonly used building materials and infrastructures. Given the hilarious compression results, it shows unsatisfactory tensile strength which is about one tenth of its compressive strength. For this purpose, in areas of immense tensile stress, where steel rebar is normally mounted, Concrete cannot be used alone. Under tensile measures, Mechanical steel attitude shows both higher strength and greater tensile strength than concrete.

New forms of concrete are constantly being produced to fulfill the increasing need for improved mechanical properties and durability. Such novel concrete forms are typically recognized as High Strength (HSC), High Performance (HPC) and Ultra High Performance concrete (UHPC). These concrete properties represent a vast improvement over ordinary concrete. However, the improved micro-structure of these new concrete forms results in a massive increase in their brittleness as well as in the volume changes that occur during the material's hardening, i.e. in autogenously shrinkage.

Nonetheless, each of these drawbacks can be easily solved by using vast quantities of short steel fibre. Such fiber-reinforced concretes are called high performance cementitious composites (HPFRCCs) reinforced with fiber. The mechanical efficiency of any HPFRCC highly depends on the equal distribution of fibers in the material's bulk. Potential sites of vulnerability are any regions with low fibers or with none. The fiber distribution in the mix depends not only on how the fibers are put into the mix but also on the shape of the cast material.

High-performance fiber-reinforced cementitious composites (HPFRCCs) are a group of fiber-reinforced cement-based composites which carry the unique ability to flex and self-strengthen before failing. This special class was built with the intention of accommodating the structural needs inherent in the standard concrete of today, such as its propensity to fail under extreme loading in a brittle manner and its lack of long-term durability. Thanks to their nature and structure, HPFRCCs possess the remarkable capacity to yield and harden plastically under excessive charge.

Strain hardening, the most critical function of HPFRCCs, occurs when a material is loaded beyond its plasticity limit and begins plastically deforming. The action of 'straining' actually strengthens the content. This phenomenon is made possible by the development of multiple microscopic cracks, in comparison to the single crack / strain softening behavior of traditional fiber-reinforced concrete. It occurs in HPFRCCs as several fibers slip past one another.

The low density is another highly positive property of HPFRCCs. A less dense, and thus lighter material means that HPFRCCs will potentially require far less energy to produce and treat, making them a more competitive material for building. Because of the lightweight structure of HPFRCCs and the potential to strain harden, it was implied that they would eventually become a more durable and effective alternative to traditional concrete.

On the other hand, a reduced crack width in tensile concrete will emerge in order to create reinforced concrete structures capable of reducing the steel corrosion caused by environmental attacks. Fibers applied to conventional concrete may be, at least in the serviceability stage, a way to fulfill this requirement. FRC (fiber-reinforced concrete) can show a higher ductility and often a higher mechanical properties compared to ordinary concrete based on the form, volume content and aspect ratio of the fibers. Nonetheless, concrete cannot generate tensile stresses totally comparable to those of the steel rebar with or without fibers. To overcome this problem, new FRCs, called High Performance Fiber-Reinforced Cementitious Composites (HPFRCC), have been recently prepared in order to develop an ultra-high ductility.

As is well known, from uniaxial tensile tests on concrete prisms a nearly linear stress-strain relationship can be obtained up to the peak stress. At this stage, failure occurs due to the presence of a single crack, and the diagram shows a softening regimen. In other words, with the increase in pressures, there is a progressive reduction in stresses that are located around the crack in the process region. Using a fictitious crack model or a crack band mode, this behavior can be effectively modelled.

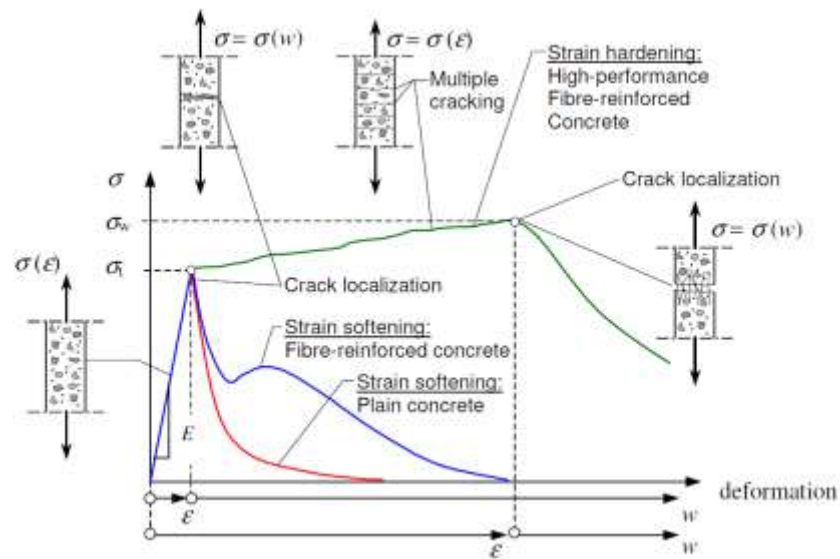


Figure 2.3: Reinforced cementitious composite structure in tension

Nevertheless, the tensile zones of reinforced concrete (PC) structures can reveal more than one crack. Too many different experiments on tensioned reinforced concrete components were conducted in order to examine this aspect of RC beams. From these formed studies, a complex crack pattern can be seen, in which both primary cracks and secondary internal cracks occur in the concrete surrounding. Crack sequence development is generally assigned to the bond-slip mechanism between steel and concrete, which allows the transfer of tensile stresses between two primary cracks even in the concrete.

Since the HPFRCC class contains many different formulae, their physical structures differ considerably. Most HPFRCCs, however, contain at least the following ingredients: fine aggregates, a super-plasticizer, polymeric or metallic fibers, cement, and soil. The key distinction between HPFRCC and conventional concrete construction therefore lies in the absence of coarse aggregates by HPFRCCs. Typically, a fine aggregate such as silica sand is used in HPFRCCs.

On the other hand some doubt will remain. How can you use a huge amount of fibers? Why do we separate the fibers? As we described before, the balling of these fibers is one of the most major problems regarding the waste steel fibers. And, when we need to disperse these fibers in the concrete parts, we'll face enormous problems. And if such fibers are in our components the probable solution is to use high quantity. At the end, the greater the better the quantity of fiber is the distribution and will be better as a result of that efficiency.



Figure 2.4: high quantity of fibers in sample

Previously Nervi used Ferro-cement. A significant amount of wire (wire meshes) was put in the formworks, and it was shielded by a cement mortar. Ferrocement or Ferro-cement is a building method using reinforced mortar or plaster (lime or cement, sand and water) spread over a metal mesh "armature," stretched metal or metal fibers woven and thin steel rods, such as rebar, that are closely spaced.

We can do the same procedure for HPFRCC growth. To do so we need to put very large concentrations of ELTs and we need to use a very fluid concrete to create a sample with this sort of properties. In this case we don't need to distinguish them because of the huge amount of concrete. And we'll somehow compensate the balling problems of these steel fibers in this process.

In the previous method, once all the other ingredients have been added, the occurrence of making fiber clumps in our mix typically known as "balling" can usually be prevented by shaking the fibers into the mix through a tube. The cycle affects the concrete characteristics of workability and strength. This has a propensity to affect concreteness and power. When fiber is added to a concrete mix, each individual fiber receives a cover of cement paste.



Figure 2.5: high amount of steel in our samples

We need a fluid concrete because of the high volume of steel in our mix which can be prepared by applying super-plasticizers to the mix. Super-plasticizers are additives used in producing high strength concrete, also known as high range water reducers. Plasticizers are chemical compounds that enable concrete to be manufactured with about 15 per cent less water content.

Super-plasticizers permit a 30 per cent or more reduction in water content. Such additives are used at a few per cent weight level. The curing of concrete is often retarded by plasticizers and superplasticizers. Super-plasticizers can be used where well-dispersed suspension of particles is necessary to improve the flow characteristics of suspensions such as in concrete implementations. They significantly improve fresh paste hardening efficiency. As we know the concrete strength increases as the ratio of water to cement dropped.

Super-plasticizers in conclusion turn solid, low-slump concrete into flowing, pourable, easily positioned concrete. They can improve workability, pace finish, increase strength, preserve cement and help minimize shrinkage and thermal crack.



Figure 2.6: super-plasticizer used for making concrete more fluid

2.4: Modelling of steel reinforced cementitious composites elements in tension

High-performance cementitious composites strengthened by fiber (HPFRCC) is a class of material that demonstrates not only high strength and low permeability, but also high ductility and micro-crack growth under tensile stress. Such properties are achieved due to the extremely dense microstructure of the cementitious matrix combined with the use of microfibers, which can reduce the width of the cracks in an appropriate proportion. Which is why the HPFRCC can be used as material for the maintenance, renovation and/or upgrading of reinforced concrete structures.

HPFRCC is a type of cemented material characterized by a substantial hardening behavior of the tensile strain and as a consequence, significantly high deformability. Such materials are manufactured from a mixture of high strength concrete and fibers with increased homogeneity since fine sand replaces typical coarse aggregates.

Figure 1 shows an image of HPFRCC's material reaction under uniaxial tension. Where a large number of cracks are uniformly distributed, the deformation is known as being macroscopically uniform. During the strain softening process, deformation is localized by only a small number of cracks growing in width. Much work has been carried out to analyze and enhance material properties, and to develop process technology, design principles and ideas for applications.

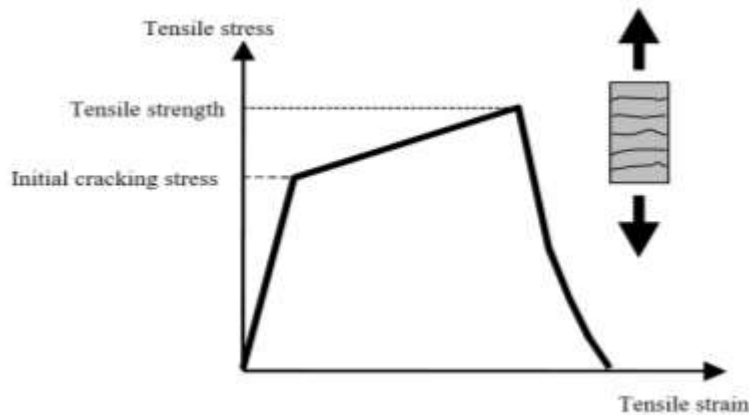


Figure 2.7: Tensile stress-strain relationship

Groundbreaking features of HPFRCC including strain hardening and multiple cracking are addressed beforehand. We must note that material should be applied appropriately for the acquisition of these novel properties, based on the performance criteria for structures. Quality based on multiple fine cracks is mostly needed, as greater durability of concrete structures is becoming increasingly a necessity in all structures, and reducing crack width is one of the approaches to obtain more robust concrete structures.

At the other hand, it is difficult to use the structural response obtained from HPFRCC's novel mechanical properties due to the lack of design principles that take the potential for deformation into account.

HPFRCC's tensile load carrying capacity, which is one of the positive points of structural use, should be properly assessed. Although the required deformation-related output has not been explained, higher energy consumption is expected for members with HPFRCC having critical stress similar to reinforcement yield strain. Different types of uniaxial tensile tests using various specimen sizes, geometries, and boundary conditions were proposed and performed to determine the shape of the tensile stress strain relation.

The tensile properties that are used in the design should match the actual application conditions. Instead, the relationship between the test and current conditions should be carefully checked by using test results obtained under conditions varying from existing conditions. The model relation of bi-linear stress strain shown in Fig. 8. The HPFRCC tensile stress strain relation (JSCE 2005a) is proposed. In the JSCE guideline, initial cracking force and strain at tensile strength are proposed as common values to assess the modelled stress strain relationships.

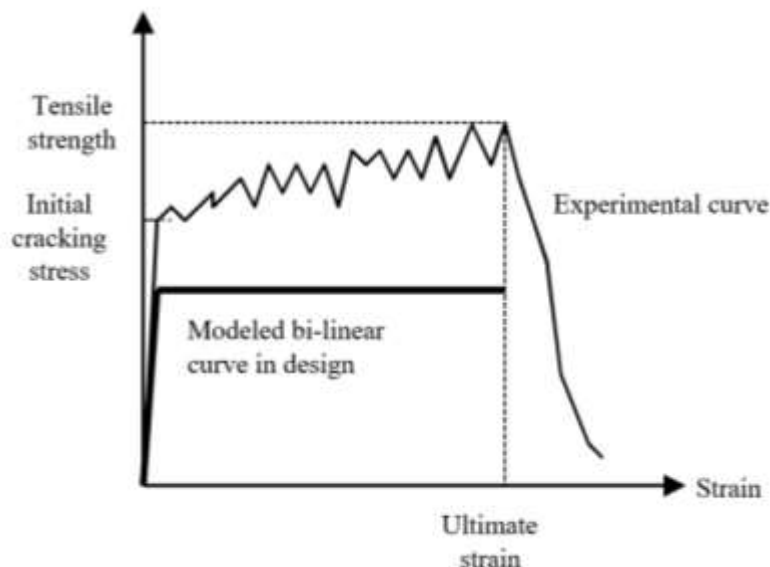


Figure 2.8: Modeled stress-strain curves in design

The novelist HPFRCC tensile properties described in the previous section also result in an increased resistance to fatigue. There were records of positive results obtained from laboratory samples. HPFRCC has longer lifetimes of fatigue at higher rates of tiredness. However, at lower fatigue stress levels, HPFRCC has shorter lifetimes of fatigue than ordinary FRC, since only a few cracks can spread in the specimen.

2.5: fundamental features and recent application of HPFRCC

Durability is an essential element of performance needed for building materials like HPFRCC. Deterioration of the material itself should be accurately calculated due to a frost attack (freeze-thaw), alkali-silica reaction, or chemical attack. Since the materials used in ordinary HPFRCC, such as Portland cement and sand, are similar to those used in ordinary cement mortar, it is possible that HPFRCC will be extended to material output assessment approaches for mortar and/or concrete.

HPFRCC's other desirable result is aesthetics. Cracking causes a loss of cosmetic appearance in normal structures constructed from concrete in the form of noticeable visible cracks, exacerbated by soiling (staining) of the concrete surface. Conversely, HPFRCC only reveals small cracks that are not clearly visible from a distance. Nonetheless, it should be remembered that visual observation of concrete structures is commonly used for ordinary maintenance inspections of concrete structures, and thus the effect of smaller crack widths on structural maintenance with HPFRCC should be addressed from the visual inspection point of view.

HPFRCC probably has decreasing pressure due to the use of fine materials such as cement and admixture. Product with no shrinkage can essentially be used to minimize shrinkage, because HPFRCC is also applied to composites with a constraint (composite system). While in HPFRCC the width of a shrinkage crack is very small, the tensile stress caused by the shrinkage may decrease the capacity of the tensile load bearing. The test method using an embedded strain gage that is applied to ordinary concrete is useful for assessing HPFRCC's shrinkage properties.

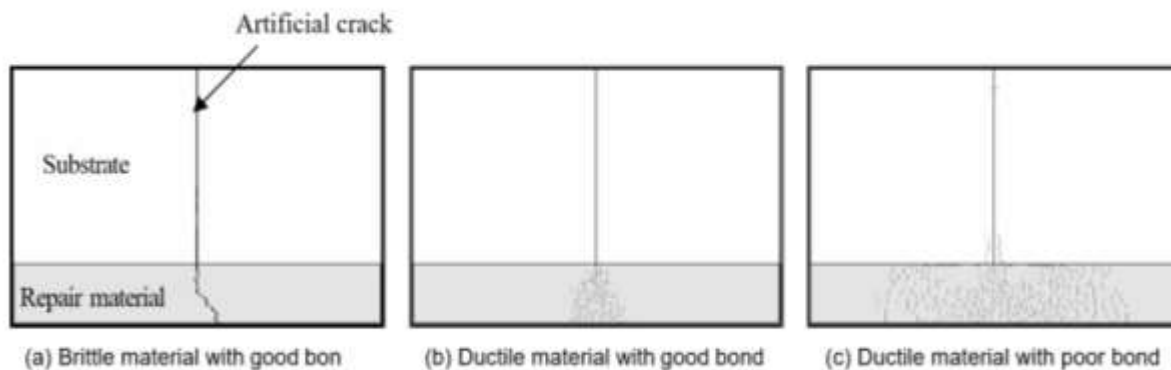


Figure 2.9: Crack patterns considering elongation around a crack

One of HPFRCC's advantages for HPFRCC after cracking is the formation of fine cracks. Some work has been done on the influence of fine cracks on the penetration of substances like oxygen, water, chloride ions and carbon dioxide. Furthermore, repeated cracking with small cracks imparts improvements to the rebar corrosion process within the HPFRCC.

Another thing to be addressed is the strong erosion resistance that can be obtained from short-fiber HPFRCC. In the case of ordinary reinforced concrete fiber, it was found that the short fiber content in FRC specimens imparts higher resistance to erosion.

Recent HPFRCC applications in structures take advantage of those composites' superior mechanical properties and fine cracking mode.

- ❖ Bridge decks to increase resistance to fatigue via HPFRCC tensile force bearing power.
- ❖ Dampers in reinforced concrete buildings to increase energy absorption and reduce vibration during earthquakes, in addition to reducing repair after heavy loading
- ❖ Surface repair of dams and irrigation channels to strengthen the shielding properties of degraded concrete surfaces
- ❖ Surface repair of retaining walls damaged by alkali silica reaction to strengthen aesthetic appearance



Figure 2.10: Outline of Mihara Bridge

Mihara Ohashi in Hokkaido, with 972 m long bridge and 340 m central span (Mitamura 2005). Half the depth of the asphalt overlay on this bridge's steel deck was replaced by 40 mm thick HPFRCC in 2004 to increase the load bearing capacity and deck stiffness while reducing the stress produced, thereby improving the stiffener's fatigue resistance to the steel deck. This was important because while the bridge was under construction, the standards for fatigue resistance were updated in the standard specifications. HPFRCC was blended in ready-mixed concrete plants, transported by large agitating trucks to the construction site and subjected to secondary mixing on the site.

A part of HPFRCC reinforced with steel bars is able to withstand a considerable amount of energy under charge. Members of the HPFRCC is used in reinforced concrete constructions as dampers. The leaders of HPFRCC were linking elements with main (core) frames of high-rise buildings, and the elements included both higher energy consumption and reduced post-earthquake repair work. HPFRCC's shielding efficiency is also excellent due to its tiny crack widths, which reduce water permeation.

HPFRCC is ideal for use in terms of aesthetics on the surface of cracked concrete buildings, due to its low cracking widths. It can be used in gravity concrete retaining wall because of its characteristic of this material. And it can also be used for restoring certain structures after construction.



Figure 2.11: Surface repair of concrete retaining wall

Some important points about HPFRCC structures need to be listed here. Firstly, it is important to forecast the performance of structures using HPFRCC through numerical analysis. To assess the advantages of HPFRCC, accurately simulate not only mechanical output (structural response) but also time-dependent output (durability).

In comparison, HPFRCC's production expense at this time is more costly than that of ordinary concrete. In addition to significant cuts in production costs, the maintenance will be encouraged taking into account the cost of the life cycle.

By using waste or recycled concrete, ordinary building materials can help to reduce the environmental impact. Achieving long-lasting structures by using HPFRCC may lead to sustainable development, and this idea should be replicated in existing structures. HPFRCC systems should also be prepared for environmental impact management approaches such as recycling, waste usage and reconstruction.

Several fiber reinforced concrete composite technologies have been developed, varying from stand-alone constructions such as cement plates, boards, pipes, slabs and prefabricated components to hybrid solutions in conjunction with other structural products (e.g. regular concrete, steel, etc.). In addition, HPFRCC is increasingly being used in the restoration and renovation process of existing buildings

Another fairly recent application is seismic retrofitting, which aims to improve the device behavior of old structures and let the structural components achieve the desired efficiency. For strength columns, beams and walls, tunnel lining and other unique structures such as specific bridges, super high-rise buildings and offshore platforms, other important examples can be found in jacketing.

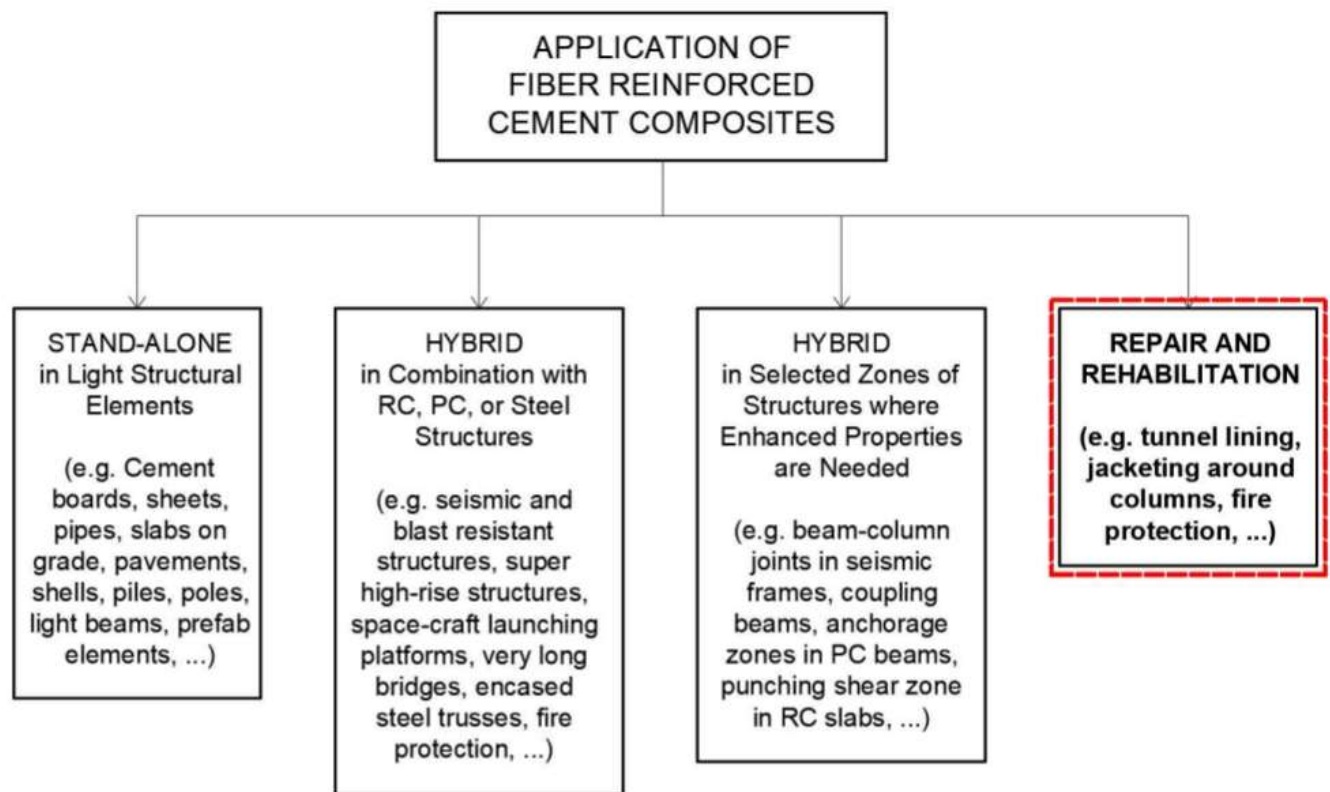


Figure 2.12: Classes of application of fiber reinforced cement composites

Owing to their intense sensitivity to harmful chemicals, such as salts and other de-icing agents, HPFRCC is often used to protect different areas of reinforced concrete structures such as bridge piers and retaining walls. In general, these components exhibit insufficient durability when built with conventional reinforced concrete. UHP-FRCC is also able to guarantee the requisite durability as well as the mechanical efficiency of these structural elements.

2.6: Use of selected waste materials in concrete mixes

Following a natural population growth worldwide, the quantity and form of waste materials have increased accordingly. Many of these waste materials that are not rotting in time will remain hundreds, maybe thousands of years in the world. As stated before, non-decaying waste materials cause a tremendous crisis in waste accumulation, thereby leading to environmental issues. The waste disposal problem exists worldwide, especially in the densely populated areas. Most of these products are left in designated areas as stockpiles around towns, landfill or illegal dumping.

Massive amounts of this waste cannot be disposed of. However, by making more sustainable use of these waste products, the environmental impact can be compensated. This is known as "the Hierarchy of Wastes." Its aim is to reduce, reuse, or recycle waste, the latter being the preferred waste disposal method. Illustration. 12 Gives a diagram of the structure of waste.

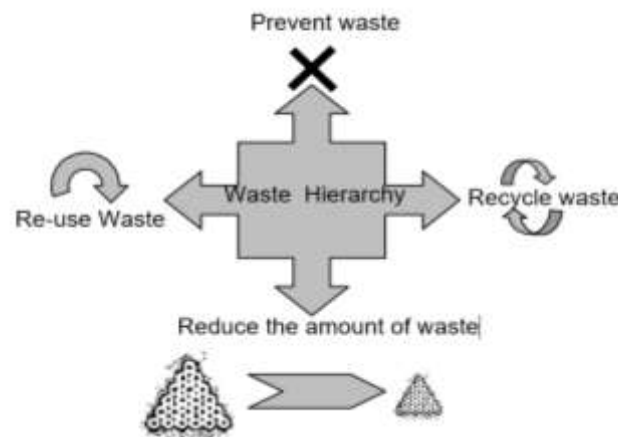


Figure 2.13: The waste hierarchy.

Discussion continues slowly on modern and novel applications of waste materials. These research efforts are trying to meet the demand from society for healthy and economical disposal of waste materials. Use recycled aggregates saves natural resources and spaces for waste, and helps maintain a healthy climate.

In general, plans for the recycling of waste materials should be formulated prior to implementation of work for any construction project. Such plans will define the types of wastes to be produced, the method of handling, and the procedures for recycling and disposal. Additionally, areas should be specifically marked for the temporary collection or storage of building waste materials.

2.7: Eco-Mechanical Analysis

One of novel construction industry's fundamental ideas is to massively reduce the use of cement in new concrete structures especially for environmental purposes. Mechanical and environmental efficiency are not usually balanced in the above analyzes, however. To pick, or tailor, new eco-friendly and high-performance cement-based composites, a comparison between the various concrete mixes is required.

For concrete structures as stated earlier, 90 percent of total life-energy is required to produce the material (i.e., mostly clinker), while only 10 percent is connected to the manufacture, transport and use of the product. Therefore, an approach to eco-design should be focused on choosing concrete components with low embodied energy and low carbon footprint, and reducing the concrete mass. To meet these goals, the following techniques can be applied:

- Product efficiency approach focused on clinker reduction by reducing the total amount of concrete, and therefore the volume of structures. Clearly, under the same loading condition the mechanical efficiency, such as the compressive strength f_c , must be improved in comparison to traditional concrete.
- Material replacement technique involving replacing clinker with cemented and/or pozzolanic mineral admixtures (e.g., fly ashes, etc.).
- Use of LCA (Life Cycle Assessment) to pick the lowest carbon footprint concrete materials.

Use these techniques from a structural point of view will cause drawbacks in concrete's mechanical performances. In fact, concrete with high strength can display very brittle behavior, particularly under compression. Even, when the cement is partially replaced by mineral additives, compressive strength does not significantly alter but the post-peak response can be much more brittle than ordinary concrete. Such behavior was observed by comparing the pre-peak and post-peak curves of two concretes having the same water-binder ratio (and therefore the same strength), but different water-cement ratio. From a structural point of view, using such techniques will cause drawbacks in the mechanical efficiency. However, if recycled aggregates with a more desirable carbon footprint are used instead of virgin aggregates, a drastic reduction in compressive strength can be observed (even greater than 50 per cent).

Among other sets of design attributes, such as strength and ductility, the environmental impacts have to be weighed according to these factors. According to these criteria, the best concrete mixture must display the highest Eco-Mechanical Index (EMI), which covers ecological as well as mechanical aspects:

$$EMI = \frac{MI}{EI} \quad (2.1)$$

MI = Mechanical Index.

EI = Ecological Index.

For example, Damineli et al. consider as possible EI values the total carbon dioxide emitted and the quantity of binder required to produce 1 MPa of compressive force. In this case, however, as also in Flower as Sanjayan's paper, MI only comprises the compressive strength of concrete, while the post-peak energy absorption (i.e. ductility) is ignored. The beneficial effects of fibers are not measured adequately in this way. If the fiber volume fraction is less than 1%, the strength (and therefore MI) will not differ, whereas the environmental effect (i.e., EI) will increase. As a result, fiber-reinforced concrete (FRC) eco-mechanical efficiency tends to be poorer than regular concrete.

Product properties should be paired with structural efficiency at serviceability and ultimate limit stages in a more sophisticated concept of EMI. The definition of MI should not only be based on concrete strength but also on structural test results.

However, such tests are much more complex to be performed in usual labs, especially when full scale concrete members need to be investigated. Thus, it is desirable that not only strength but also other mechanical properties of concrete are considered. As the serviceability stage and the durability of concrete structures are associated with the fracture mechanism of concrete in tension, in the opinion of Fantilli and Chiaia the work of fracture can be effectively used to evaluate MI. This is especially true for bending beams made of reinforced concrete (RC), whose code rules allow narrow crack widths. Within the following section a new eco-design method is presented to prove this conjecture in the case of normal strength concrete (NSC) with recycled and industrial steel fibers.

Fantilli and Chiaia research is carried out using a chart. The mechanical response is recorded on the horizontal axis: It is defined by the Mechanical Index (MI) divided by MI_{inf} , the mechanical characteristics' lowest bound value. In addition, ecological performance is recorded on the vertical axis, defined by the Ecological Index (EI) divided by EI_{sup} , which is the upper limit value of ecological impact expressed by EI_{sup} .

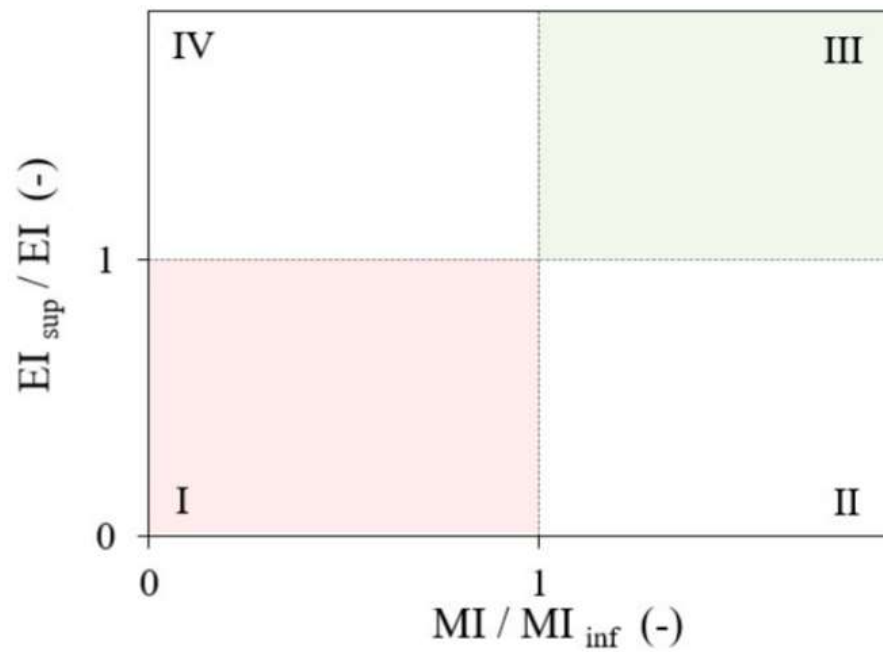


Figure 2.14: Schematic chart for evaluation of Eco-mechanical performances

Four different zones can be distinguished within the chart:

1. Zone I: Low mechanical performances – Low ecological performances
2. Zone II: High mechanical performances – Low ecological performances
3. Zone III: High mechanical performances – High ecological performances
4. Zone IV: Low mechanical performances – High ecological performances

For conclusion, if mineral additives and fiber reinforcement are properly mixed, a new class of cement-based composites can be created, providing the mechanical strength of a conventional concrete with a reduced effect on the environment and a better durability.

2.8: Evaluation of Ecological and mechanical indexes:

The most important ecological parameters are carbon footprint, embodied energy and water which is used to create a cubic meter of concrete according to fib-Guidelines for Green Concrete Structures.

Consequently, EI can be determined using the following equation:

$$EI = (\alpha \cdot wc_a) \cdot (\beta \cdot wc_\beta) \cdot (\gamma \cdot wc_\gamma) \quad (2.2)$$

α = quantity of carbon dioxide (CO₂);

β = quantity of embodied energy

γ = volume of water

As the ecological performances are related to the local condition in the place of use, three weighting coefficients (wc_a , wc_β , wc_γ), which can be properly adjusted depending on water shortage, transportation, grabbing of raw materials, etc., are also introduced within Eq.(1.2). For instance, the longer the distance between concrete plant and building site, the higher the value of wc_γ due to the impact of transportation.

Moreover, Eq. (2.2) can be enriched by other available parameters, such as biodiversity, toxic substances, and resource depletion. However, in the evaluation of ecological performances only the carbon footprint and the embodied energy of cement and steel fibers are assumed to be relevant. Such values, taken from fib and from the Eco Invent database, are reported in Table 1. It must be noted that the procedure here introduced is suitable only for comparison among similar types of concrete, cast in the same place and having the same type and amount of aggregates, and not for detailed calculation.

Although shredding tires and separating rubber and steel result in processing leads to some expenses, it is acceptable to neglect that and assume recycled steel fibers have zero carbon and energy impacts. On the other hand it is critical to keep in mind the impacts regarding the treatment of the product at the end of its life. In other words, assuming no environmental impact for the recycled steel fibers gives credit for the net CO₂ that is saved when a product is reused or recycled.

	Carbon footprint	Embodied energy
	kgCO ₂ /kg	MJ/kg
Normal Portland Cement	0.83	4.73
Industrial Steel fibers	1.5	20.6
Recycled fibers	0	0

Table 2.1: Carbon footprint and embodied energy of concrete components

In accordance with fib, both the material and the structural performances must be incorporated into the mechanical index. Thus MI can be estimated by means of the following equations:

$$MI = m_{pm} * m_{ps} \quad (2.3)$$

m_{pm} = mechanical parameter of concrete material.

m_{ps} = mechanical parameter of concrete structure.

If the durability needs to be taken into account, m_{ps} is in inverse proportion to the crack width measured at a pre-established external load. Indeed, in a reinforced concrete structure, permeability is mainly influenced by the presence of cracks in the tensile zones, rather than the concrete porosity. Such cracks are the results of the so-called “tension stiffening” interaction between concrete and steel. Both numerical and experimental results, show that the higher the fracture energy of concrete, the lower the crack width produced by tension-stiffening. In other words, the work of fracture in tension inevitably characterizes the durability performance of RC structures, and m_{pm} can be considered equal to the work of fracture.

Consequently, not only material examinations (tensile and/or bending tests) are required to compute MI, but also the measure of crack width in full-scale structures (e.g., RC ties or beams) needs to be tested.

2.9: Research significance

At the serviceability stage of concrete structures, recycled tire fibers minimize the crack width and can therefore substitute the imported fibers without penalizing structural efficiency. In this analysis, a large amount of tire fibers (more than 2 per cent in amount) will be tested to find the best combination.

Nonetheless, the synergetic effect of generated fibers and reused fibers improves concrete efficiency while maintaining low environmental impact.

In other words, we need to use significant quantities of recycled steel fibers to compensate for the lack of force when implementing the replacement strategy. We know that the use of large amounts of waste steels in our mix will solve the problems with the uneven distribution of fiber in our samples and thus we believe that we can obtain better test results. To order to check our initial conclusions, specific experiments will be conducted on those samples.

Considering high amount of steel in our samples we need to use a very fluid concrete. In order to have this type of concrete as mentioned before, we can use Super-Plasticizers in our mix. Looking to the samples it is easily visible the steel fibers.



Figure 2.15: high amount of steel in our samples

2.10: Industrial fibers VS ELTs (End Life Tires)

After characterizing the raw materials, determining the concrete's mechanical properties for the chosen application, optimizing the correct mix-design and mechanical characterization of the compressive strength and post-cracking behavior. The outcome of samples made with ELTs was contrasted with industrial fibers by means of a statistical method, the final part of the project was the realization of some panel prototypes reinforced with ELT steel fibers.

In this phase the thesis is developed to assess:

- Assess the contribution of waste fibers to overall structural efficiency and create concrete mixtures of different types of fibers that classify the optimal ones based on both mechanical behavior and environmental effects. This will allow design guidelines for the use of steel fibers from waste tires as concrete reinforcement to be created, which will create new market opportunities for RTSF.
- Investigate the effect of spatial fiber delivery on the overall mechanical efficiency of 3PBT-subjected prismatic specimens. Experimental tests are based on current concept equations with predictions. In this way, the effects of casting and compaction on the fiber distribution may be mitigated, thus reducing the likelihood of structural defects from spots with a smaller or zero fiber.
- Compare the performances of recycled fibers with those of industrial fibers.



Figure 2.16: Industrial fibers VS ELTs

Chapter 3 Materials Review

3.1: Waste-Tire management and recycling techniques

The that amount of waste tires worldwide makes tire disposal a real and critical issue that needs to be solved. In recent years, over three million tons of waste tires have been produced in the EU states In order to comply with the two EU directives on recycling, all European countries need to build markets (which will use used tires as secondary raw material) to accommodate the quantity of non-reused or recycled tires. The need to build new markets is also justified by increasing environmental concerns about the more common alternative of energy recovery in cement kilns, as pollutants are released into the atmosphere.



Figure 3.1: Used tires dumped in stockpiles

Aims to significantly reduce the landfill disposal of waste tires, the development of new markets for the tires becomes fundamental.

The tire life cycle can be identified by the following six steps:

1. Product developments and innovations such as tire shaping increase tire life, increments of replacement, consumer safety, and reduce tire waste.
2. Proper manufacturing and high quality of delivery reduces waste at production.
3. Direct distribution through retailers, reduces inventory time and ensures that the life span and the safety of the products are explained to customers.
4. Consumers' use and maintenance choices like [tire rotation](#) and alignment affect tire wear and safety of operation.
5. Manufacturers and retailers set policies on return, [retread](#), and replacement to reduce the waste generated from tires and assume responsibility for taking the 'tire to its grave' or to its reincarnation.
6. Recycling tires by developing strategies that combust or process waste into new products, creates viable businesses, and fulfilling public policies

3.2: Tire constituents

A tire is a ring-shaped component that surrounds a [wheel's rim](#) to transfer a vehicle's load from the axle through the wheel to the ground and to provide [traction](#) on the surface traveled over. Most tires, such as those for automobiles and bicycles, are [pneumatically](#) inflated structures, which also provide a flexible cushion that absorbs shock as the tire rolls over rough features on the surface. Tires provide a footprint that is designed to match the weight of the vehicle with the bearing strength of the surface that it rolls over by providing a bearing pressure that will not deform the surface excessively.

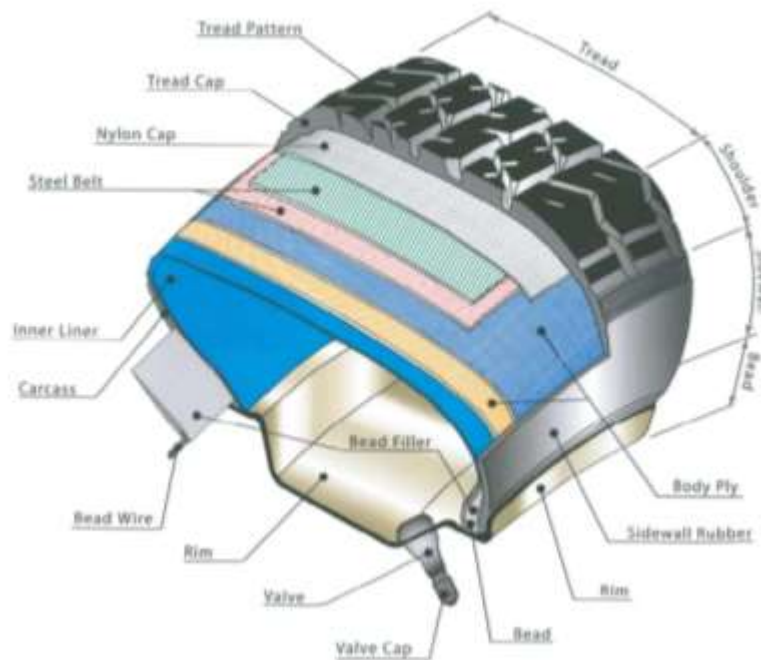


Figure 3.2: Tire structure

The materials of modern pneumatic tires are [synthetic rubber](#), [natural rubber](#), fabric and wire, along with [carbon black](#) and other chemical compounds. They consist of a [tread](#) and a body. The tread provides [traction](#) while the body provides containment for a quantity of [compressed air](#).

Before [rubber](#) was developed, the first versions of tires were simply bands of metal fitted around wooden wheels to prevent wear and tear. Early rubber tires were solid (not pneumatic). Pneumatic tires are used on many types of vehicles, including [cars](#), [bicycles](#), [motorcycles](#), [buses](#), [trucks](#), [heavy equipment](#), and [aircraft](#). Metal tires are still used on [locomotives](#) and [railcars](#), and solid rubber (or other polymer) tires are still used in various non-automotive applications, such as some [casters](#), [carts](#), [lawnmowers](#), and [wheelbarrows](#).

Tires vary in weight between 7 kg for a car to 60 kg for a truck or a lorry. The calorific value of a tire is around 30 to 35 MJ per kg (8.3 to 8.5 kWh per kg), which means that used tires have greater energy content than wood or coal. The principal raw materials for modern tire production are rubber compounds kept together with steel and textile reinforcement. The proportions of rubber, steel and textile vary with construction and tire type (for example car or truck).

Tires contain so many different compounds and ingredients because they are engineering miracles, expected to handle the tortures of heat and cold, high speed, abrasive conditions, and often not enough air pressure. They are expected to perform for tens of thousands of miles and retain their essential properties despite horrendous driving habits and sometimes poorly maintained or built roads.

Type	Size	Weight (kg)
Car	165-13	7.5
Car/van	175-14 / 700-14	8
Light truck	800 R16	25
Truck	1100 / 20	50–60
Truck	1200 / 20	60–70
Truck	1200 / 22.5	80–90

Table 3.1: Approximate tire weights

Component	Steel-braced radial	Textile-braced radial	Cross-ply
Rubber Compound	83	90	76
Steel	12	3	3
Textile	5	7	21

Table 3.2: Main constituents of tires by weight

Tires contain different types of fibers according to the particular purpose of the tire. Some tires have cords made of nylon, polyester, and kevlar and other have steel.

3.3: Tire recycling techniques

Used tires are either reduced to rubber “crumb” and steel fibers by means of mechanical recycling (such as shredding and cryogenic processes) or reduced to their chemical constituents by means of anaerobic thermal degradation (such as pyrolysis and microwave induced pyrolysis processes). The feasibility of a new mechanical process (where tires are reduced to rubber crumb and steel by means of ultra-high water pressure) has been investigated recently.



Solution

Capacity	500-4000 kg/h
Application	Diameter of the tire : 380-3000mm , including car tyre/truck tyre/OTR tyre.
Output Size	5-220 mesh, Can be customized
Characteristic	<ul style="list-style-type: none">• Complete separation: The Rubber Crumbs, Steel and Fibre can be separated automatically.• Control system: Adopt PLC control system, it is simple and easy to control and maintain.• Low energy consumption
Blade	Long life cycle, High utilization, Multiple maintenance.
Area	About 500 square meter, 5.5 meter high

Table 3.3: example of tire recycling solution

The shredding process reduces tyres into rubber and steel through a number of stages, the number of which depends on the size desired for the rubber endproduct. In the first stage of processing, a complete tyre is chopped or shredded until it is reduced to pieces ranging in size from about 50 to 150 mm. The rubber, which still contains steel, can be used as tyre derived fuel (TDF) and possibly as fill to assist drainage. Unless destined for these limited uses, the rubber pieces are normally then fed into a second shredder which reduces them to smaller pieces. The rubber crumb is then fed into a knife or hammer mill where it is pulverised to approximately 1 to 10 mm in size.

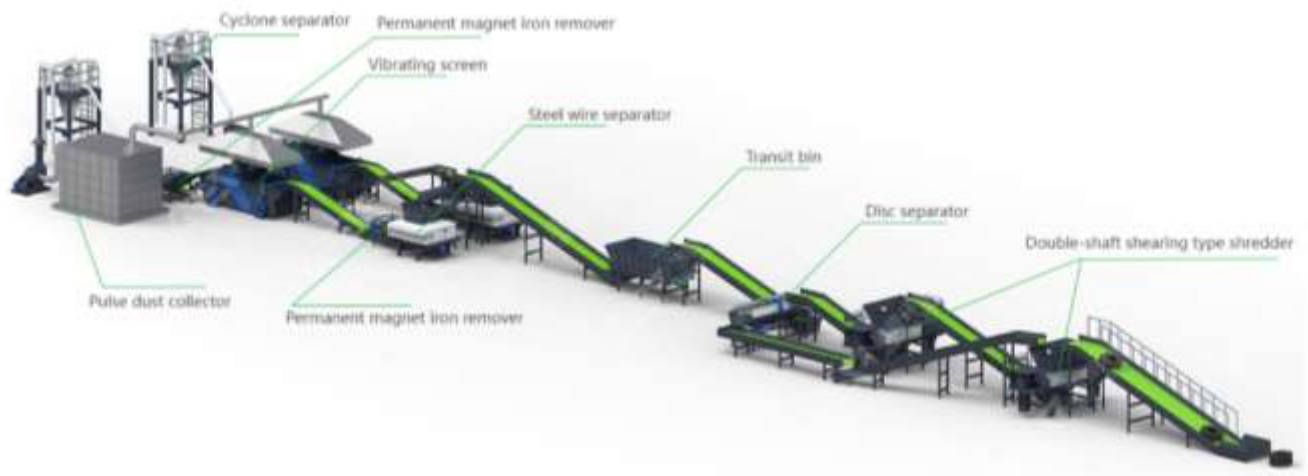


Figure 3.3: processing technique



Figure 3.4: first shredding process

By the second stage of shredding, the steel fibers have been subjected to the chopping, shredding, and pulverizing operations. As a result, much of it will have been broken, and its thread or cord-like configuration destroyed. The broken, pulverized textile fibers form “fluff” that entraps and holds rubber particles and steel together. In order for the rubber to be usable, the steel and fluff need to be separated and removed. The use of magnets removes the free steel pieces, but the magnets also remove rubber particles, in which the rest of the steel is embedded. To avoid losing substantial amounts of steel-bearing rubber, and to obtain finer rubber particles, the rubber must be subjected to a second regrinding. This is normally done in a knife mill capable of disintegrating the rubber into smaller particles or in a hammer-mill. Steel and fluff are extracted at this final stage as well.

The steel extracted after the second stage and the final stage of shredding differs in quality. The former contains large pieces of rubber as well as much of the textile wire in long lengths. The cord is sometimes undamaged, but most of it is deteriorated into individual wires. The latter is much finer, comprising mostly of thin individual steel wires, but still containing around 10% rubber and much fluff and as a result, it is considered a waste material and usually it is sent to landfill. The by-products at the different stages of shredding are shown in Figure 3.5.



Figure 3.5: crumb made from tires

Crumb rubber is recycled [rubber](#) produced from [automotive](#) and [truck scrap tires](#). During the recycling process, [steel](#) and tire cord (fluff) are removed, leaving tire rubber with a granular consistency. Continued processing with a granulator or cracker mill, possibly with the aid of [cryogenics](#) or by mechanical means, reduces the size of the [particles](#) further. The particles are sized and classified based on various criteria including color (black only or black and white). The granulate is sized by passing through a [screen](#), the size based on a dimension (1/4 inch) or mesh (holes per inch: 10, 20, etc.). Crumb rubber is often used in [artificial turf](#) as cushioning.

Old tires can be used as a substituted material in the [Portland cement](#) production, a key ingredient in concrete. Whole tires are commonly introduced into [cement kilns](#), by rolling them into the upper end of a preheater kiln, or by dropping them through a slot midway along a long wet kiln. In either case, the high gas temperatures (1000–1200 °C) cause almost instantaneous, complete and smokeless combustion of the tire.

3.4: Properties of concrete

Concrete is an artificial conglomerate stone made essentially of Portland cement, water, and aggregates. Portland cement is produced by mixing ground limestone, clay or shale, sand and iron ore. This mixture is heated in a rotary kiln to temperatures as high as 1600 degrees Celsius. The heating process causes the materials to break down and recombine into new compounds that can react with water in a crystallization process called hydration.

The raw ingredients of Portland cement are iron ore, lime, alumina and silica. These are ground up and fired in a kiln to produce a clinker. After cooling, the clinker is very finely ground. When first mixed the water and cement constitute a paste which surrounds all the individual pieces of aggregate to make a plastic mixture. A chemical reaction called hydration takes place between the water and cement, and concrete normally changes from a plastic to a solid state in about 2 hours. ζ Concrete continues to gain strength as it cures. Heat of hydration - is the heat given off during the chemical reaction as the cement hydrates

The single most important indicator of strength is the ratio of the water used compared to the amount of cement (w/c ratio). Basically, the lower this ratio is, the higher the final concrete strength will be. This concept was developed by Duff Abrams of The Portland Cement Association in the early 1920s and is in worldwide use today. A minimum w/c ratio (water-to-cement ratio) of about 0.3 by weight is necessary to ensure that the water comes into contact with all cement particles (thus assuring complete hydration). Typical values are in the 0.4 to 0.6.

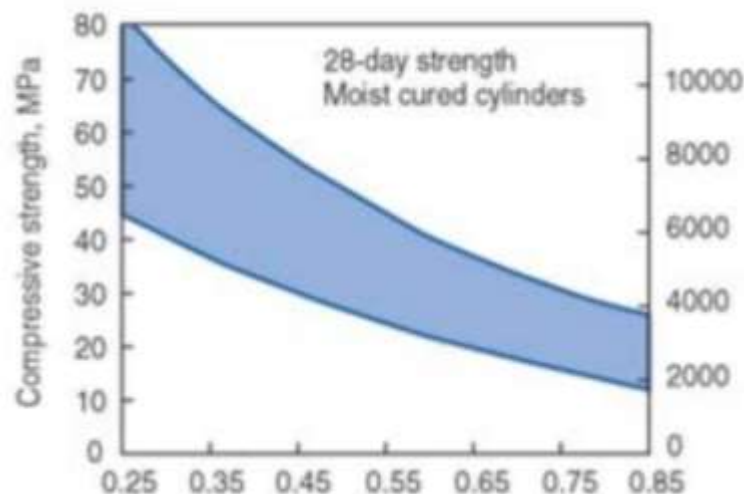


Figure 3.6: water cement ratio

Advantages of low water/cement ratio:

- Increased strength
- Lower permeability
- Increased resistance to weathering
- Better bond between concrete and reinforcement
- Reduced drying shrinkage and cracking
- Less volume change from wetting and drying

Hardened concrete has a number of properties, including:

- Mechanical strength
- Durability.
- Porosity and density.
- Fire resistance.
- Thermal and acoustic insulation properties.
- Impact resistance.

Compressive Strength

Is defined as the measured maximum resistance of a concrete or mortar specimen to an axial load, usually expressed in psi (pounds per square inch) at an age of 28-days. During the first week to 10 days of curing it is important that the concrete not be permitted to freeze or dry out. In practical terms, about 90% of its strength is gained in the first 28 days the first 28 days. Concrete compressive strength depends upon many factors: quality and proportions of the ingredients and the curing environment.

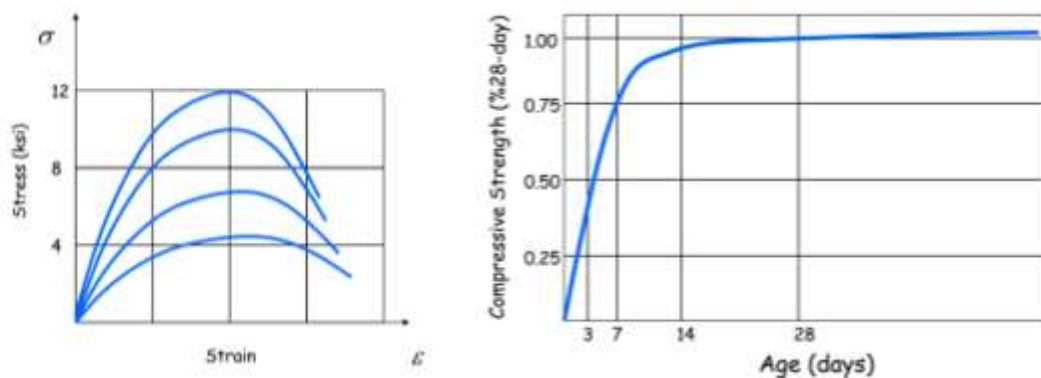


Figure 3.7: compressive strength of concrete

3.5: Properties and application of HPFRCC

As mentioned before a fiber-reinforced composite (FRC) is a [composite building material](#) that consists of three components.

1. The fibers as the discontinuous or dispersed phase,
2. The matrix as the continuous phase
3. The fine interphase region, also known as the interface.

FRC is high-performance fiber composite achieved and made possible by cross-linking cellulosic fiber molecules with resins in the FRC material matrix through a proprietary molecular re-engineering process, yielding a product of exceptional structural properties. This technology involves a method of refining, blending, and compounding natural fibers from waste materials to form a high-strength fiber composite material in a new matrix. The designated waste or base raw materials used in this instance are those of waste thermoplastics and various categories of cellulosic waste including rice husk and saw dust.

Strengthening concrete with steel fibers is not a recent idea. Berard (1874) received a patent for the idea of improving concrete behavior by introducing metallic wastes. However, for almost a century, SFRC was used very rarely. It was only in the 1960s, that the application of SFRC increased worldwide.

In the early phases of the development of SFRC, it was hoped that it would be possible to increase the relatively weak tensile strength of the concrete substantially. Until now, only small strength increases are possible. In addition, the load-carrying capacity of reinforced concrete (RC) and pre-stressed concrete (PC) structural members cannot be substantially increased by fiber addition. However, improvements in the behavior of RC & PC structural members in some areas are possible, especially when there is ductility in demand in the tension zone.

Moreover, steel fibers can increase the serviceability behavior of RC and in some cases, when this limit state dominates, replace steel reinforcement altogether.

The application of SFRC is particularly economical in those areas, where a relatively high compression stress is present in combination with a small bending load, such as in tunnel structures. SFRC is used both for cast-in-situ and precast applications, sprayed concrete is also widely used.

High-performance fiber-reinforced cementitious composites (HPFRCCs) are a group of fiber-reinforced cement-based composites which possess the unique ability to flex and self-strengthen before fracturing. This particular class of [concrete](#) was developed with the goal of solving the structural problems inherent with today's typical concrete, such as its tendency to fail in a brittle manner under excessive loading and its lack of long-term durability.

For producing HPFRCC fine aggregates are mostly used. Accordingly, demonstrating remarkable properties such as improved resilience and sustainability. HPFRCC materials also show improved properties compared with normal concrete and/or Fiber Reinforced Concrete (FRC) in terms of higher ductility, durability and energy dissipation capacity. This material can be characterized by a pseudo-ductile tensile strain hardening behavior with multiple cracking prior to failure. Tensile behavior of NC, FRC and HPFRCC materials are compared in the next figure.

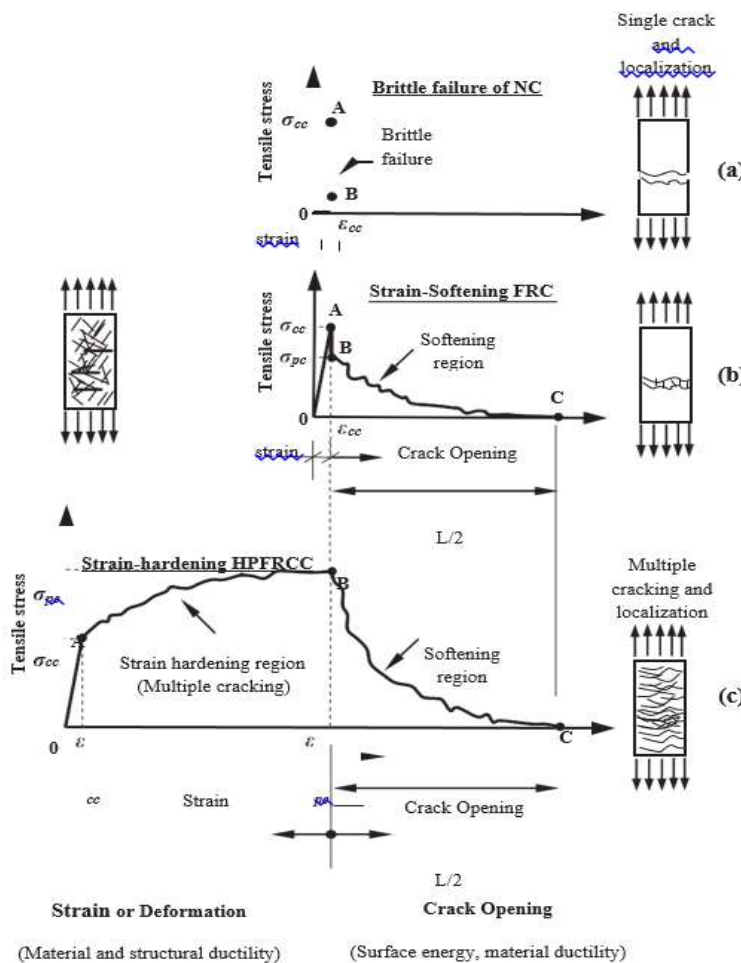


Figure 3.8: Typical tensile behavior of HPFRCC

This figure clearly exhibits three distinct behavior upon cracking. When concrete, mortar or FRC are subjected to tension, brittle degrading behavior at first cracking due to inability to transfer tensile stresses across the crack surface is observed. In contrary, HPFRCC materials undergo multiple cracking after first cracking, exhibiting a hardening behavior, strength increase after first cracking. Only for the HPFRCC materials the post cracking strength, is higher than the first cracking strength.

Rossi suggested the following concepts for a deeper and simpler interpretation of UHPFRCC's cracking mechanism:

“A micro-crack is a crack whose length can be considered to be very small in relation to the size of a specimen or a structure”;

“A macro-crack is a crack whose length cannot be considered to be very small in relation to the size of a specimen or a structure”;

“An active crack is a crack whose edges undergo normal or tangential displacements”;

“A critical and active crack is a crack which leads to a concentration of stresses and a localization of strains within a volume of concrete”.

The transformation from material behavior to structure behavior can be defined as a two-phase series. At first the micro-cracks are distributed spontaneously and without predominant orientation: the mechanical macroscopic behavior remains fundamentally the same and is intrinsic to the material. Afterwards, macro-cracks occur and they are initially distributed in the same way as the micro-cracks, in different orientations. In this case, on the contrary, the macroscopic mechanical behavior may depend on the location of the macro-cracks in the specimen, and is found structural in this case.

In general, short fibers are needed mainly to function on micro-cracks, while long fibers are mostly engaged in macro-cracks. In next figure the position of the micro and macro fibers during the cracking process is exemplified.

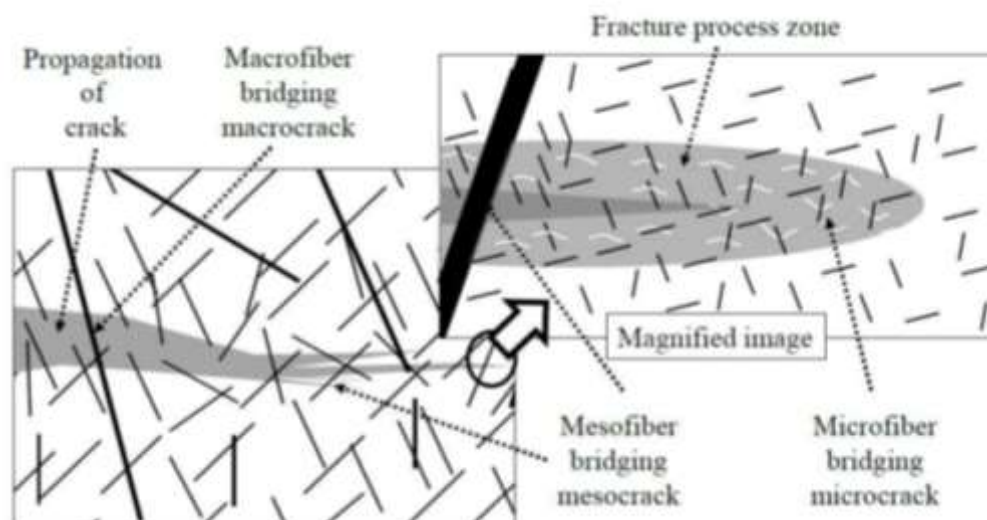


Figure 3.9: Representation of multi-scale fiber-reinforcement element

Chapter 4 Experimental program

4.1: Introductory remarks And Work Methodology

This chapter presents experimental work on Waste Steel Fiber Reinforced Concrete (WSFRC) made by reused steel fibers from end life tires with different dosages and blends using cubes. The performance of a typical concrete mix was evaluated using

Before discussing the test procedure and experimental part, it is necessary to briefly mention the laboratory that these tests were performed. The present experimental report has been carried out at Politecnico di Torino DISEG Laboratory. The laboratory is a high-tech office which lots of different research projects are developed inside that.

Correspondingly, this lab, operated by trained and specialized staff, contributes significantly to the study and education of civil engineering. The Laboratory is fitted with many mechanical and physical measurement equipment and measuring instruments. The practices range from research on buildings and structural components, to construction materials chemical-physical and mechanical research. The laboratory is equipped to perform experimental tests on innovative materials, including steel, in addition to tests on concretes.

The analysis and research of fiber reinforced cement-based composite materials and structural components, in particular for structural reinforcement and anti-seismic adaptation of buildings and civil structures, are sectors that play an important role in this study.

Each and every test can be separated into two part. The first phase is the preparation of specimens and the second phase is performing the tensile and compressive tests. In the following figures we will take a brief look at these two steps. In the first step according to the mix we need to mix the different particles.



Figure 4.1: Specimens preparation mode

The second phase is performed using a loading machine which can be seen in the following figure, regarding the indicated loading rate. The loading rate had been specified according to the code rules.



Figure 4.2: Testing machine

To fulfill the primary requirements of each project in the most productive and successful way, a working methodology has been needed to achieve the research goals, which defines the main phases of the process.



Figure 4.3: Work Methodology Scheme

4.2: Molds, casting and curing

For the casting of the prism specimens, metallic molds were used. Each mold included three compartments for prisms (width of 40 mm, depth of 40 mm and length of 160 mm). For each mix, all of the mold was used.



Figure 4.4: Testing Mold

The test specimens were cast and cured in compliance with EN 12350-1 and EN 12390-2.

De-molding oil was applied on the molds, 15 to 30 minutes before the concrete arrival. The molds were then placed on the laboratory vibrating table, waiting to be filled with concrete. The molds were filled in various layers and vibration was applied after each layer and the vibration time ranged from 10 to 20 seconds depending on the concrete consistency. For fluid concrete the vibration is not necessary.

The specimens were cast in one day and cured in the molds for 48 hours. After de-molding, the specimens kept together on pallets and stored inside the Laboratory. After 28 days of curing in an interior environment, all hessian and plastic sheets were removed and specimens were left to dry.

The casting routine is described below and shown in following figures.



Figure 4.5: separating fibers from tire particles



Figure 4.6: filling the mold with fibers



Figure 4.7: filled mold by waste fibers



Figure 4.8: provide the mix materials

As mentioned before, we need to find the proper mix and in order to do it we perform different tests on them. According to each mix we provide three samples and perform a flexural and compressive test on them. The tested mix are presented in the following sections.



Figure 4.9: mix and produce concrete



Figure 4.10: pouring mortar in mold



Figure 4.11: filled mold



Figure 4.12: specimens after de-molding

Mixing of fiber reinforced concrete needs careful conditions to avoid balling of fibers, segregation and in general the difficulty of mixing the materials uniformly. An increase in the aspect ratio, volume percentage, size and quantity of coarse aggregate intensify the difficulties and balling tendency. Steel fiber content in excess of 2% by volume and aspect ratio of more than 100 are difficult to mix. In the experimental program Mix K was scrapped due to severe balling (see Fig. 4.9)



Figure 4.13: balling of fibers

The preparation of the fibers included screening to remove any residual rubber from the fibers and to remove the majority of short fibers (below 15 mm). The dust was also removed to enhance the bond of the fibers with the concrete.

For the different mixes three prisms were cast for each to comply with the BS EN196-1 (2016) in order to obtain the flexural and compressive properties of HPFRCC, respectively. The purpose is to form a comprehensive parametric study on how small variations of fiber dosages affect the flexural properties of concrete.

The method comprises the determination of the compressive and especially flexural strength prismatic test specimens 40mm*40mm*160mm in size. At the specified age the specimens are taken from their wet storage and broken in flexure, determining the flexural strength where required, and each of the half are tested for the compressive strength.

The laboratory where the test take place shall be maintained at a temperature around 20°C and the relative humidity not less than 50%.

According EN 196-1 CEN, Standard sand is used. This sand shall have been granted a CEN certificate by the national standardization organization. In view of the difficulties of specifying CEN Standard sand completely and unambiguously it is necessary during certification and quality control testing to standardize the sand against the CEN Reference sand, as described in EN 196-1.

When the cement to be tested is kept for more than 24 h between sampling and testing, it shall be stored in completely filled and air tight containers made from material which does not react with cement. Distilled water shall be used for reference testing. For other test, drinking water may be used.

To facilitate the filling of the mold a tightly fitting metal hopper with vertical walls 20mm to 40mm in height shall be provided. When viewed in plan the hopper walls shall overlap the internal walls of the mold by nor more than 1 mm. The outer walls of the hopper shall be provided with a means of location to ensure correct positioning over the mold.

The mixer shall operate at the speeds given in following Table.

	Rotation [min ⁻¹]	Planetary movement [min ⁻¹]
Low speed	140 ± 5	62 ± 5
High speed	285 ± 10	125 ± 10

Table 4.1: Speeds of mixer blade

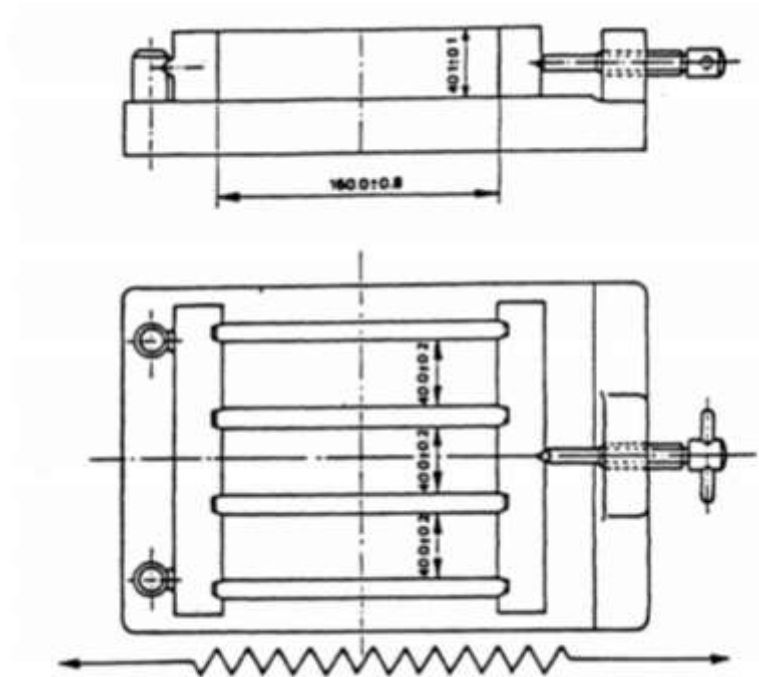


Figure 4.14: Typical mold

For curing the specimens the following steps must be followed.

- Place a 210 mm x 185 mm plate glass sheet (or from other impermeable material such a steel) of 6 mm thickness on the mold
- Place each covered mold on a horizontal base in the moist air room. Mold shall not be stacked one upon the other
- Each mold shall be removed from storage at its appropriate time for de-molding.
- carry out de-molding with due precautions
- Keep the de-molded specimens selected for testing at 24 h covered by a damp cloth until tested
- Place the specimens on non-corrodible gratings and keep them apart from each other so that the water has free access to all six sides of the specimen. At no time during storage shall the spaces between the specimens or depth of water above the upper faces of the specimens be less than 5 mm
- Remove the specimens from the water not more than 15 min before the test is carried out. Cover the specimens with a damp cloth until tested

4.4: Flexural tests

According to code rules we need to place the prism in the testing machine (see Figure) with one side face on the supporting rollers and with its longitudinal axis normal to the supports. The distance between supports is $100 \text{ mm} \pm 0.5 \text{ mm}$. Apply the load vertically by means of the loading roller to the opposite side face of the prism and increase it smoothly at the rate of $50 \pm 10 \text{ N/s}$ until fracture.

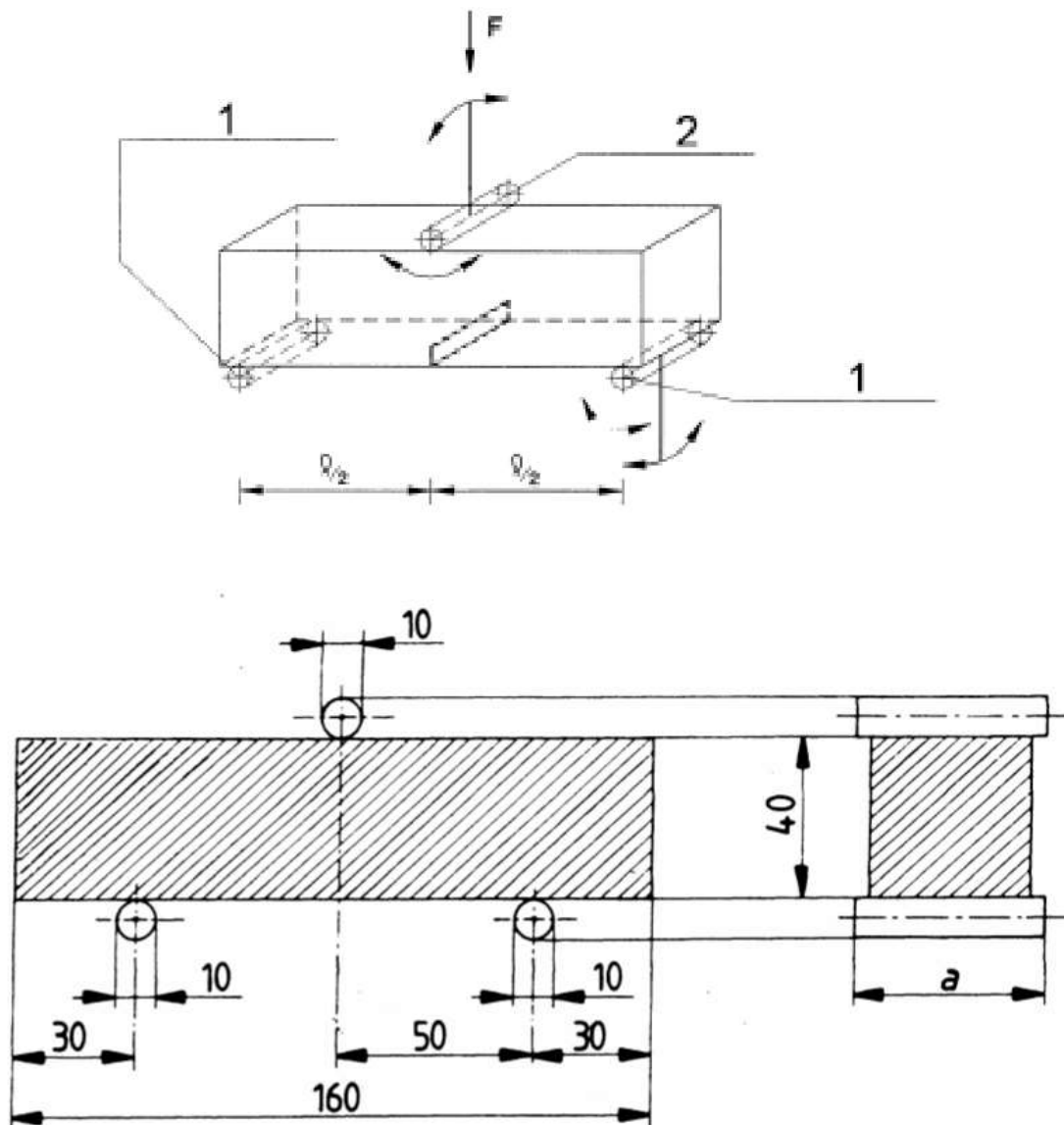


Figure 4.15: Arrangement of loading of test specimen, 1-Supporting roller, and 2-Loading roller

The test specimens were placed in the testing machine, correctly centered and with the longitudinal axis of the specimen at right angles to the longitudinal axis of the upper and lower rollers.



Figure 4.16: 3-Point Bending Test

The tensile behavior of metallic fiber concrete is evaluated in terms of residual flexural tensile strength values determined from the load-crack mouth opening displacement curve or load-deflection curve obtained by applying a center-point load on a simply supported prism.

The three-point bending flexural test provides values for the [modulus of elasticity in bending](#) , [flexural stress](#), flexural strain and the flexural stress–strain response of the material. The main advantage of a three-point flexural test is the ease of the specimen preparation and testing. However, this method has also some disadvantages: the results of the testing method are sensitive to specimen and loading geometry and strain rate.

Calculate the flexural strength from:

$$R_f = \max \sigma_f = \frac{\max M}{W}$$

where

- R_f is flexural strength [MPa]
- σ_f is maximum flexural stress [MPa]
- M is bending moment [N.mm]
- w is section modulus [mm³]

The terms bending moment and section modulus shall be explained in the course Structural mechanics.

Some basic examples of loading and appropriate formulas for bending moment and section modulus are given in next table.

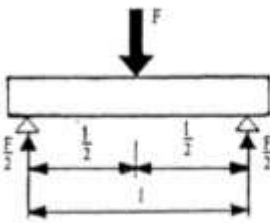
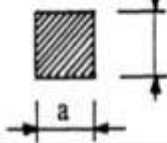
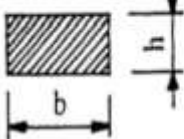
Loading diagram	Bending moment	Form of section	Section modulus
	$M = \frac{1}{4} F \times l$		$W = \frac{1}{6} a^3$
			$W = \frac{1}{6} b h^2$

Table 4.2: Basic examples of bending moment and section modulus

4.4: Compressive tests

The prism after test of flexural strength are becoming halves, then they are tested in compression Centre the prism halves laterally to the auxiliary platens of hard steel, which exactly determine the compressive area (because the prism halves have an irregular form). According EN 196-1 the size of the platens is 40 mm x 40 mm and they are at least 10 mm thick .During loading the relative attitude of the upper and lower platens shall remain fixed. The resultant of the forces shall pass through the center of the specimen. Increase the load smoothly at the rate of 2400 ± 200 N/s over the entire load application until fracture.

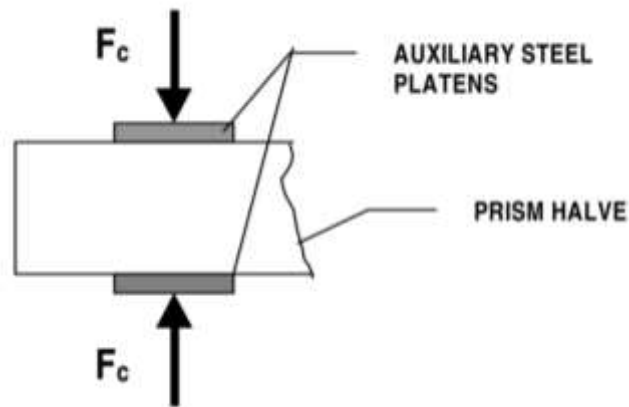


Figure 4.17: Scheme of loading for compressive test



Figure 4.18: Preparation of specimen for compressive test

4.5: Mixes and fiber used

In order to verify the proper mix using these fibers we perform a series of test according to the mentioned regulations, for each mix we provided 3 different specimens in 1 day and after 28 days we performed the flexural and compressive tests according to the code rules.

After the preparation of the specimens a preliminary check is performed in order to see if the samples are satisfying the basic requirements or not. For example in the case that we used larger aggregates we need to check if the specimen is capable of accepting these materials. We need to check the specimens not having big crack or holes after the de-molding.

In the following tables you can see the different mixes and the date which they are made.

1° series: Test on 23_9:

test on 23-09	value	note
W/C ratio	0.6	
Water(g)	690	
Cement(g)	1150	Cement 52.5 type 1
Fiber(%volume)	2	



The result of preliminary evaluation was satisfying but the amount of used cement is so high. So is possible that we face some difficulties for satisfying the embodied energy.

2° series of tests: not tested

second test	value	note
W/C ratio	0.5	
Water(g)	400	
Cement(g)	800	Cement 52.5 type 1
super-plasticizer(g)	9.6	mapei Dynamon SR1/AV
aggregate(g)	800	mas 0.2(mm)
Fiber(%volume)	2.1	



From literature Two-Stage Concrete (Najjar, 2016) with fibers (volume of cement paste 0.7 l; volume of sand 0.3 l) Second series of tests which didn't have a satisfying result and was rejected before testing

3° series of tests: 15_10:

test on 15-10	value	note
W/C ratio	0.5	
Water(g)	430	
Cement(g)	860	Cement 52.5 type 1
super-plasticizer(g)	9.6	mapei Dynamon SR1/AV
aggregate(g)	680	mas 0.2(mm)
Fiber(%volume)	2.1	



With respect to 2° series the sand is reduced (volume of cement paste 0.75 l; volume of sand 0.25 l)

And the final result was much better.

4° series of tests: 29_10

test on 29-10	value	note
W/C ratio	0.5	
Water(g)	430	
Cement(g)	860	Cement 52.5 type 1
super-plasticizer(g)	9.6	mapei Dynamon SR1/AV
aggregate-sand(g)	510	max 0.2mm
aggregate-fine(g)	45	max 0.125mm
Fiber(%volume)	2.1	



With respect to 3° series (volume of cement paste 0.75 l; volume of sand 0.35 l) substitute 25% of sand with the same volume of Plastic P2 from (max 0.125 mm)

5° series of tests: 6_11

test on 06-11	value	note
W/C ratio	0.5	
Water(g)	430	
Cement(g)	645	Cement 52.5 type 1
fly-ash(g)	215	
super-plasticizer(g)	7.2	mapei Dynamon SR1/AV
aggregate-sand(g)	510	max 0.2mm
aggregate-fine(g)	45	max 0.125mm
Fiber(%volume)	2.1	



With respect to 4° series (volume of cement paste 0.75 l; volume of sand 0.35 l) substitute 25% of cement with the same weight of fly ash/silica fume Mapei. Also the $\frac{\text{super-plasticizer}}{\text{cement}}$ ratio is the same

6° series of tests: not tested

In the next step we tried to replace the waste fibers from end life tire with the industrial fibers. But before introducing the next mix it is necessary to mention the procedure which we followed in order to get the size of the industrial fibers.

In order to do that we followed a statistical procedure and we choose a sample of around 600 fibers and we measured these fibers with the accuracy of .01mm.

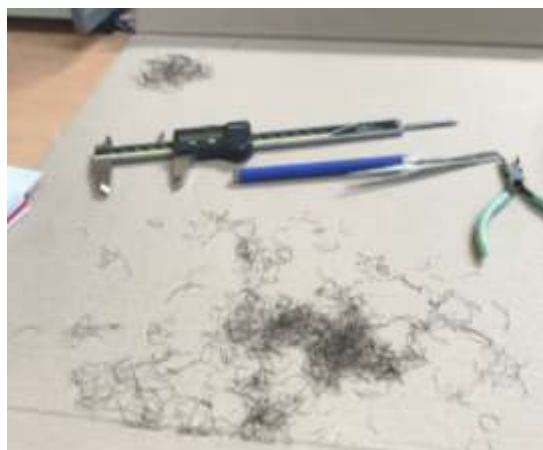


Figure 3.19: Measurement of the fiber sample

In measuring the fibers we just need to mention that we neglect the dust-like materials with small dimensions.

After finishing this step we put the result in one excel file and we draw a Gaussian curve in order to find the average size of these fibers. Here in the following figure we provided the result of our calculation.

1	length	diameter
2	21.19	0.39
3	27.14	0.88
4	29.69	0.19
5	25.65	0.39
6	29.63	0.19
7	42.28	0.31
8	23.06	0.56
9	29.53	0.23
10	22.63	0.44
11	18.72	0.31
12	28.44	0.56
13	23.57	0.34
14	14.59	0.22
15	30.58	0.38

Figure 3.20: Excel file provided for length measurement

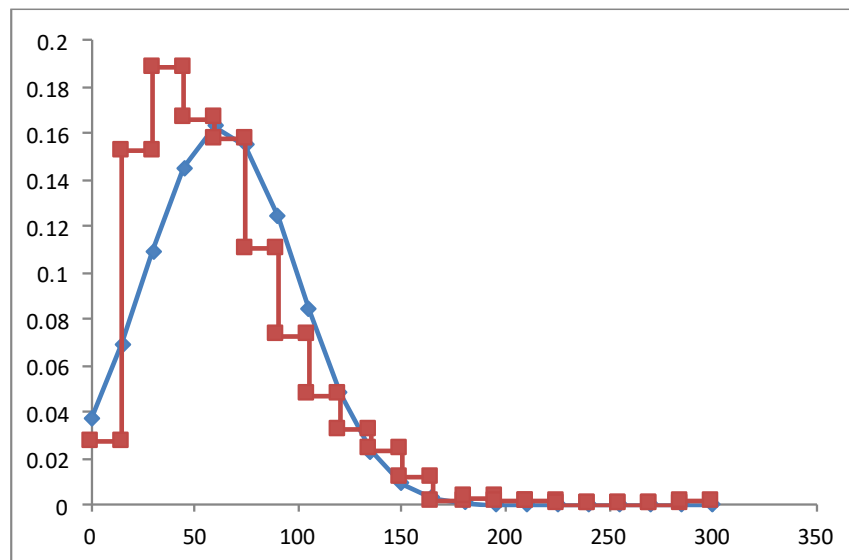


Figure 3.21: Statistical calculation

The result of our calculation is to use 2.1% in volume of industrial steel fibers having the aspect ratio close to the average aspect ratio of the recycled fibers with the length of 62mm.

The fibers DE 35/0.55 M (Krampe Harex diameter=0.55 and length=35) has an aspect ratio of 63.



Figure 3.22: industrial fibers which have been used in our mix

Now we decided to use the composition of the HPFRCC for the first attempt. And here is the mix:

	con la legge di	con i dati
	gauss	reali
n=	590	590
sqm=	36.5166848	
min=		7.97435897
fratt_5%=	2.784772437	16.721519
fratt_25%=	38.24247338	35.3333333
Media=	62.85471894	62.8547189
fratt_75%=	87.4669645	82.6944444
fratt_95%=	122.9246654	128.933333
max=		297
mediana=		56.4444444

According to the preliminary checks we figured out that the composition of our mix does not work in the case of:

- the same composition of Two-Stage Concrete (Najjar, 2016) with fibers (volume of cement paste 0.7 l; volume of sand 3 l)
- Less past then Two-Stage Concrete (Najjar, 2016) with fibers (volume of cement paste 0.55 l; volume of sand 0.45 l)

So we didn't perform the tests on these samples and they were rejected in the preliminary stage.

second test	value	note
W/C ratio	0.5	
Water(g)	400	
Cement(g)	800	
super-plasticizer(g)	9.6	mapei Dynamon SR1/AV
aggregate(g)	800	mas 0.2(mm)
Fiber(%volume)	2.1	industrial fibers

We need to mention also in the next mixes the same statistical concept is applied and only the ratio of other particles were changed. So the main idea of industrial fiber size in our thesis is to use 2.1% in volume of industrial steel fibers having the aspect ratio close to the average aspect ratio of the recycled fibers 62. And the fibers DE 35/0.55 M (Krampe Harex diameter=0.55 and length=35) has and aspect ratio of 63.

7° series of tests: 21_11:

test on 21-11	value	note
W/C ratio	0.5	
Water(g)	290	
Cement(g)	580	Cement 52.5 type 1
super-plasticizer(g)	0.45	mapei Dynamon SR1/AV
aggregate-sand(g)	510	normal sand dmax=2mm
Fiber(%volume)	2.1	industrial steel fiber



As mentioned before we just need to change the ratio of our paste material in this step. The composition of HPFRCC has less paste than Two-Stage Concrete (Najjar, 2016) with fibers (volume of cement paste 0.5 l; volume of sand 0.5 l). We need to mention that the density of these fibers is around 7200 kg/m³.

8° series of tests: 10_12:

test on 10-12	value	note
W/C ratio	0.5	
Water(g)	430	
Cement(g)	645	
fly-ash(g)	215	
super-plasticizer(g)	7.2	mapei Dynamon SR1/AV
aggregate-sand(g)	510	max 0.2mm
aggregate-fine(g)	45	max 0.125mm
Fiber(%volume)	4.2	



With respect to 5° series (volume of cement paste 0.75 l; volume of sand 0.35 l, 25% of cement is made by fly-ash/silica fume Mapei and 25% of aggregate is made by Plastic P2 from (max 0.125 mm) the content fiber is 4.2%

9° series of tests: 18_2:

test on 10-12	value	note
W/C ratio	0.5	
Water(g)	430	
Cement(g)	645	
fly-ash(g)	215	
super-plasticizer(g)	7.2	mapei Dynamon SR1/AV
aggregate-sand(g)	510	max 0.2mm
aggregate-fine(g)	45	max 0.125mm
Fiber(%volume)	3	



With respect to previous series (volume of cement paste 0.75 l; volume of sand 0.35 l, 25% of cement is made by fly-ash/silica fume Mapei and 25% of aggregate is made by Plastic P2 from (max 0.125 mm) the content fiber is 3%.

10° series of tests: 25-6-A:

test on 25-06-A	value	note
W/C ratio	0.5	
Water(g)	430	
Cement(g)	580	
fly-ash(g)	280	
super-plasticizer(g)	7.2	mapei Dynamon SR1/AV
aggregate-sand(g)	680	max 0.2mm
Fiber(%volume)	3	



With respect to 3°series (volume of cement paste 0.75 l; volume of sand 0.35 l) substitute 33% of cement with the same weight of fly ash/silica fume Mapei. Also the superpl/cement ratio is the same. The fiber content is 3 %.

11° series of tests: 25-6-B:

test on 25-06-B	value	note
W/C ratio	0.5	
Water(g)	430	
Cement(g)	580	
fly-ash(g)	280	
super-plasticizer(g)	7.2	mapei Dynamon SR1/AV
aggregate-sand(g)	680	max 0.2mm
Fiber(%volume)	6	



With respect to 10°series-A (volume of cement paste 0.75 l -33% of cement substituted with the same weight of fly ash/silica fume Mapei. ;

volume of sand 0.35 l) The fiber content is 6 %s

4.5: Fly-Ash and Silica Fume

Fly ash:

In thermoelectric plants, fly ash is produced as a by-product of the combustion of pulverized coal. It occurs sometimes hollow in the form of nearly spherical particles (5-90 microns). The circular shape of these particles enhances the UHP-FRCC's workability, increases the dough's stability and decreases its vulnerability to water containing changes.



Figure 4.23: Fly ash Particles

Fly ash particles have no independent binding capabilities but they work as a binder when combined with mortar. They also have beneficial effects on the hardened concrete, allowing mechanical strength to increase further even after 28 days, reducing creep phenomena and rising durability. Owing to the low porosity, concrete mixtures containing fly ash have lower water permeability and greater resistance to chemical attack.

Advantages of fly ash in concrete:-

- Reduced water content for a given workability or improved workability at the same water content.
- The rate of bleeding is reduced while workability is increased.
- Improved long term strength and durability performance.
- Lower shrinkage and porosity as a result of the lower water content.
- Lower permeability and better resistance to sulphate attack.

Disadvantages of fly ash in concrete:-

- Concrete changes from a liquid to a solid a few hours after pouring, but the curing process may take much longer.
- Fly ash admixtures can lengthen the time it takes for concrete to set.
- Fly ash reduces the amount of air entrainment, and concrete mixtures high in fly ash often require more air-entraining admixture.
- It is more difficult to control the colour of concrete containing fly ash than mixtures with Portland cement only.

Figure 4.24: Pros and Cons of fly ash in Concrete

The fact that fly ash is Pozzolan, is of no minor importance; it is also an excellent agent in combating the alkali-aggregate reaction phenomenon. The fly ash also contributes to the resilience of the products exposed to chloride attack; it allows for a constant increase in the mechanical resistance especially evident between 7 and 28 days, exceeding the limits reached by concretes of similar characteristics but made with Portland cement only.

Silica Fume:

Silica fume is a by-product of metallic silicone and ferrosilicon alloys developed by the electric furnace industry. It occurs as amorphous silica in the form of microspheres smaller than $0,1\text{ }\mu\text{m}$ which can be distributed in the mixtures in the interstices between the granules of cement ($1\text{-}50\text{ }\mu\text{m}$)

Clearly the filler feature is related to the extreme fineness that this material holds, which is around 100 times finer than cement, both as the average granulate diameter and as a particular surface. This makes it possible to place silica fume granules between the cement's larger granules to create an incredibly compact structure that leaves a limited space open to the water.



Figure 4.25: Silica Fume Particles

The pozzolanic feature on the other hand is related to the chemical composition and morphological structure of highly reactive silica granules. Hence, silica fume does not come and should not be considered simply an aggregate but an integral part of the binder volume.

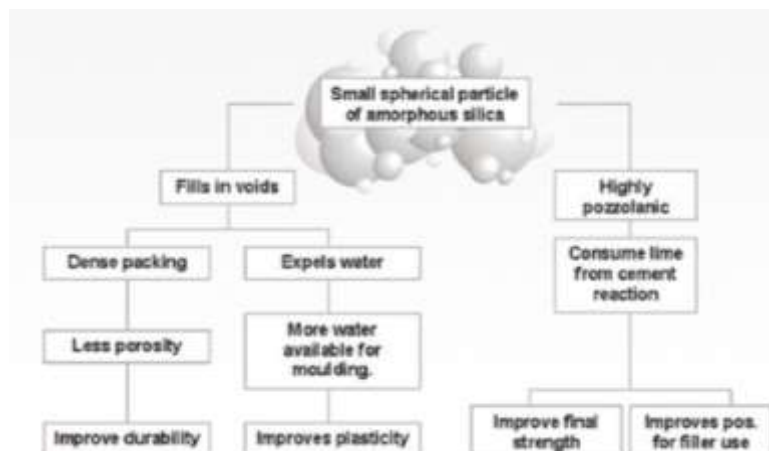


Figure 4.26: Silica Fume characteristic features

Chapter 5 Experimental results and behavior

5.1: General overview

This chapter presents the average stress-mid-span deflection curves for all mixes.

After 28 days, before performing the tests on our specimens we measured the diameter and weights of our samples in order to calculate the density of our specimens. In this section before discussing the results of the tests we need to mention the results which is obtained from different mixes.

Result of this measurements have been gathered in 1 table which you can see below.

Date	sample number	Density (kg/m ³)	average
test on 23_9	1	6157.0	6242.7
	2	6148.3	
	3	6422.9	
test on 15-10	1	6515.6	6623.4
	2	6665.9	
	3	6688.8	
test on 29-10	1	6798.7	6766.1
	2	6765.6	
	3	6734.1	
test on 6-11	1	6318.9	6218.5
	2	6111.9	
	3	6224.6	
test on 21-11	1	6094.7	6158.2
	2	6175.8	
	3	6204.2	
test on 10-12	1	6094.7	6080.9
	2	6056.8	
	3	6091.3	
test On 18-2	1	6066.3	6180.3
	2	6106.2	
	3	6368.4	
test On 25-06-A	1	5971.1	5890.1
	2	5971.1	
	3	5728.2	
test On 25-06-B	1	5453.9	5462.9
	2	5527.9	
	3	5406.9	

Table 5.1: Density of specimens calculated before testing

But before performing any analysis we take a brief look to the type of the failure which happened in these specimens under the flexural test. By knowing the different type of possible failure modes, we will have a better mindset when we see the results of our tests.

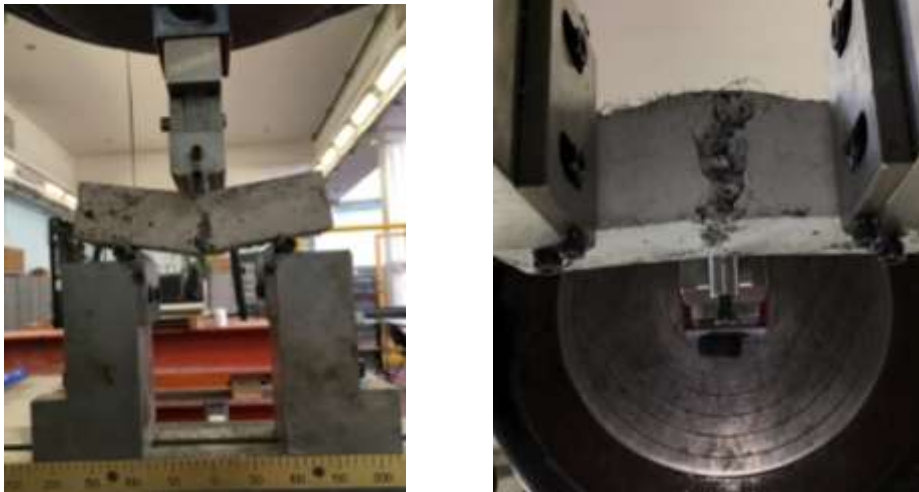


Figure 5.1: specimens after 3PB test

In our specimens because of the high volume of the fibers, we didn't face the problems regarding the distribution of fibers.

The presence of fiber contributes to a more ductile failure for specimens than for plain concrete, and fiber pull-out is primarily responsible for the failure. The potential for tensile deformation is enhanced, which results in an increased critical crack opening. The critical opening of the crack is characterized as one where no stress can be transferred, as shown in the following Figure.

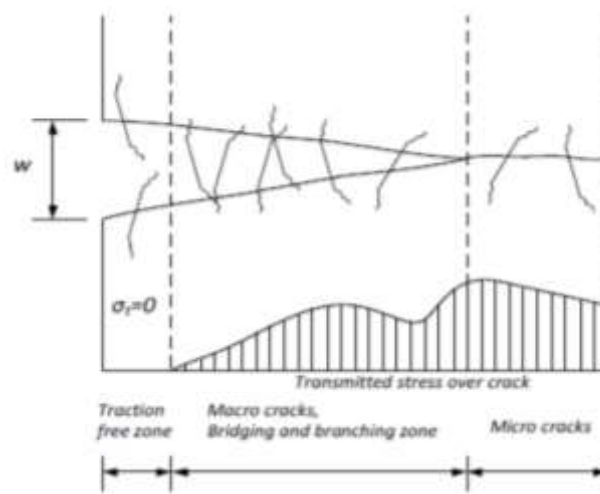


Figure 5.2: Steel Fiber Reinforced Concrete cracking zone

SFRC failure due to pull-out of the fiber is beneficial to obtain ductility and strength during failure. Hence, due to bending, the fibers must be sufficiently ductile to prevent fiber fracture. In addition, the bond strength between the fiber and the matrix must be equal to or greater than the matrix's tensile strength.

Compared to ordinary concrete, neither the tensile strength nor the fiber-reinforced concrete elasticity modulus is greatly impacted. The fiber primarily affects the behavior of the tensile fracture and the properties after cracking. The stress-strain curve is characterized by a strain-softening pattern for FRC with a low to moderate fiber content (< 1 percent), as shown in Figure 2. The curve in this case decreases fairly steeply after the tensile strength is reached, even whereas the curve for plain concrete tends to decrease until zero. Usually the curve for FRC increases again as the fiber continues to work by bringing tensile stresses through cracks.

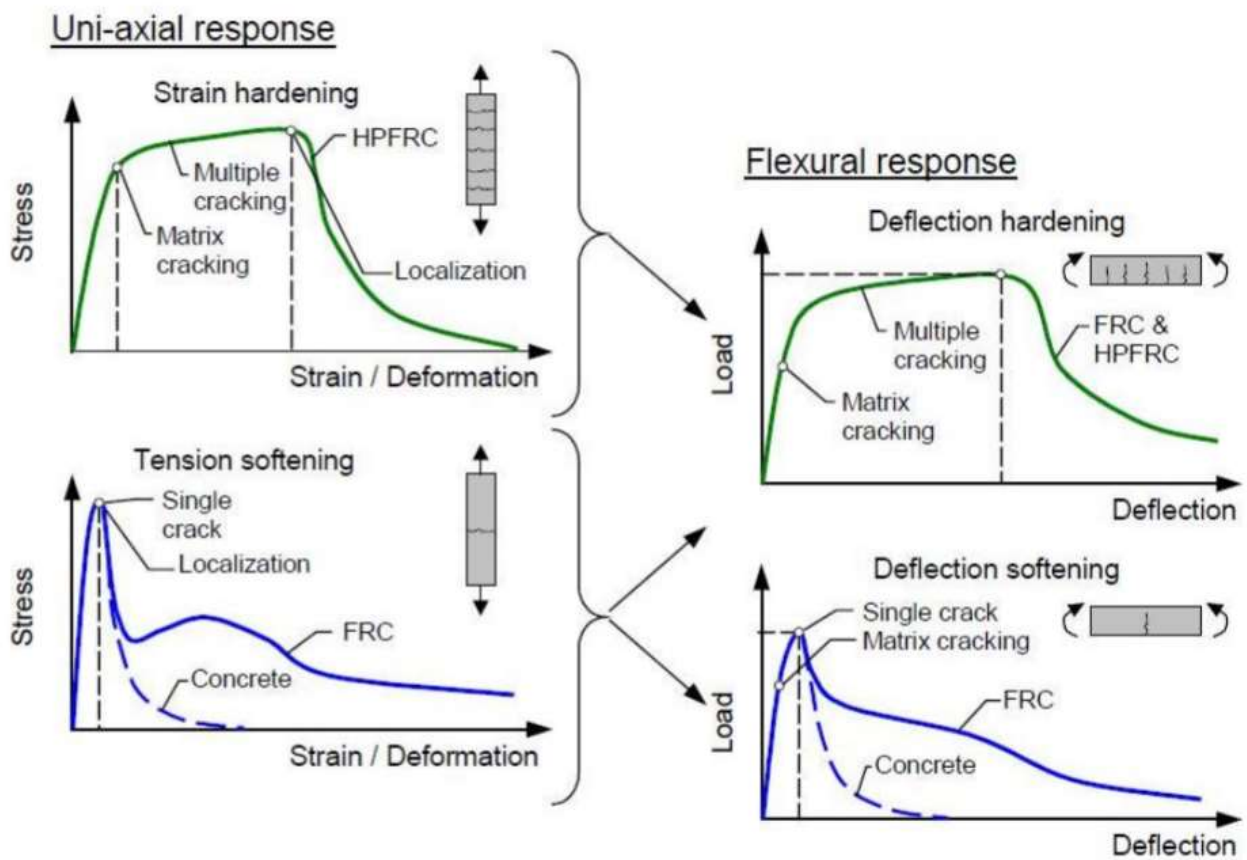


Figure 5.3: Typical tensile behavior of Fiber Reinforced Concrete

As it could be seen in the figure above, given the softening response in uni-axial stress, FRC can provide deflection hardening in bending. It should also be noticed that the deformations locate in one crack in the case of softening behavior, while the hardening one contributes to several cracking before the peak value reaches.

Keeping this in mind in the next section we will provide the result from 3PB test of different mixes. Note that in each graph there are different curves due to the number of the test performed on each mic.

In this part, the full test results are given for each individual prism: After the test, stress-deformation curves are obtained for each individual prism. The graph shows the bending tension versus the deflection of the typical mid-span.

For comparison purposes an overall graph showing bending stress against the average mid-span deflection is given for all specimens of each combination. This section summarizes the key results for evaluating the efficiency of the different mixes using average bending stress-mid-span deflection curves.

In the first part we are reporting the average result of flexural test gained from 3 different prisms. After that we try to combine all these averaged graphs from different tests and make a comparison between different mixes.

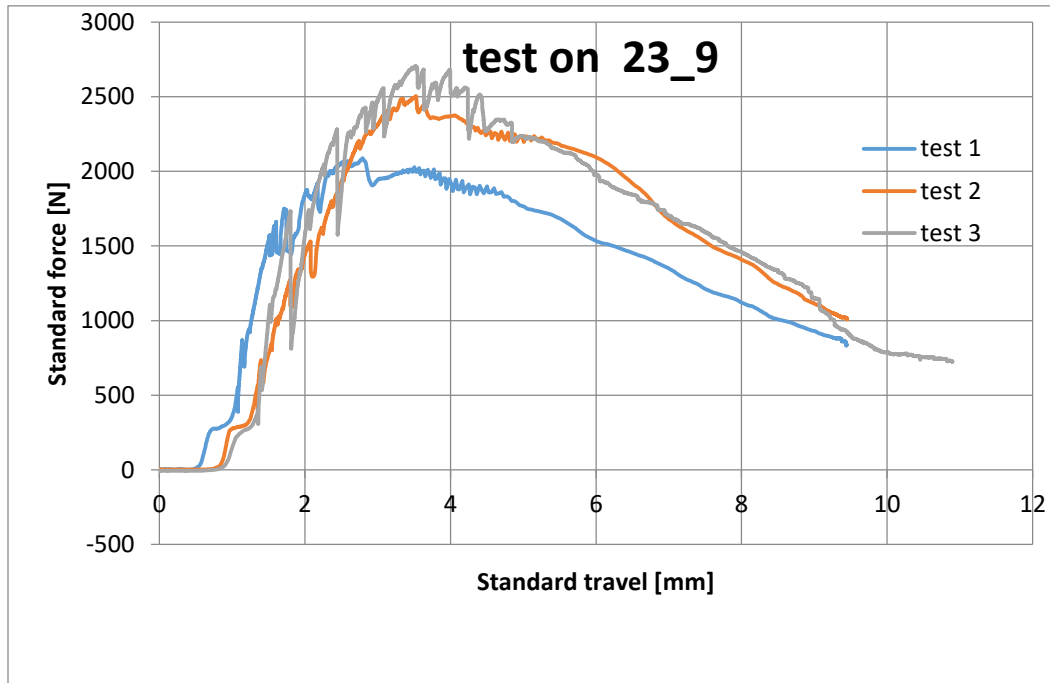
After performing the 3PB test on each of the specimens, we will approximately half the specimens and then perform 2 sets of compressive test. Each half of the specimens are placed under the testing machine. In the following figure this process can be seen.



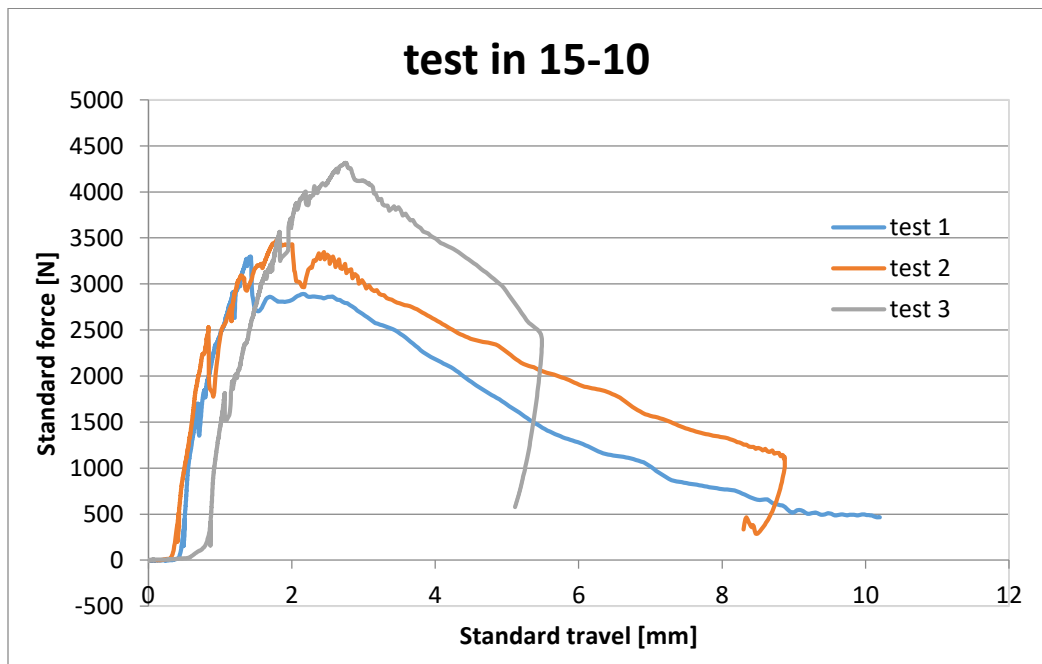
Figure 5.4: Compressive Test

5.2: 3PB Test Result

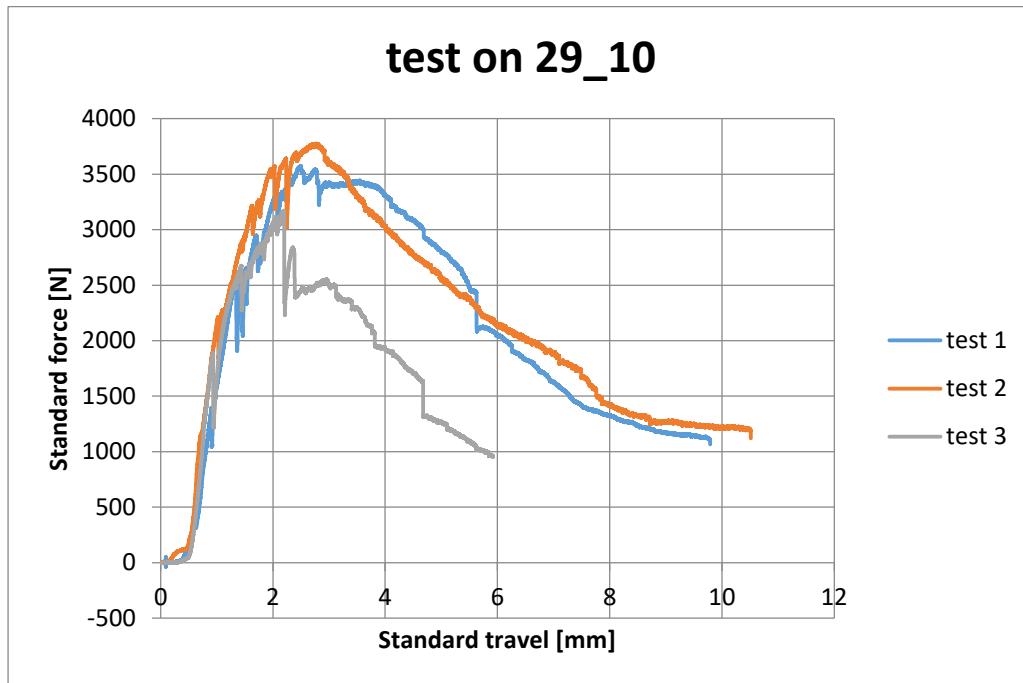
1° series: Test on 23_9:



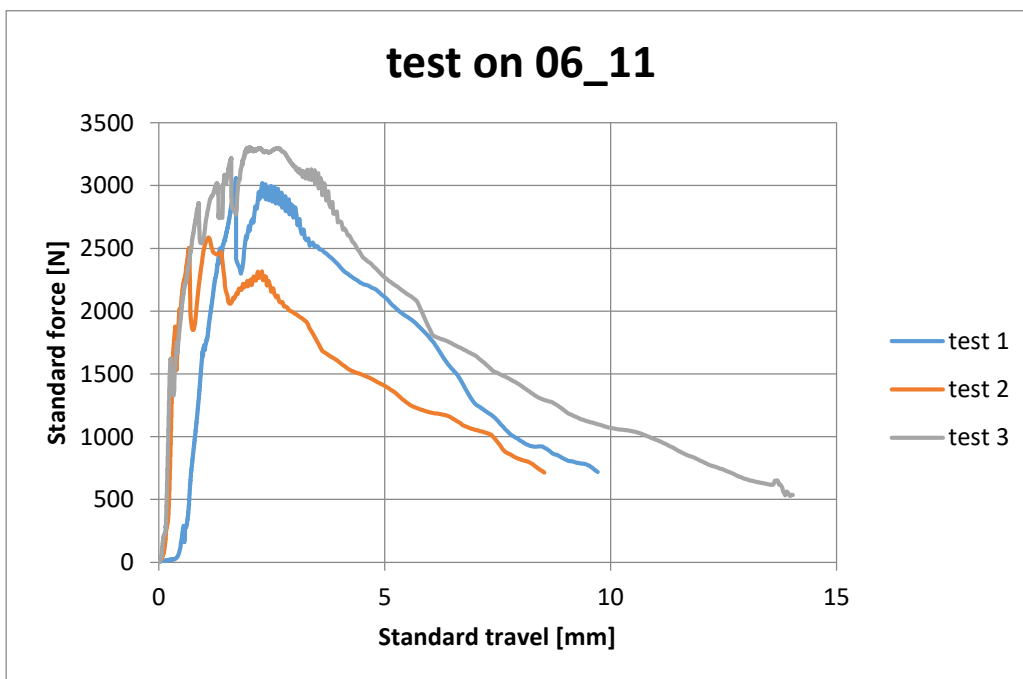
2° series of tests: 15_10:



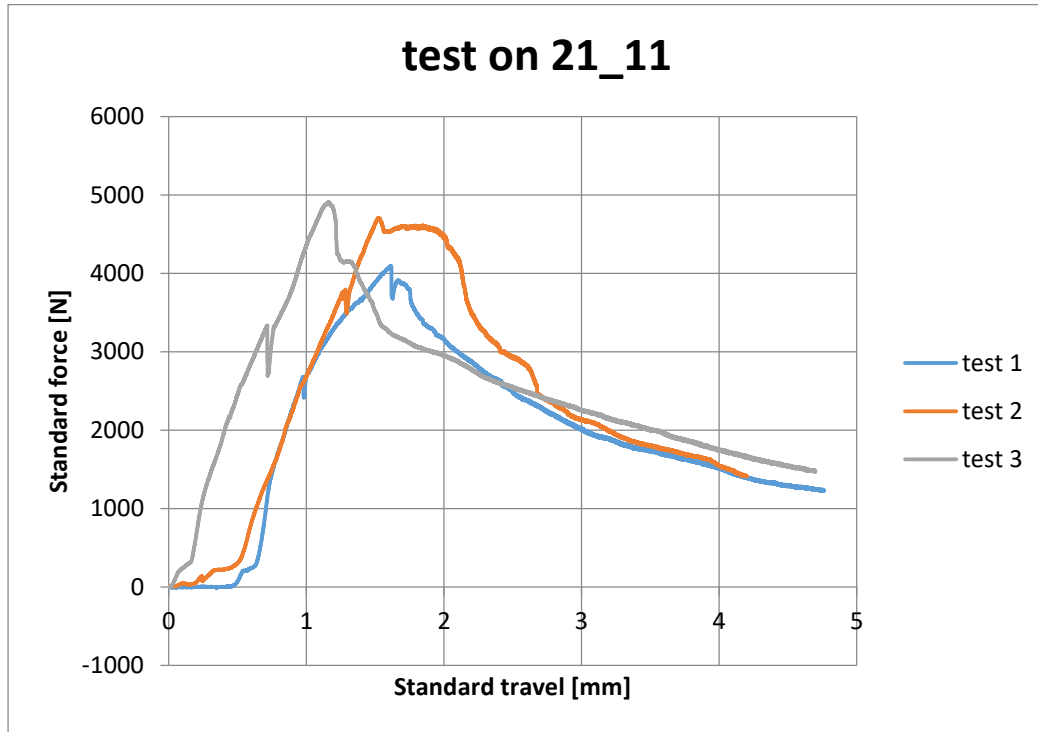
3° series of tests: 29_10:



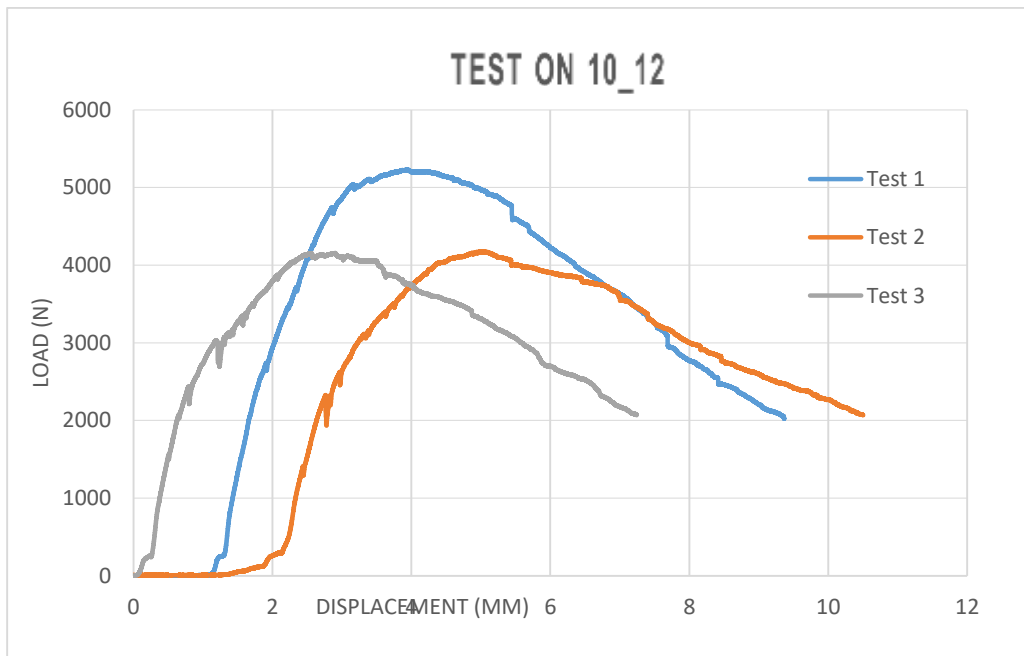
4° series of tests: 6_11:



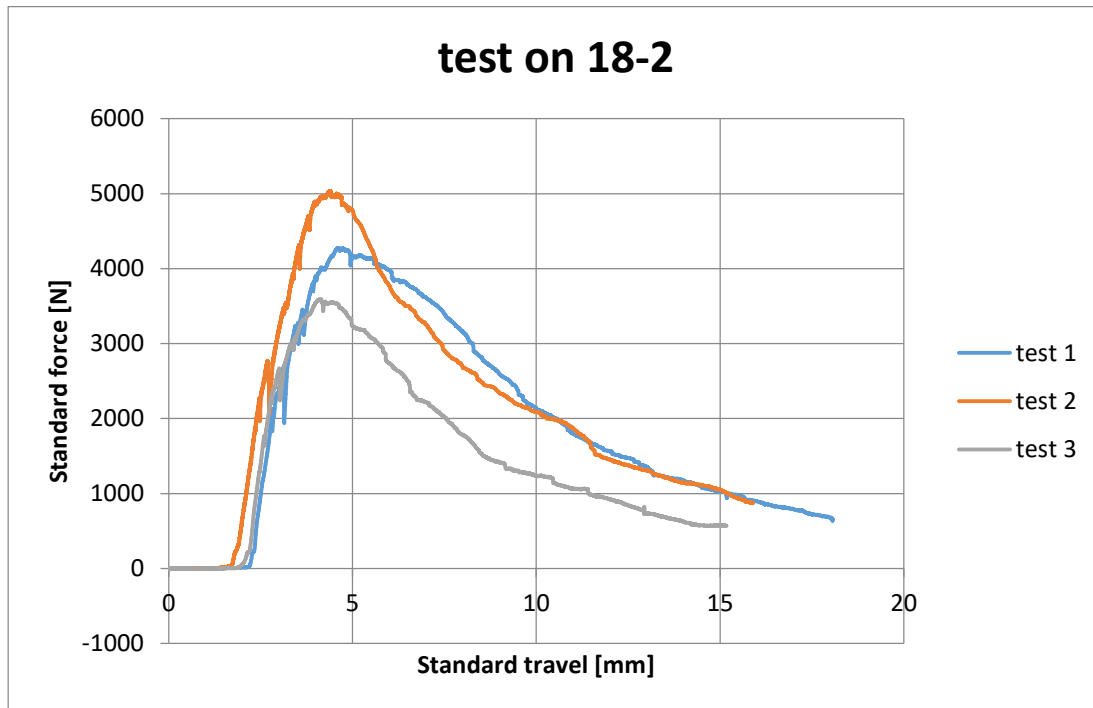
5° series of tests: 21_11:



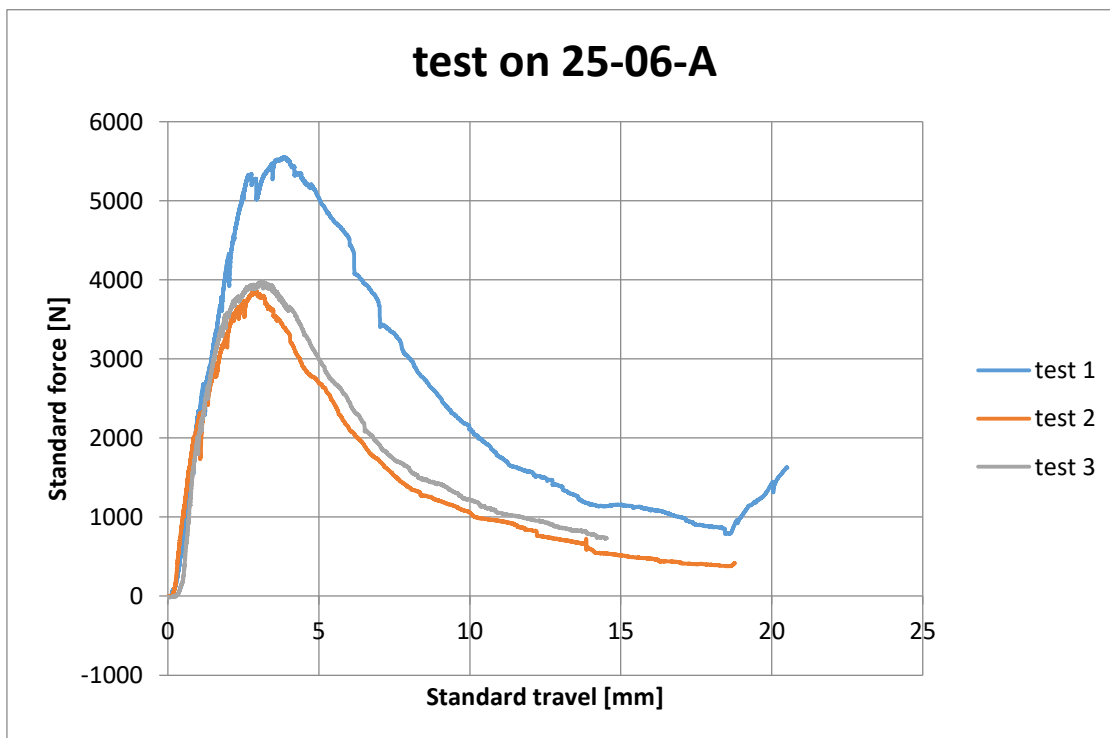
6° series of tests: 10_12:



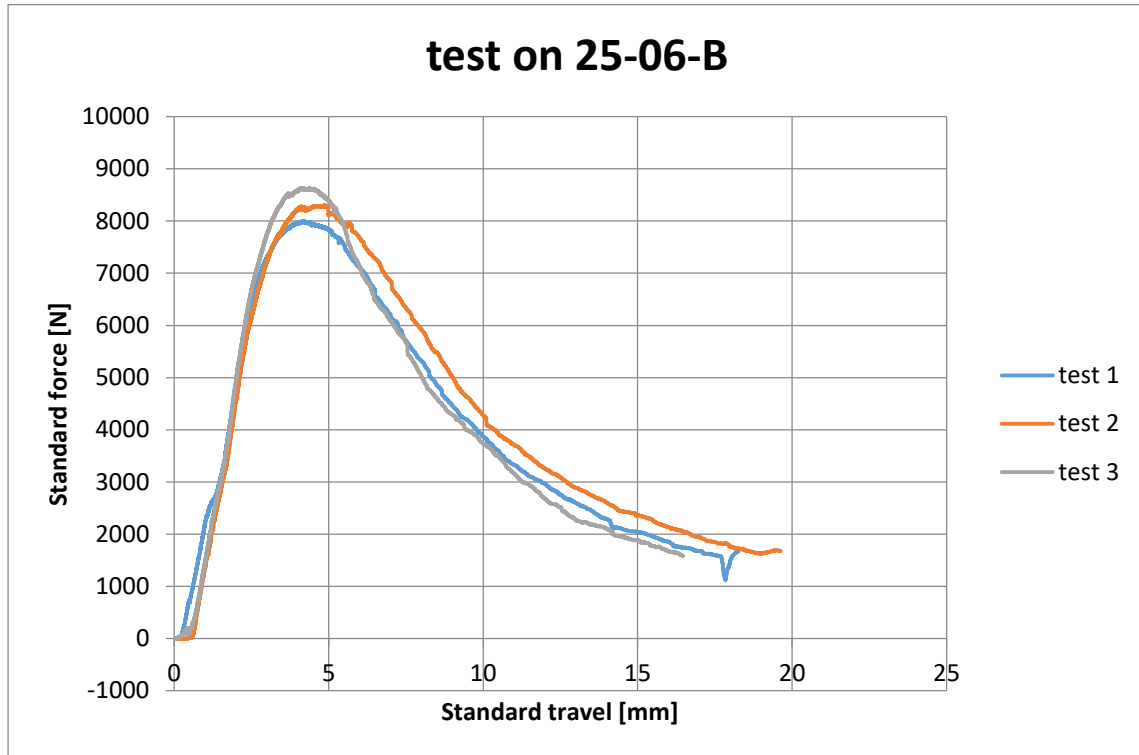
7° series of tests: 18_2:



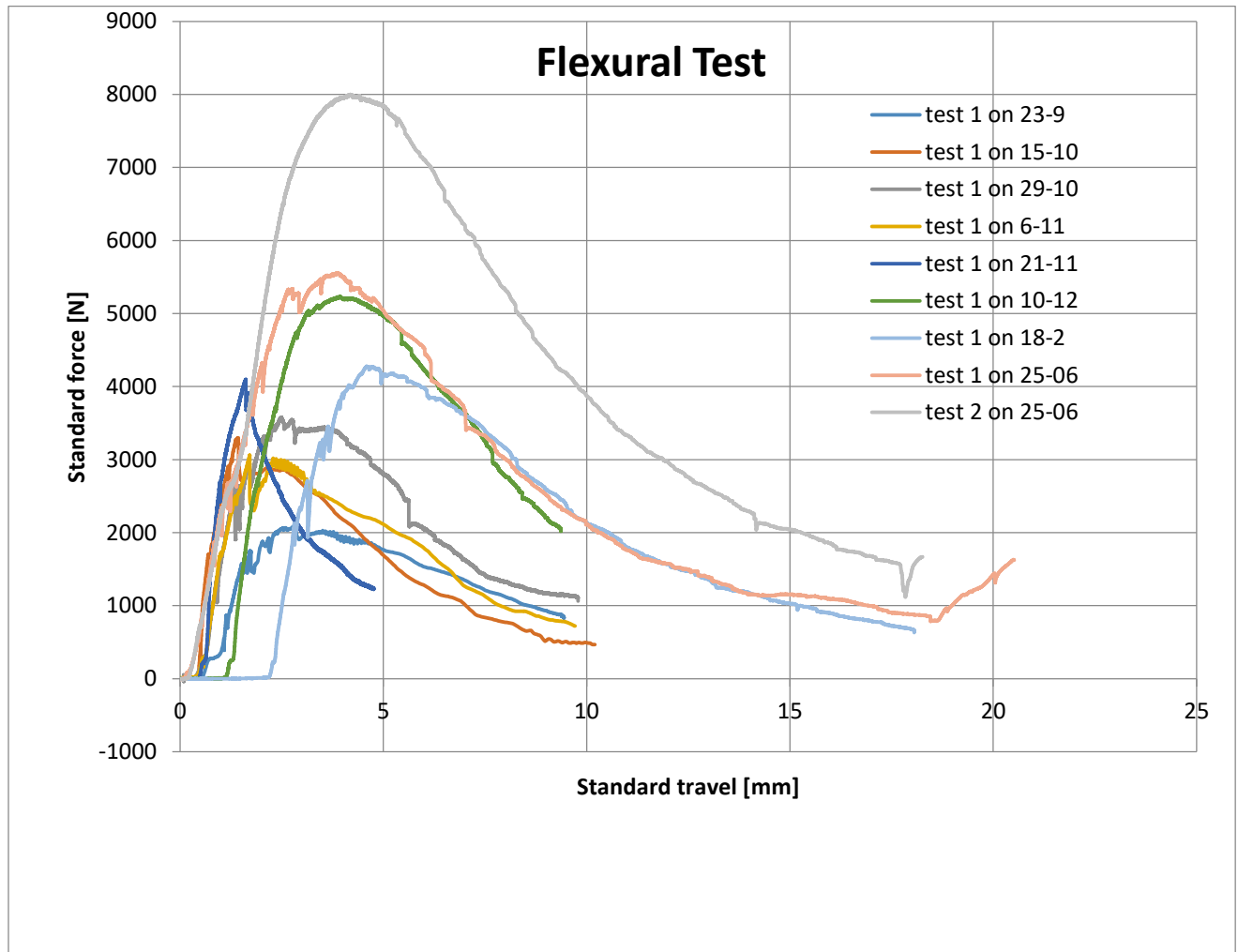
8° series of tests: 25_06-A:



9° series of tests: 25_06-B:



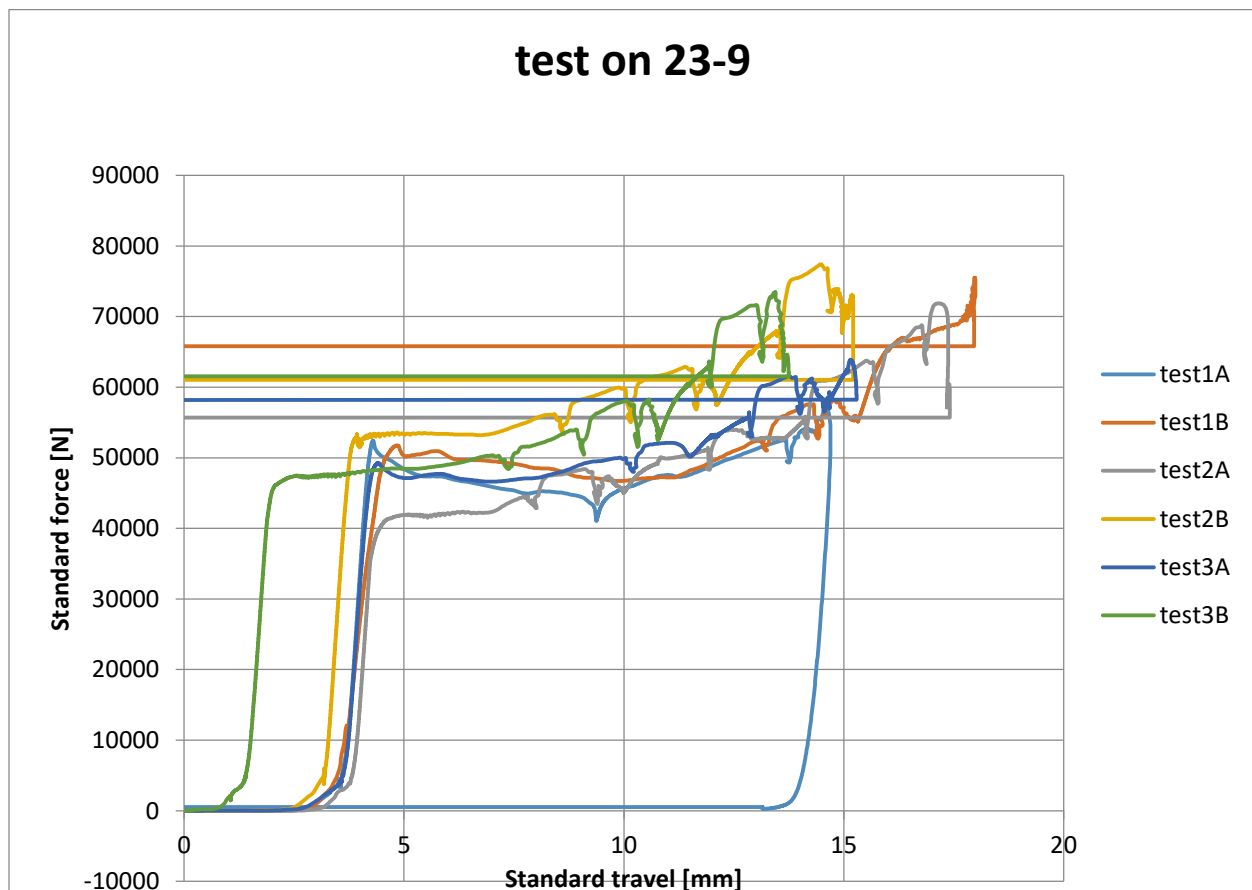
Comparison of test results:



Date	sample number	Pmax(N)	Average	Pcr(N)	Average
test on 23_9	1	2087.3	2433.6	839.0	745.7
	2	2504.8		734.0	
	3	2708.8		664.0	
test on 15-10	1	3299.4	3700.4	1639.0	1952.7
	2	3485.2		2483.0	
	3	4316.5		1736.0	
test on 29-10	1	3573.8	3507.3	1352.0	1800.7
	2	3777.3		2202.0	
	3	3170.9		1848.0	
test on 6-11	1	3058.3	2984.1	1635.0	1703.0
	2	2587.9		1874.0	
	3	3306.0		1600.0	
test on 21-11	1	4095.8	4571.4	2651.0	3231.3
	2	4709.1		3753.0	
	3	4909.3		3290.0	
test on 10-12	1	5230.4	4520.5	2658.0	2445.7
	2	4176.4		2319.0	
	3	4154.8		2360.0	
test On 18-2	1	4276.6	4302.6	2183.0	2047.7
	2	5035.8		2234.0	
	3	3595.5		1726.0	
test On 25-06-A	1	5552.6	4470.6	2654.0	2356.0
	2	3874.0		2382.0	
	3	3985.2		2032.0	
test On 25-06-B	1	7999.8	8308.7	2364.0	3641.3
	2	8297.8		4638.0	
	3	8628.4		3922.0	

5.3: Compressive Test Result

The result of compressive test on 23-9 is reported as a graph. The result of other days is presented in a table which can be seen afterwards. It is worth mentioning that the shape of the graphs are pretty much similar in the compressive mode.



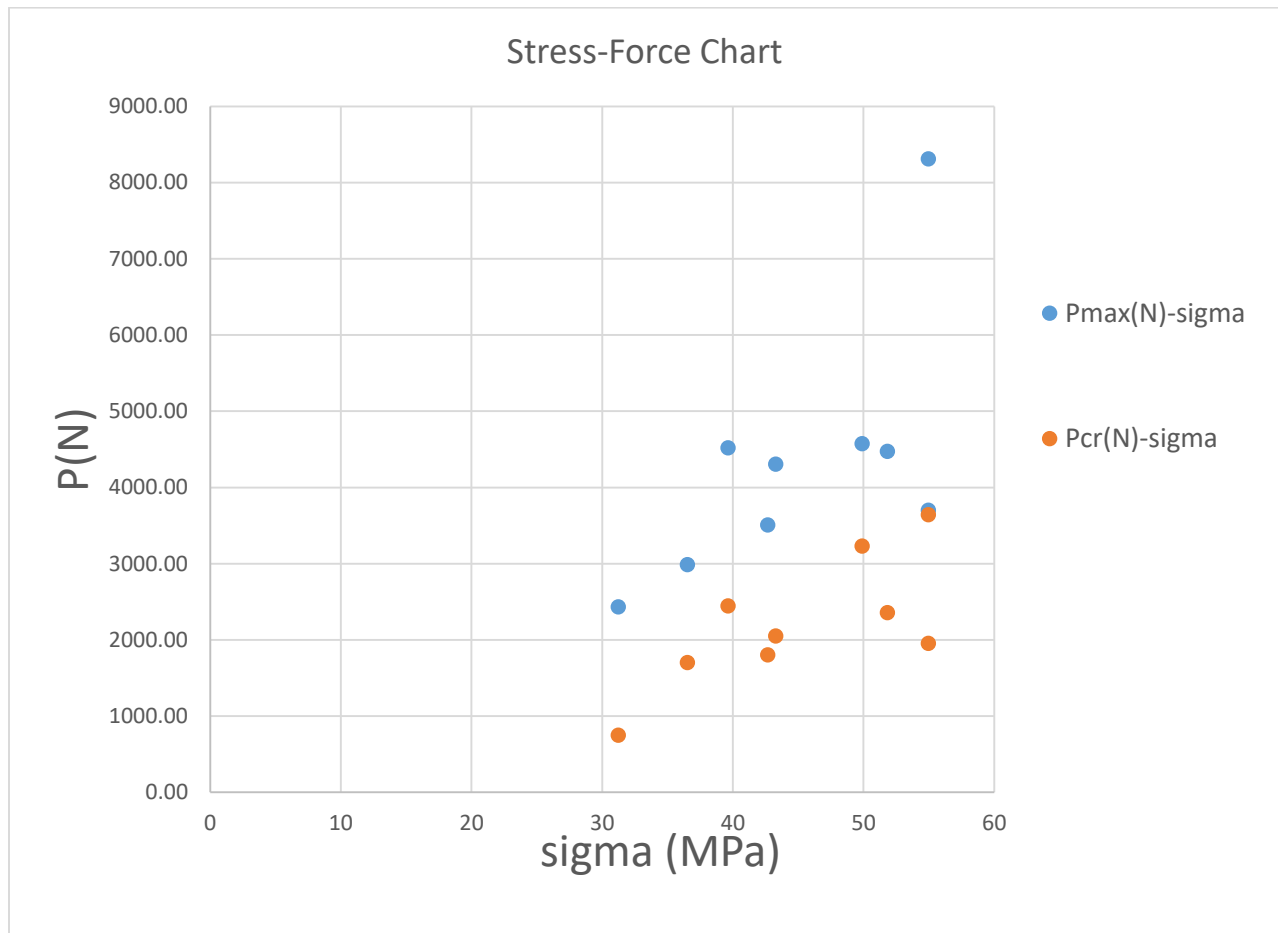
Date	sample number	F _{max} (N)	Average
test on 23_9	1A	57062.7	69882.20
	1B	75495.4	
	2A	71897.9	
	2B	77423.6	
	3A	63892.4	
	3B	73521.2	
test on 15-10	1A	83394	94232.92
	1B	119322.4	
	2A	89062.1	
	2B	95737.2	
	3A	93331.1	
	3B	84550.7	
test on 29-10	1A	65688.3	68283.18
	1B	63931.6	
	2A	66413.3	
	2B	70691.9	
	3A	74003.4	
	3B	68970.6	
test on 6-11	1A	58880.7	72441.98
	1B	73147.6	
	2A	81030.5	
	2B	69892	
	3A	75044	
	3B	76657.1	
test on 21-11	1A	82705	79835.50
	1B	80901.3	
	2A	87853.4	
	2B	79385	
	3A	58640.7	
	3B	89527.6	
test on 10-12	1A	94755.3	77447.37
	1B	69198	
	2A	70112.7	
	2B	87044.9	
	3A	60161.2	
	3B	83412.1	

Date	sample number	F _{max} (N)	Average
test on 18-2	1A	62913.36	69250.99
	1B	70576.46	
	2A	66075.07	
	2B	74125.84	
	3A	78877.14	
	3B	62938.05	
test on 25-06-A	1A	97573.8	82933.86
	1B	81303.3	
	2A	78120.9	
	2B	72456.3	
	3A	100121.7	
	3B	68027.2	
test on 25-06-B	1A	90686.8	87951.33
	1B	89137.2	
	2A	88316.6	
	2B	78523.8	
	3A	74534.9	
	3B	106508.6	

Table 5.2: Compressive Test Result

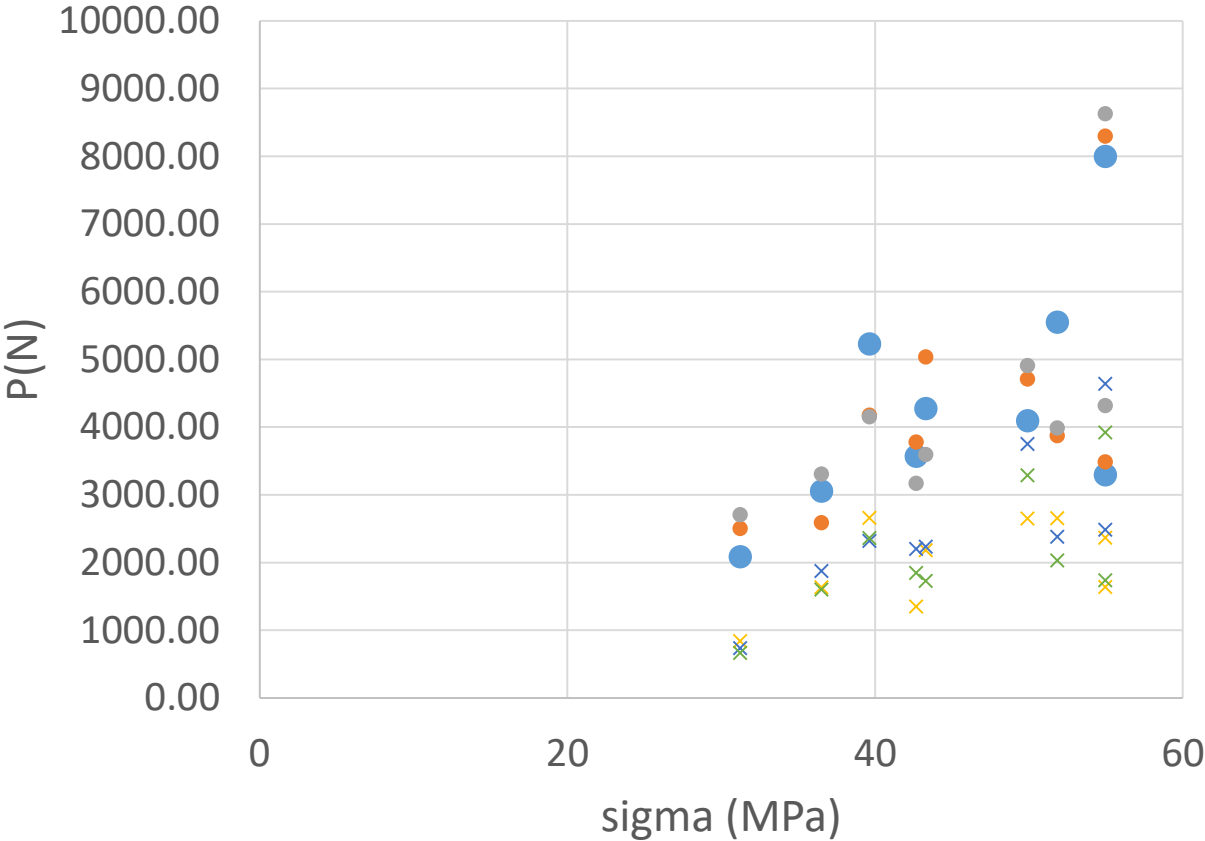
Average results evaluated from compressive test and flexural test can be also represented in one chart. In this case regarding the 3PB test we need to consider the cracking value, and also the maximum value which is estimated in tests. For each mix, we performed 6 different compressive test and average of these values can be used in order to evaluate the value of stress.

Mixes	sigma (MPa)	Pmax(N)	Pcr(N)	(Pmax-Pcr)/Pcr
23_09	31.23	2433.65	745.67	2.26
15_10	54.96	3700.36	1952.67	0.90
29_10	42.68	3507.33	1800.67	0.95
06_11	36.52	2984.06	1703.00	0.75
21_11	49.90	4571.42	3231.33	0.41
10_12	39.64	4520.53	2445.67	0.85
18-02	43.28	4302.65	2047.67	1.10
25-06-A	51.83	4470.61	2356.00	0.90
25-06-B	54.97	8308.66	3641.33	1.28



The previous chart is made up of the average values of the P_{max} and P_{cr} . The complete figure is shown in the next step.

Stress-Force Chart



5.4: Advantageous of Adding Fiber

Several studies and tests performed over the years have demonstrated some important properties, Figure 3 shows the impact of fiber on crack bridging under sectional forces M , V and N .

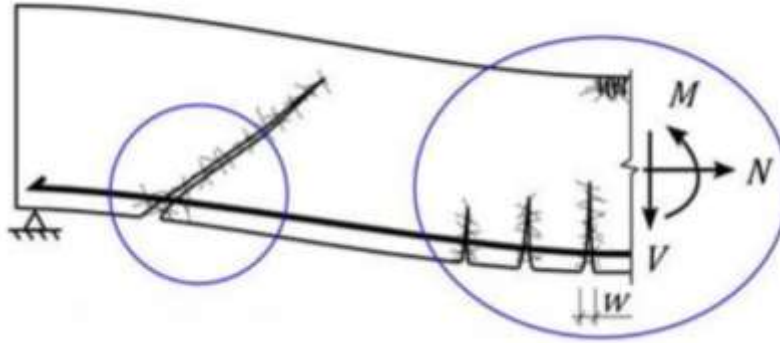


Figure 5.5: Structural Behavior after fiber Addition

Here is a list of positive impacts that adding fiber has on structural behavior of our specimens according to the literature:

- Reduction of crack spacing
- Reduced crack widths
- Increased moment resistance
- Increased flexural stiffness
- Increased ductility in compression
- Enhancing shear resistance
- Enhancement of punching resistance
- Inhibits growth of splitting cracks
- Enhanced confinement of anchored bars
- Increased punching resistance

5.5: Substitution Strategy

Among all different type of industries, concrete is the most used material worldwide. It's roughly annual production passes 10 billion m^3 . The building and development sector in the European countries accounts for around 40% of total energy consumption; moreover, the construction industry in these Countries accounts for about 70% of the total material flow.

Moreover, the concrete industry accounts for huge amount of total anthropogenic CO_2 emissions on a global scale. These facts demonstrate the drastic importance the building sector will offer to sustainability. Consequently, in addition to the initiatives in the production of new building materials, the issue of sustainability has gained more and more attention in the last few years and has become one of the key focuses in the construction materials industry.

A significant potential reduction of concrete's environmental and ecological effect may lie in limited replacement of cement with other materials that can serve as binders. This is of particular importance for what concerns concrete materials with a high cement content, as used for this research by the UHPFRCC.

The tremendous volume of cement used for UHPFRCC is the leading cause of the substantial high environmental effects in this experimental investigation. To assess ecological efficiency, the parameter considered is the amount of CO_2 released during the activities associated with UHPFRCC generation.

Accordingly a substitution strategy for reducing CO_2 emissions will be discussed in the following section.

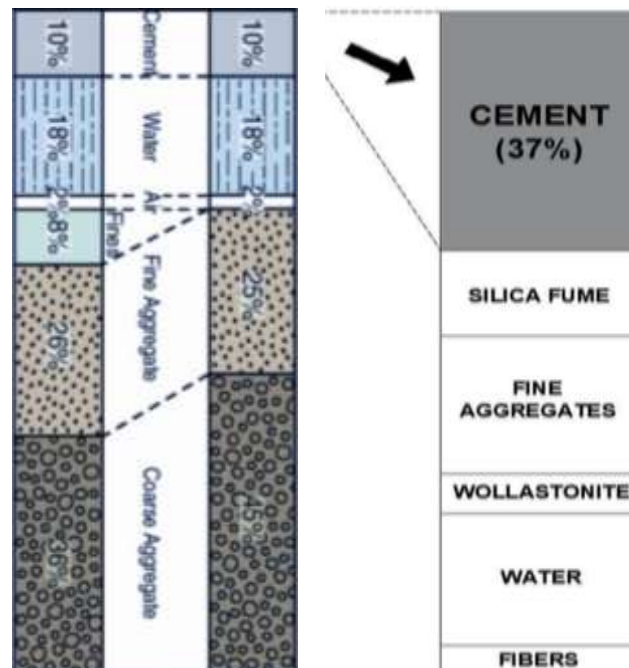


Figure 5.6: Cement ratio increase in HPFRCC mix

According to what mentioned before, we realize that the cement manufacture has a drastic impact on environment. According to this baseline, the material substitution strategy which is shown in Habert and Roussel's work needed to be implied.

As the name of this strategy suggest, it is based on the partially replacement of cement with other materials which have lower impact on environment.

In our experimental phase in one of the tests, some of cement were substituted with fly ash, a waste by-product derived from coal burning. Usage of fly ash in concrete increases the workability of plastic concrete, as well as the strength and durability of hard concrete. Usage of fly ash is also cost-effective. Adding fly ash to concrete can reduce the amount of Portland cement.



Figure 5.7: Fly-ash

As discussed earlier, since fly ash fragments are finer and more spherical than those of Portland cements, the UHPFRCC microstructure is denser and features a low porosity and therefore has excellent durability.

Fly ash is chosen because its CO_2 emissions are much smaller than those of cement and, in addition, fly ash combined with mortar serves as a binder. Even though the major advantage of fly ash lies in minimizing the environmental effect resulting from cement removal, it also offers other advantages such as enhancing concrete workability, enhancing strength, water tightness and concrete longevity at advanced ages.

As mentioned earlier, since fly ash particles are finer and more spherical than those of Portland cements, the HPFRCC micro-structure is denser and features a low porosity and therefore has outstanding durability

Fantilli et al. (2009) examined the effect on cement replacement of a reinforced concrete beam with different mixtures containing equal amount of fly ash. The graph below (Figure 4.5) shows how f_{CA} values can be achieved with different quantities of cement substitution, given varying quantities of CO_2 produced in the atmosphere.

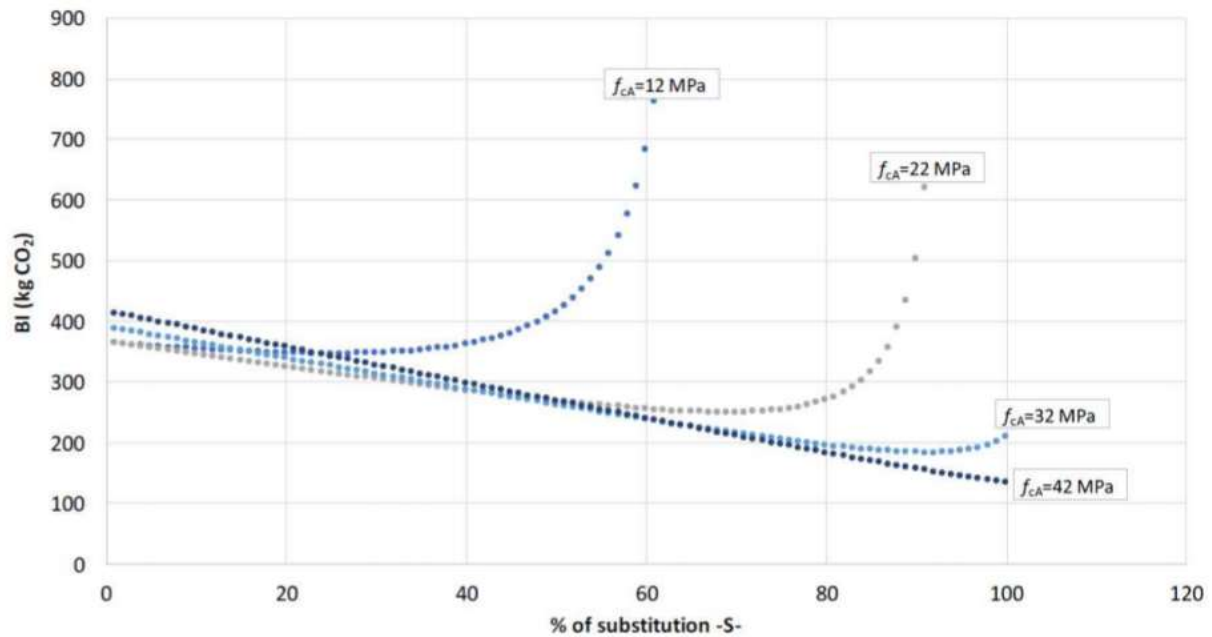


Figure 5.8: impact of substitution strategy to achieve different values of f_{CA}

Result of a previous study indicates a steady decrease in the ecological effect of CO_2 , NO_x , SO_x and PM emissions of mixtures of different percentages of fly ash (Figure 4.6)

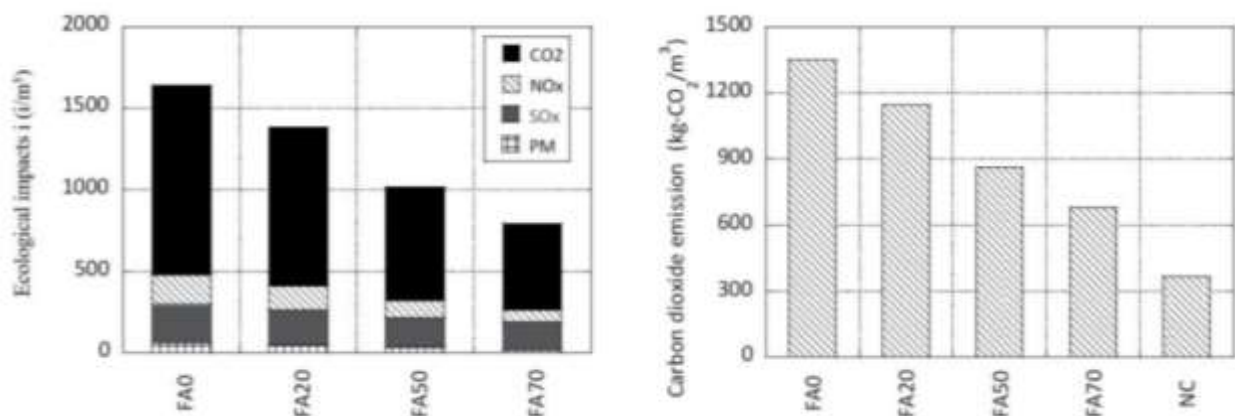


Figure 5.9: emission of greenhouse gasses and carbon footprint of 1 cubic meter of UHPFRCC

Chapter 6 Analysis of Results

6.1: Mechanical Parameters

The Young's modulus and the Poisson's ratio are two crucial mechanical parameters for evaluation and characterization of the cement composites. It is necessary to estimate the value of these two parameters, regarding the mechanical evaluation of different mixes.

➤ Young's Modulus (E_{cm})

According to different formulas which are presented in literature, the value of young's modulus is dependent on the compressive strength of concrete. This rule is stating also for the HPFRCC.

However, in normal concrete, the compression young's modulus is fundamentally dependent on the mechanical properties of the cement matrix and is not affected by the properties of the aggregates; in high-performance fiber-reinforced cement composites it can also be substantially dependent on the mechanical properties of the aggregates, due to the high strength of the matrix. This statement is what we want to investigate in this part of our work.

An empirical relation which is prepared by Euro-code 2 permit to evaluate the value of modulus.

$$E_{cm} = 22000 \left(\frac{f'_c}{10} \right)^{0.3}$$

The value of young's modulus in this formula is dependent on the maximum compressive strength (f'_c), expressed in (MPa), which is estimated from the test results.

➤ Poisson ratio

The definition of the Poisson ratio is defined as the division of transverse contraction strain to longitudinal extension strain in the direction of the applied load.

$$\nu = - \frac{\epsilon_t}{\epsilon_l}$$

ϵ_t : Transverse strain (m/m)

ϵ_l : Longitudinal strain (m/m)

Considering our case study the evaluation of transvers strain was not possible. So we just estimated the longitudinal strain in order to also have a preliminary evaluation considering this aspect. It is worth mentioning this is not a specific parameter which we can rely on, but considering the testing properties that we faced, is the only possible option.



Figure 6.1: specimens after compressive test

As it is obvious in the figure measurement of transverse strain doesn't have any sense and the result of this type of measurements is not reliable.

The parameter which we want to evaluate instead of the Poisson ratio is the longitudinal strain which as we estimated is showing an unstable behavior. We need to point that according to the code rules, before performing compressive test on our specimens, we performed the tensile 3PB test. So this can be a factor in not having a so stable and steady result. In the next table we evaluated the values of elastic modulus and also longitudinal strain.

Date	sample number	F _{max} (N)	f _c (Mpa)	E _{cm} (Mpa)	mean E _{cm} (Mpa)
test on 23_9	1A	57062.7	33.41	31.59	33.63
	1B	75495.4	44.20	34.36	
	2A	71897.9	42.40	33.93	
	2B	77423.6	45.66	34.70	
	3A	63892.4	38.18	32.88	
	3B	73521.2	43.93	34.30	
test on 15-10	1A	83394.0	50.15	35.69	36.88
	1B	119322.4	71.76	39.74	
	2A	89062.1	53.19	36.32	
	2B	95737.2	57.18	37.12	
	3A	93331.1	55.32	36.75	
	3B	84550.7	50.12	35.68	
test on 29-10	1A	65688.3	40.65	33.51	33.83
	1B	63931.6	39.56	33.24	
	2A	66413.3	40.80	33.55	
	2B	70691.9	43.43	34.18	
	3A	74003.4	45.29	34.61	
	3B	68970.6	42.21	33.89	
test on 6-11	1A	58880.7	36.94	32.56	34.25
	1B	73147.6	45.83	34.74	
	2A	81030.5	48.24	35.27	
	2B	69892.0	41.61	33.74	
	3A	75044.0	44.74	34.49	
	3B	76657.1	45.70	34.71	
test on 21-11	1A	82705.0	48.29	35.28	34.97
	1B	80901.3	47.11	35.02	
	2A	87853.4	51.98	36.07	
	2B	79385.0	47.47	35.10	
	3A	58640.7	34.86	32.00	
	3B	89527.6	53.22	36.33	
test on 10-12	1A	94755.3	59.22	37.51	35.22
	1B	69198.0	43.25	34.14	
	2A	70112.7	43.82	34.27	
	2B	87044.9	54.40	36.57	
	3A	60161.2	37.60	32.73	
	3B	83412.1	52.13	36.10	
test on 18-2	1A	62913.4	39.32	33.17	34.12
	1B	70576.5	44.11	34.34	
	2A	66075.1	41.30	33.67	
	2B	74125.8	46.33	34.85	
	3A	78877.1	49.30	35.50	
	3B	62938.0	39.34	33.18	

Date	sample number	F_{\max} (N)	f'_c (Mpa)	E_{cm} (Mpa)	mean E_{cm} (Mpa)
test on 25-06-A	1A	97573.8	77.65	40.69	38.67
	1B	81303.3	64.70	38.52	
	2A	78120.9	62.17	38.06	
	2B	72456.3	57.66	37.21	
	3A	100121.7	79.67	41.00	
	3B	68027.2	54.13	36.51	
test on 25-06-B	1A	90686.8	72.17	39.80	39.39
	1B	89137.2	70.93	39.60	
	2A	88316.6	70.28	39.49	
	2B	78523.8	62.49	38.12	
	3A	74534.9	59.31	37.53	
	3B	106508.6	84.76	41.77	

Table 6.1: Mechanical parameters evaluation

One point which I necessary for us to mention in this point is that the value which is considered as the failure for the compressive tests, is not equal to the maximum value which is gained from the tests. The reason is that after the failure we usually have a post-peak part which shows a hardening behavior. Due to that the maximum value of the compressive test can't be considered as the failure value.

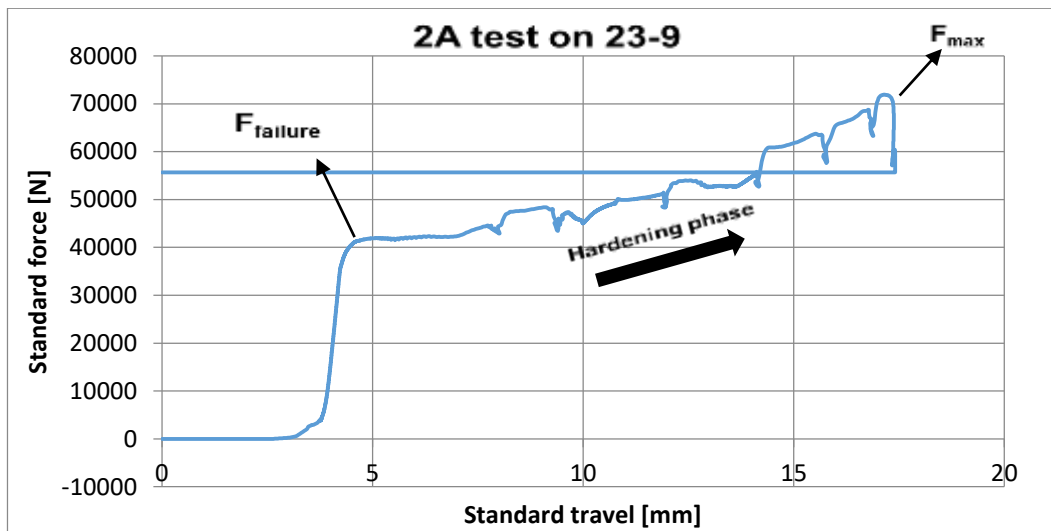


Figure 6.2: Hardening post-peak behavior

As it is represented in the previous figure after the failure, which is the first peak, the specimens is hardened. This hardening behavior leads to a second peak which is higher than the first one. There is also another case which the specimen after the failure doesn't show a hardening behavior.

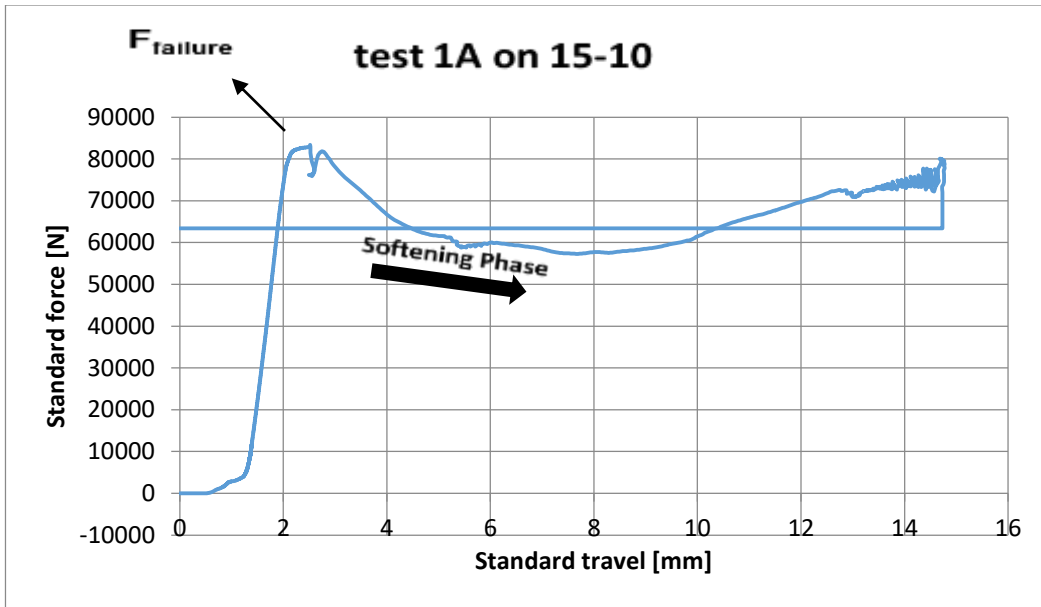


Figure 6.3: softening post-peak behavior

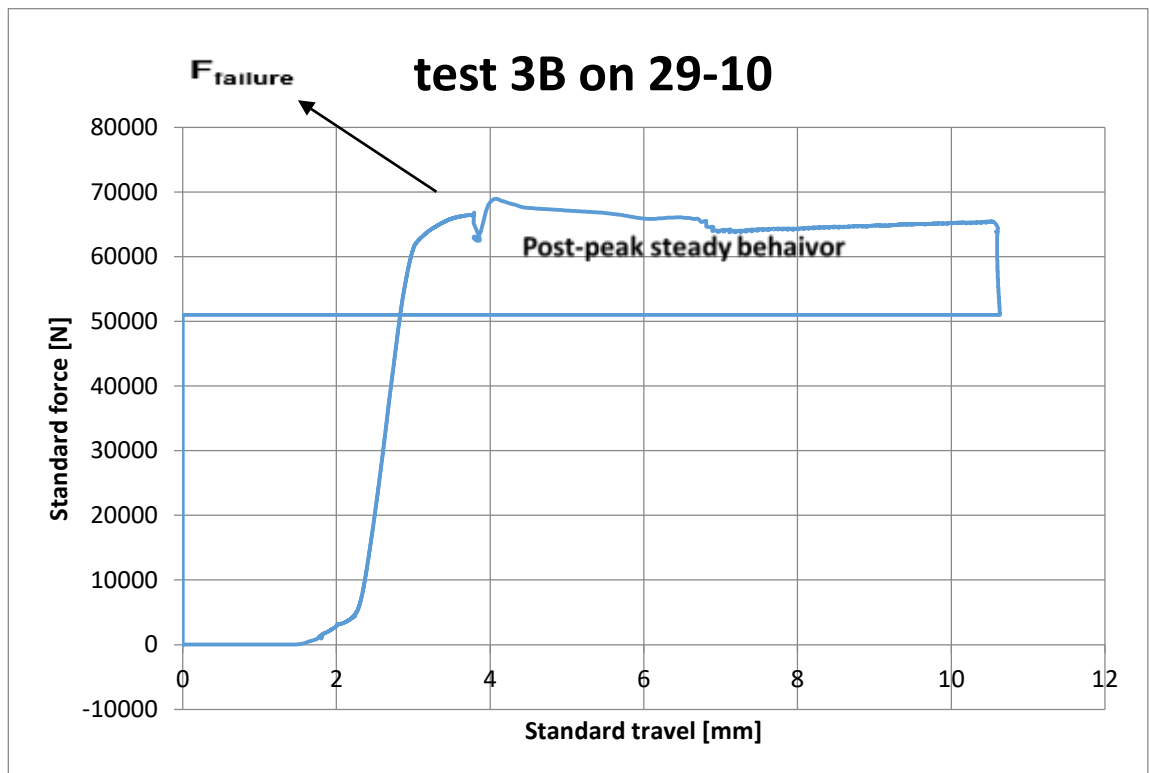


Figure 6.4: steady post-peak behavior

Here in this case after the failure we will face a steady tail and the specimen shows a stable behavior.

The young's modulus can also be represented in the format of a graph.

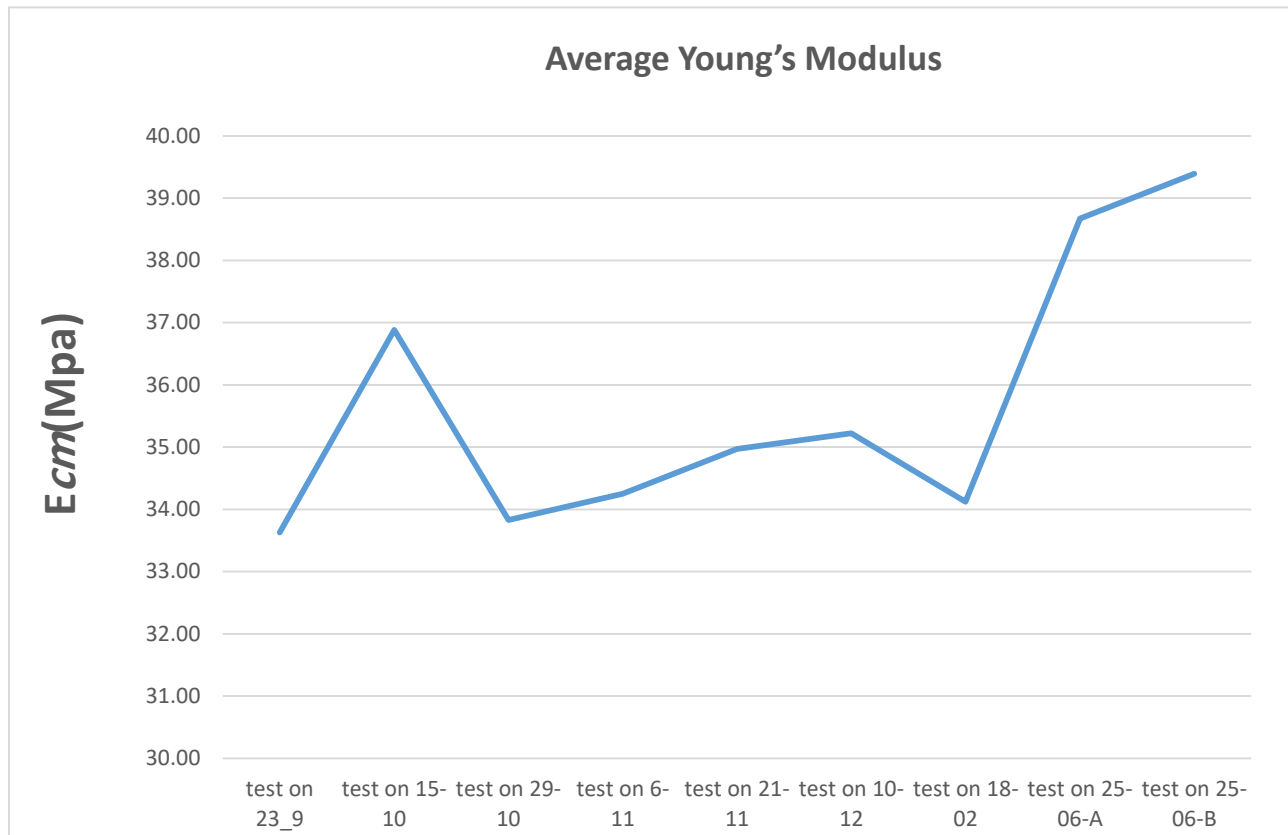


Figure 6.4: Average Young's Modulus

6.2: Ductility of HPFRCC

A material's ductility is a physical property that demonstrates its ability to deform under load by exhibiting plastic deformations before breaking: the greater the plastic deformation accomplished before breaking, the more ductile the material is. Moreover, the structure's ability to bear stresses derived from a telluric event without collapse depends on its ability to dissipate the created energy.

From these considerations can be evaluated a basic principle of the design approach of structures in seismic regions: the structures must have high deformation resources beyond their own elastic limits to withstand without totally or partially collapsing to high-intensity earthquakes.

As previously expected, one of HPFRCC's main characteristics is the ability to withstand loads long before the break is reached, above all due to the role played by steel fibers. The main added benefit that the fibers offer is the improvement of the ductility in the phase following the first cracking phenomenon.

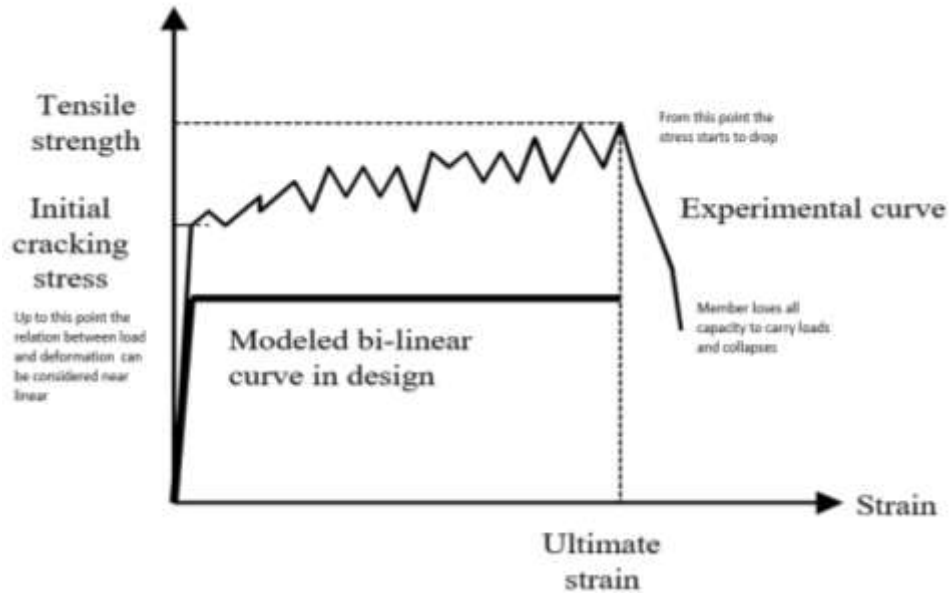
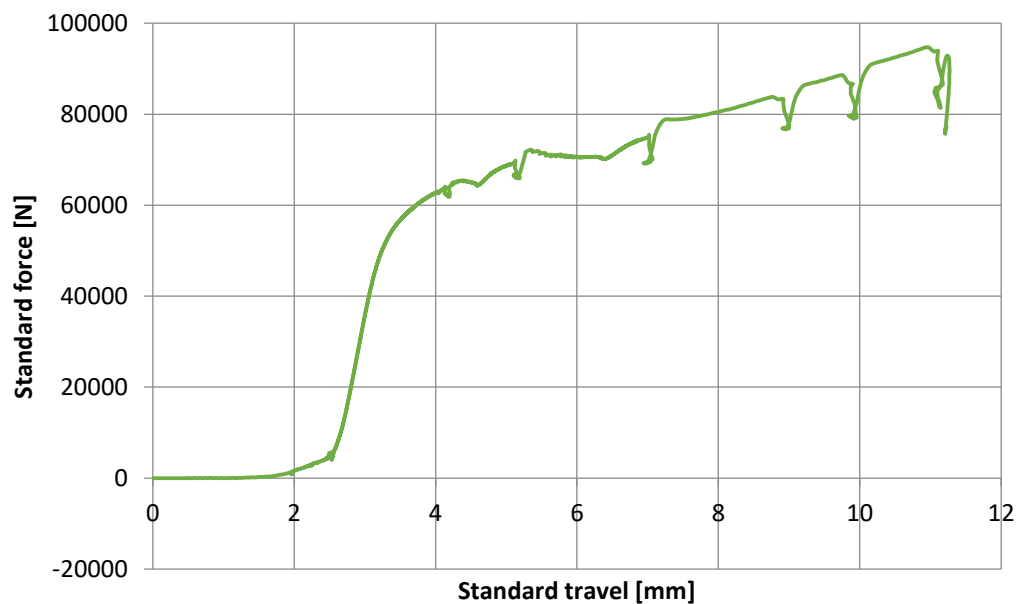
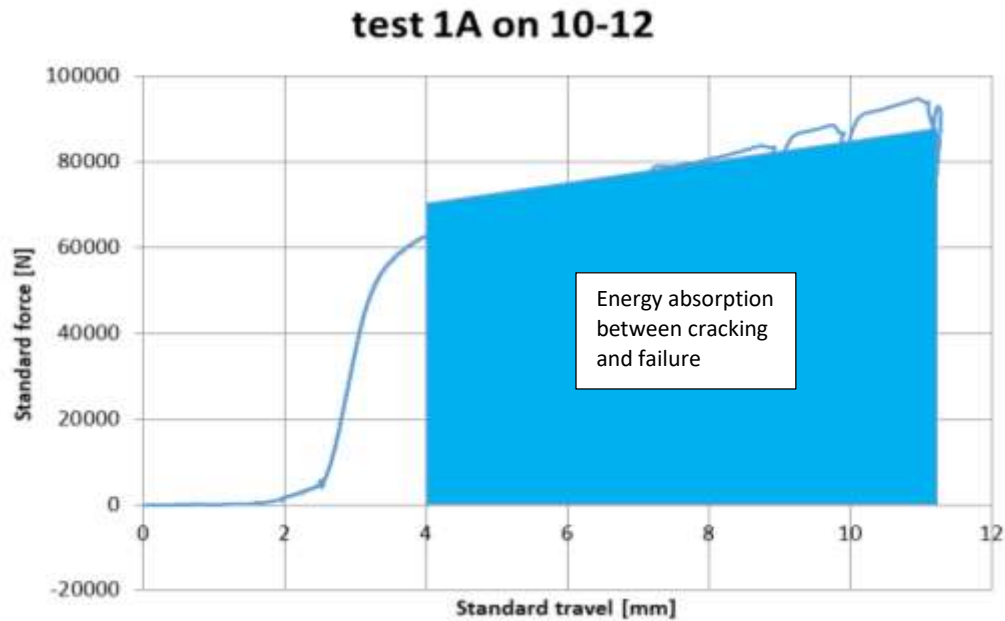


Figure 5.5: Ductile behavior of HPFRCC

It is obvious that enormous amount of energy is dissipated after the initial cracking. As an example when we have a hardening tail after first cracking which is accompanied by multiple cracking, the energy which is dissipated during this part is considerable and can lead to a ductile behavior of our mix.

test 1A on 10-12





6.3: Practical assessment of the Ecological performances

As mentioned in Chapter 1.7, cement composites are the key factor of environmental pollution and a significant reduction in this ecological impact may be due to partial replacement of cement with fly ash, which is more eco-friendly. The parameter that is needed to be considered for assessing the ecological performance is the amount of CO_2 generated during the production of 1 m^3 HPFRCC.

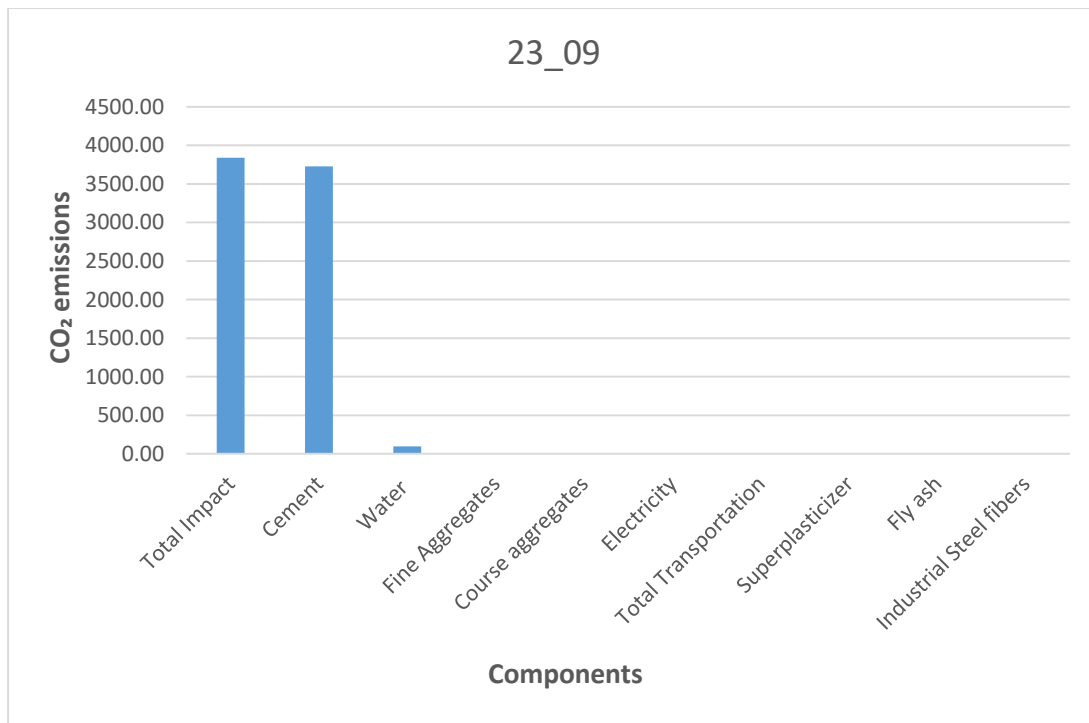
	Carbon footprint
	kgCO_2/ton
Normal Portland Cement	830
Industrial Steel fibers	1500
Recycled fibers	0
Fly ash	29
Silica sand	4,9
Water	34,8
Super-plasticizer	150

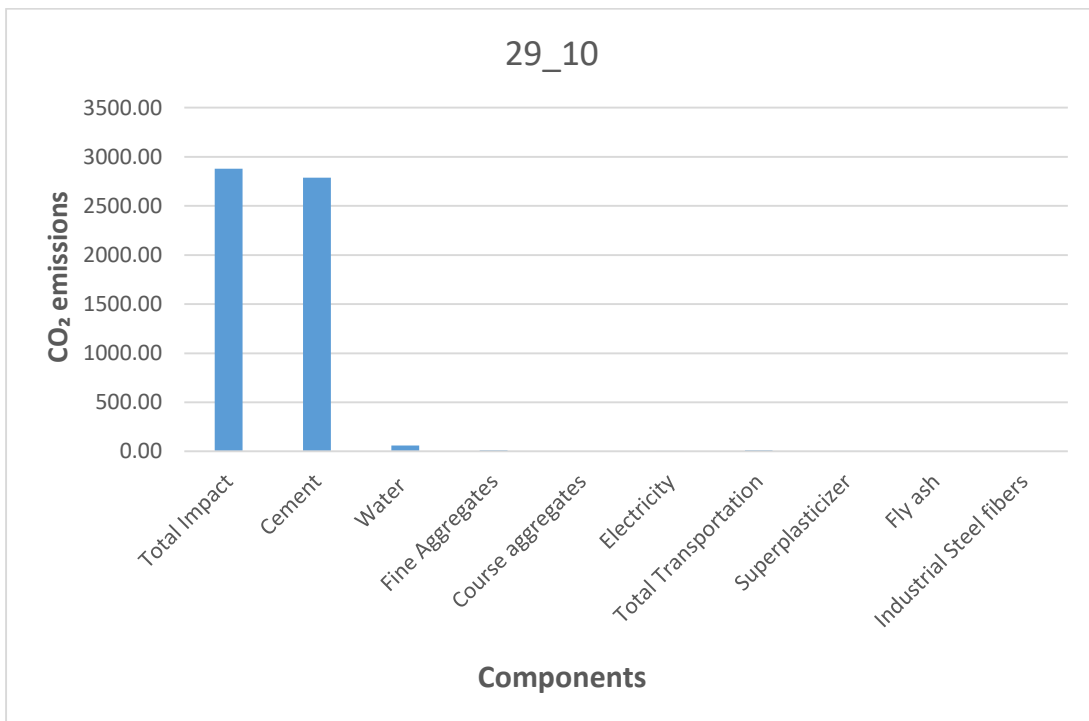
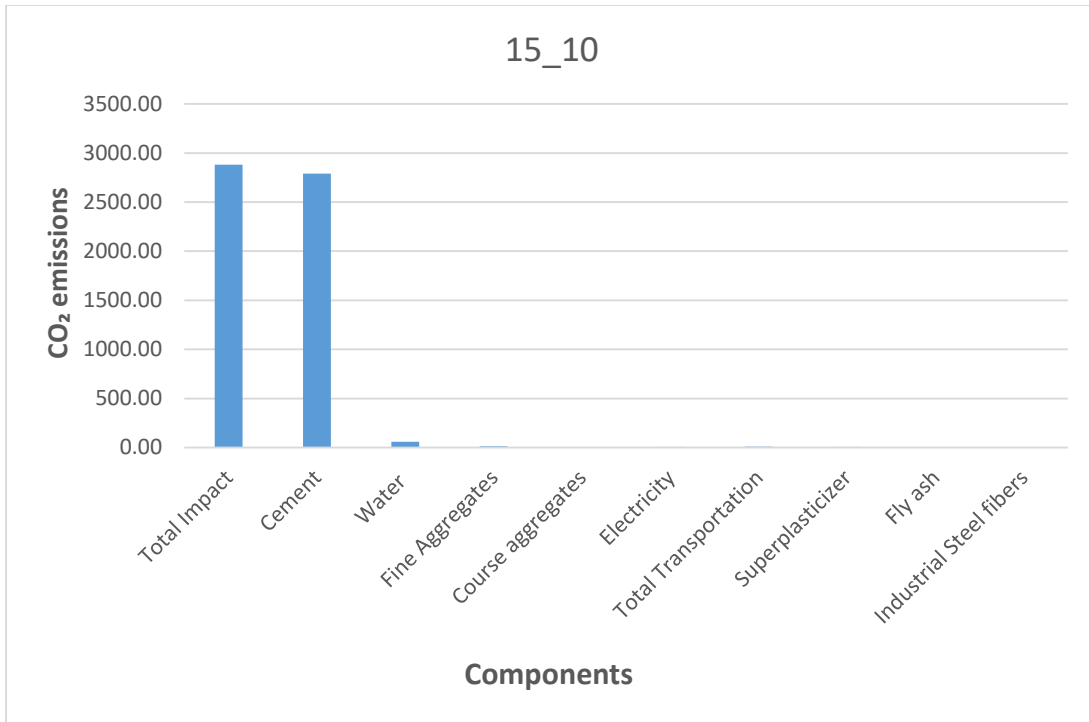
Table 6.2: Carbon footprint of used materials

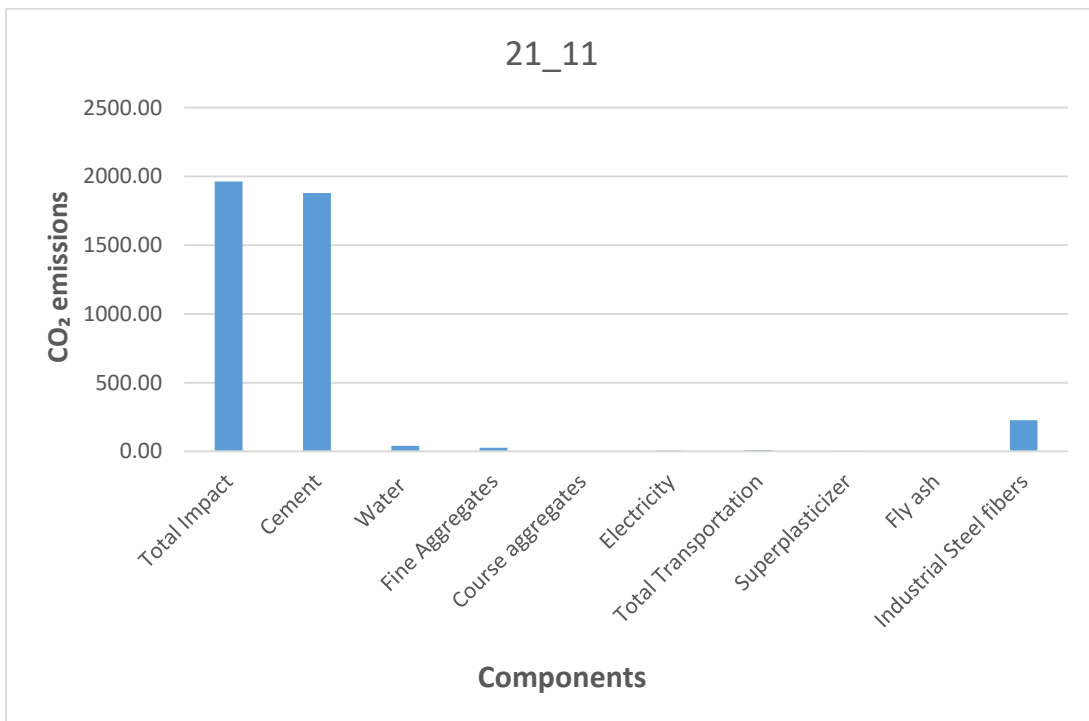
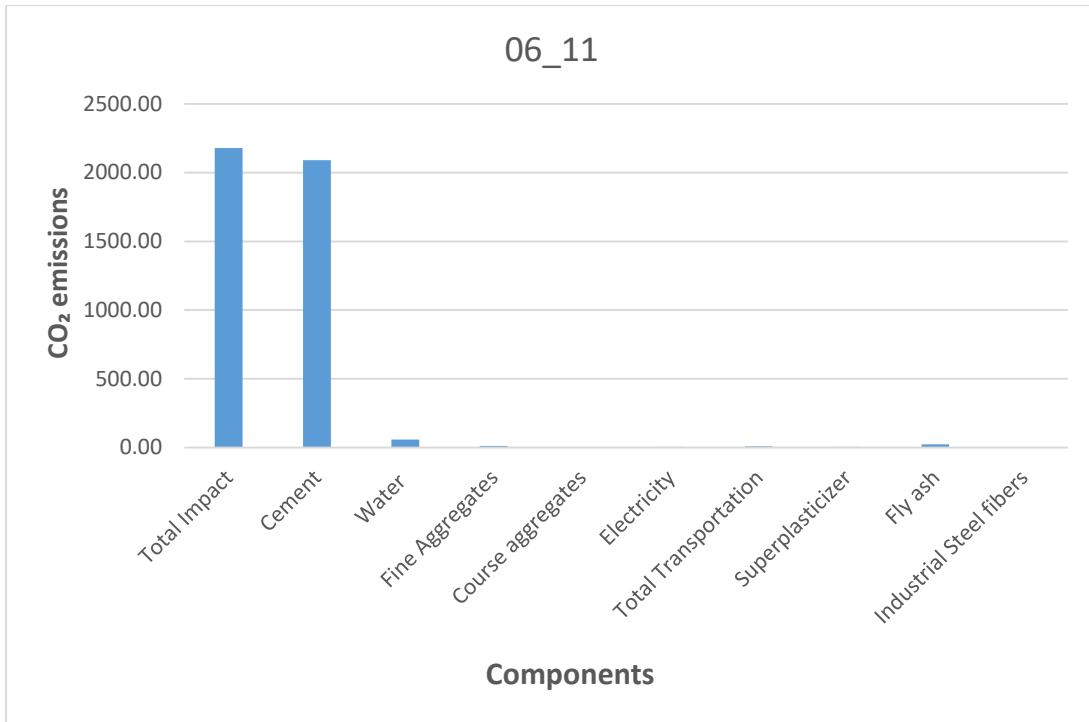
Mixes	Density	Total Impact	Reduction CO ₂
23_09	6242.71	2376.90	-84.56%
15_10	6623.44	1826.67	-41.84%
29_10	6766.12	1818.90	-41.23%
06_11	6218.47	1374.14	-6.70%
21_11	6158.24	1287.87	0.00%
10_12	6080.93	1374.14	-6.70%
18-02	6180.28	1374.14	-6.70%
25-06-A	5890.10	1247.87	3.11%
25-06-B	5462.88	1247.87	3.11%

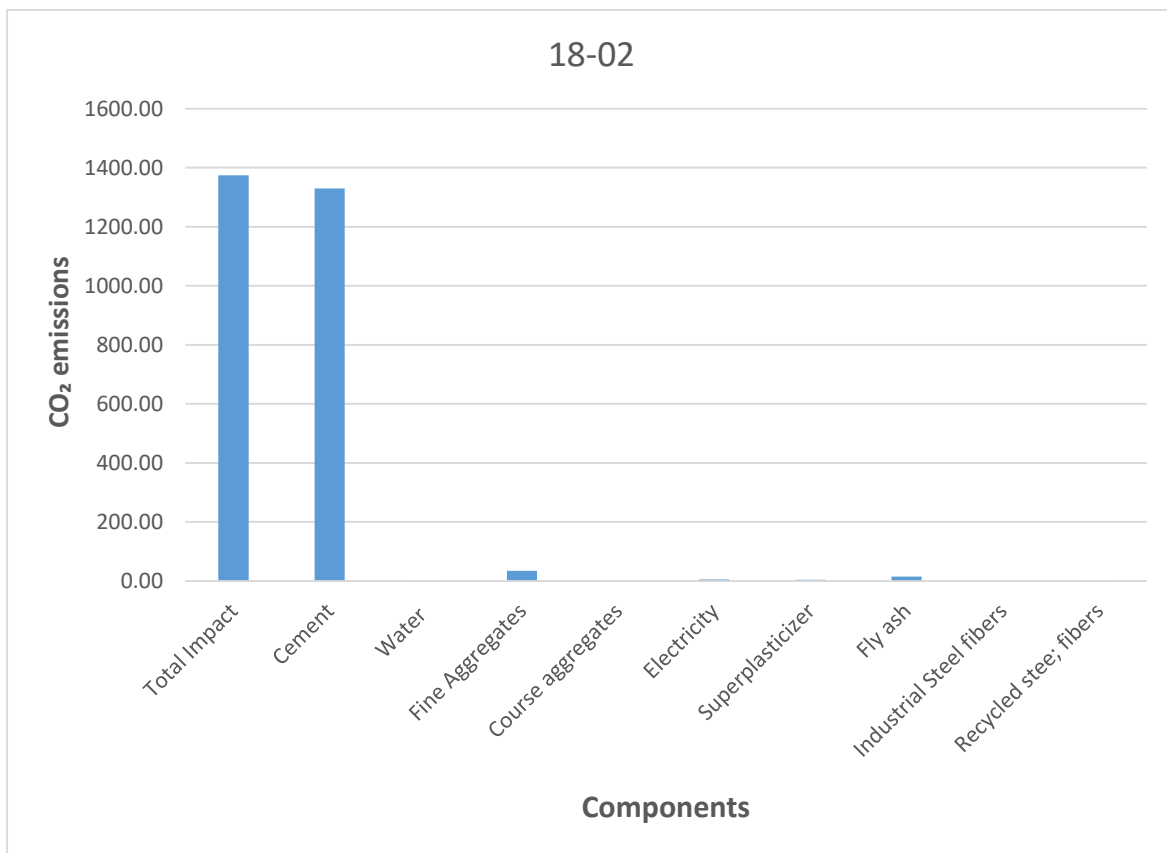
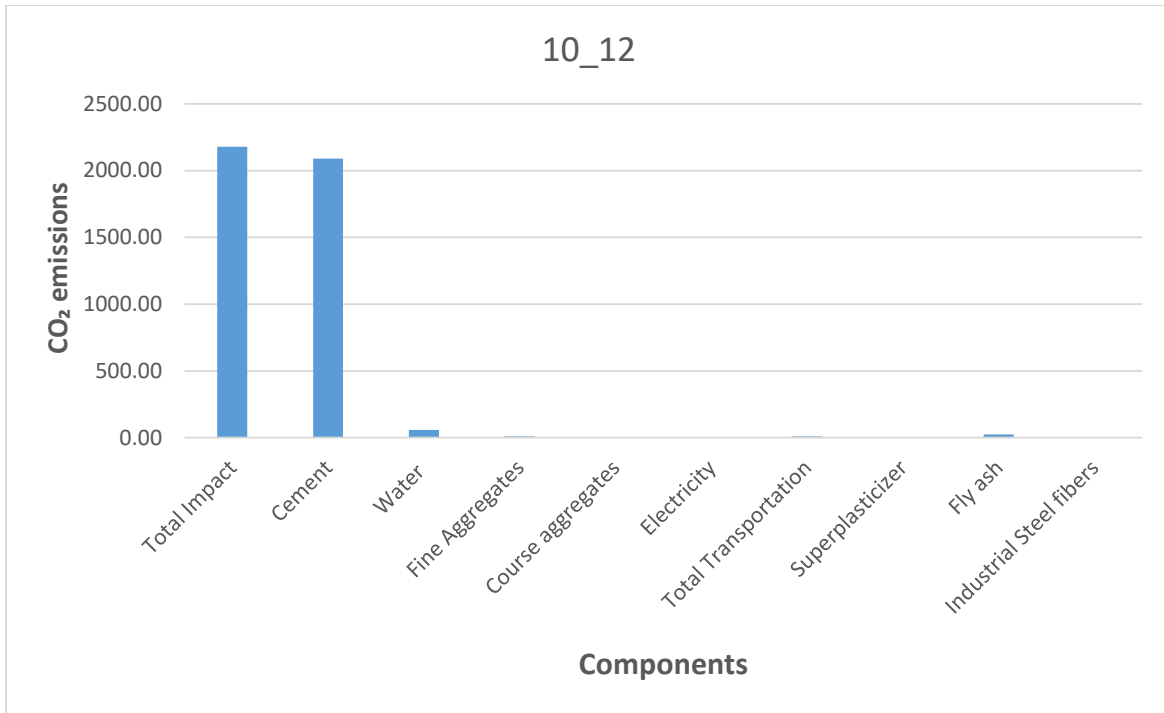
Table 6.3: CO₂ emission of HPFRCC

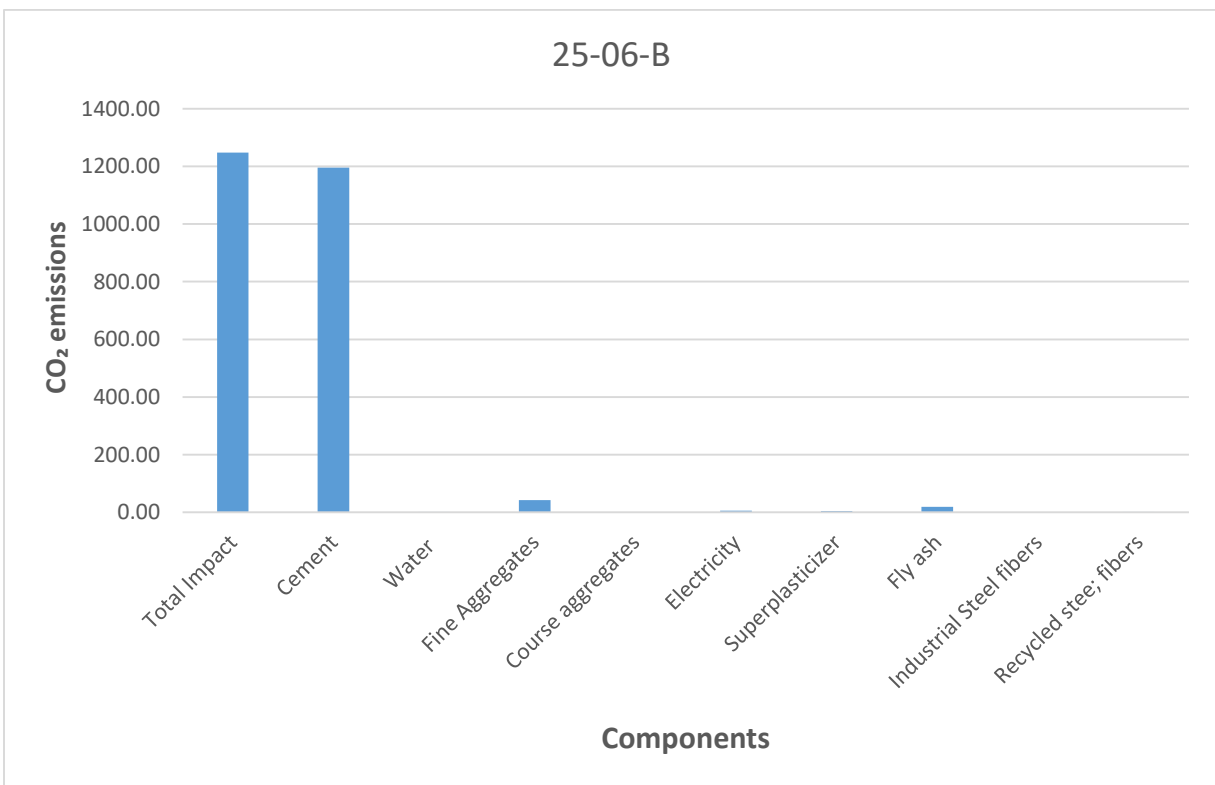
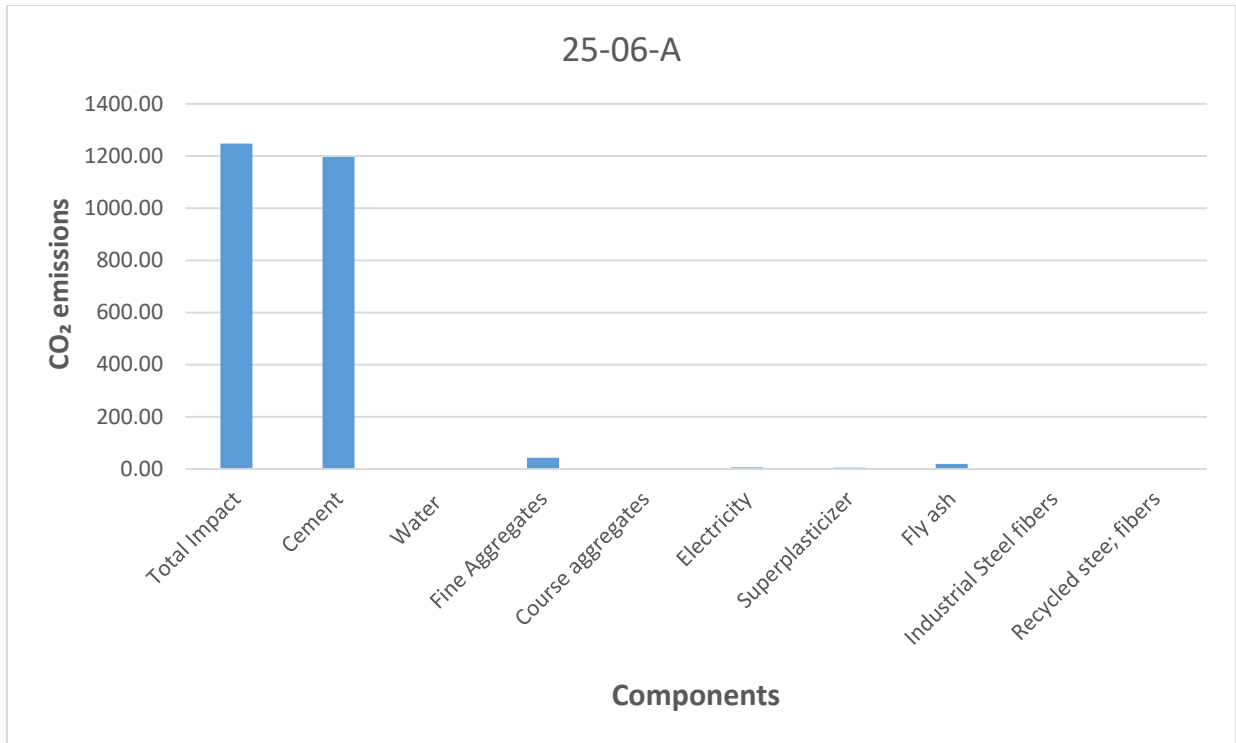
In the following chart the evaluated value of CO₂ emission is investigated for every mix.











In the next part for the evaluation of embodied energy it is necessary to have a data base. As it is mentioned before, the embodied energy (carbon) of a building material can be taken as the total primary energy consumed (carbon released) over its life cycle. Ideally, the boundaries of the life cycle would be set from the extraction of raw materials until the end of the product life time (including energy form manufacturing, transport, maintenance, disposal etc.), there by following the approach “from cradle to grave”.

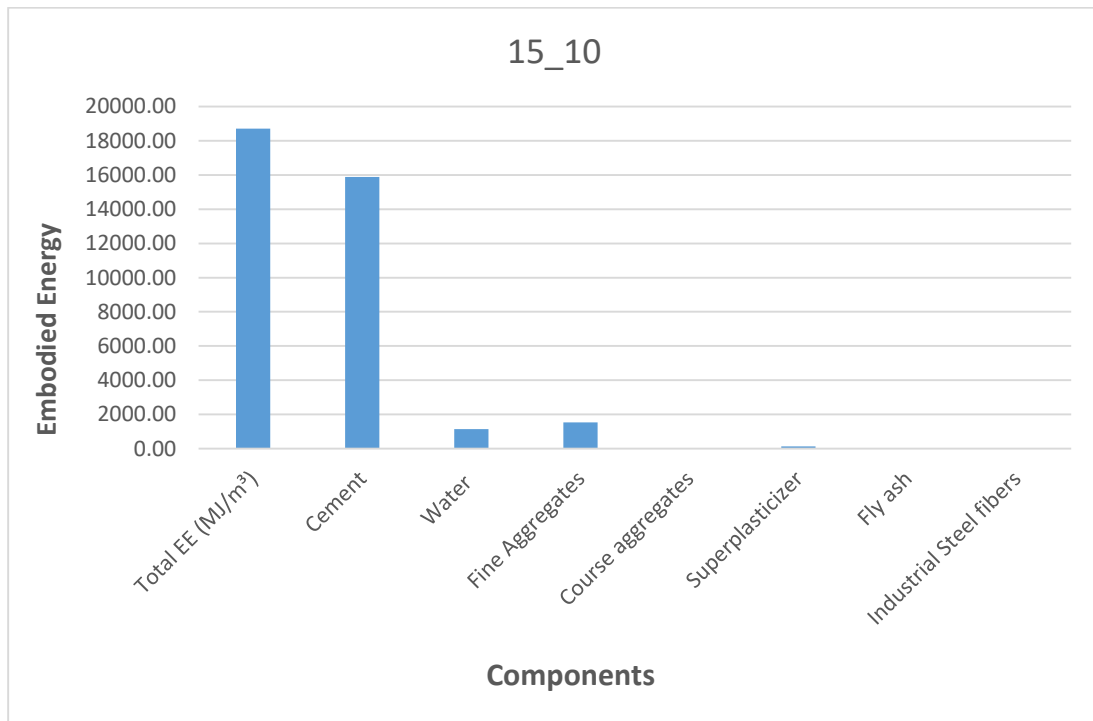
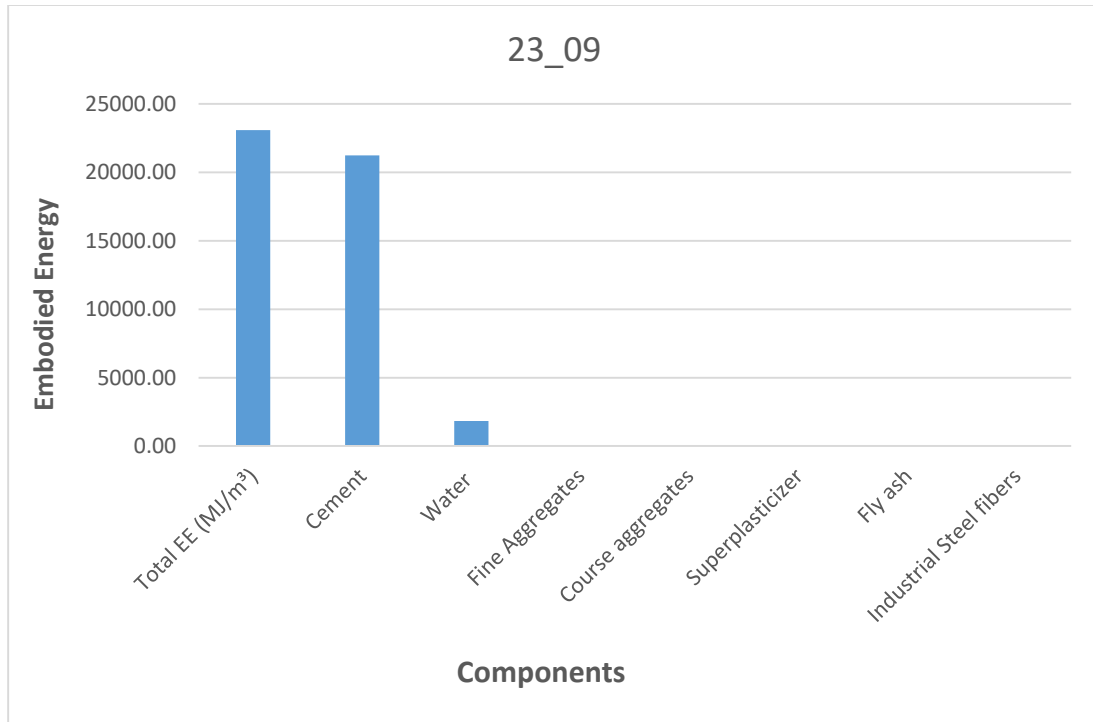
	Embodied energy
	MJ/kg
Normal Portland Cement	4.73
Industrial Steel fibers	20.6
Recycled fibers	0
Fly ash	0.93
Silica sand	0.58
Water	0.68
Super-plasticizer	3.68

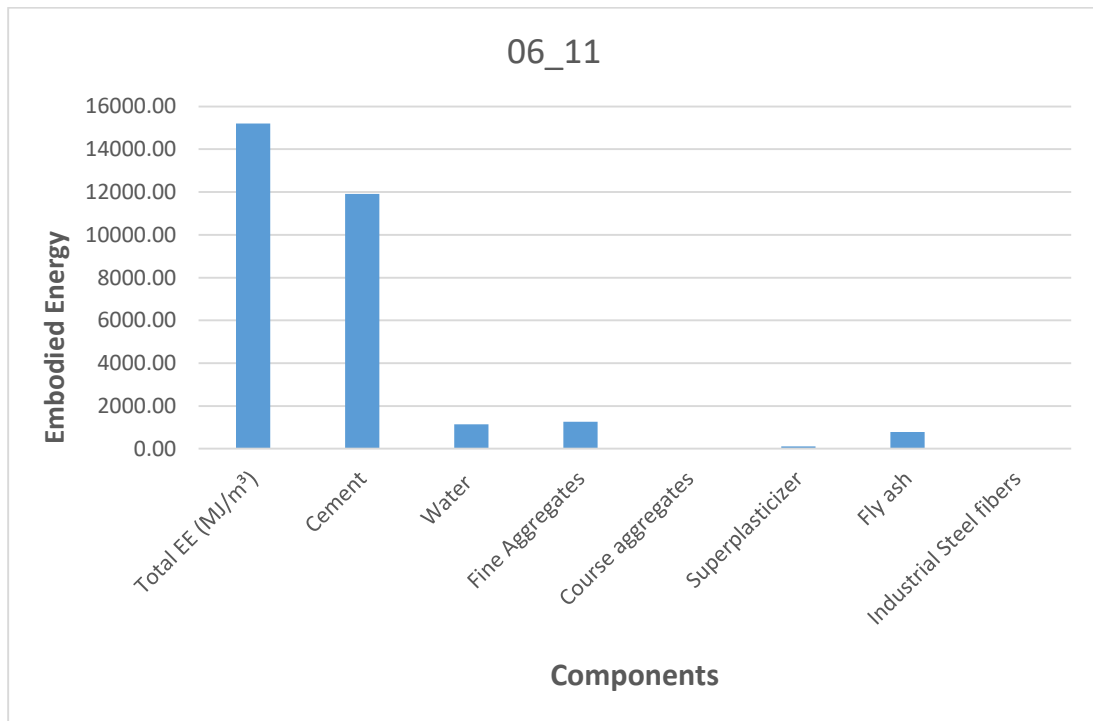
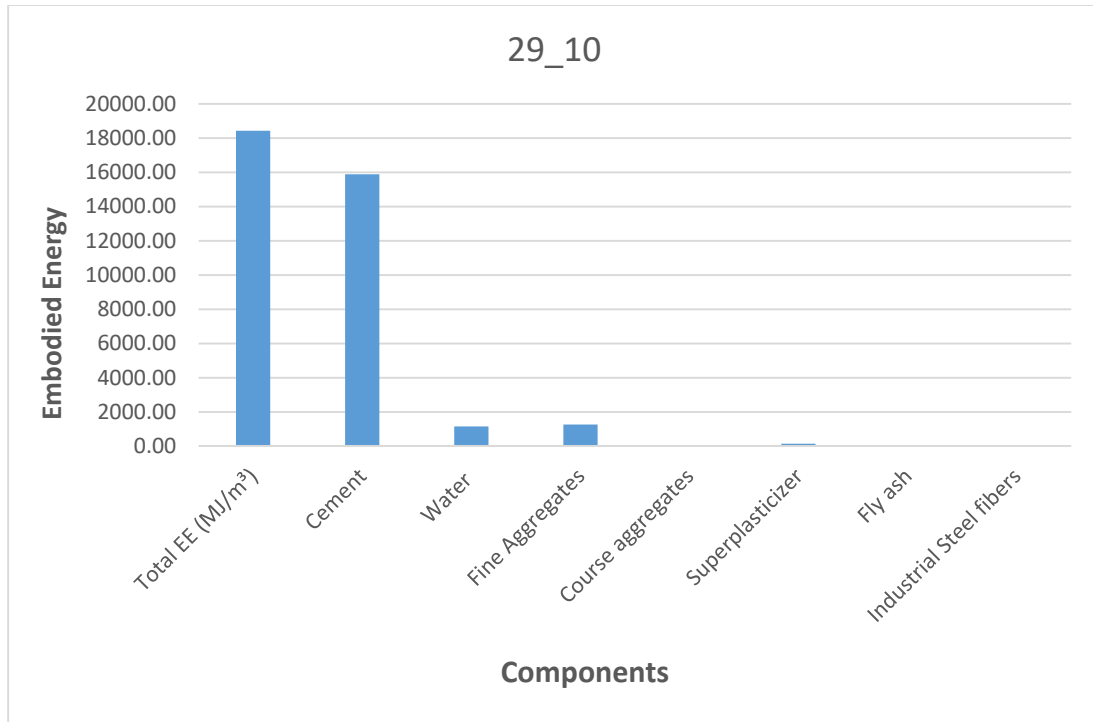
Table 6.4: Embodied energy of different components

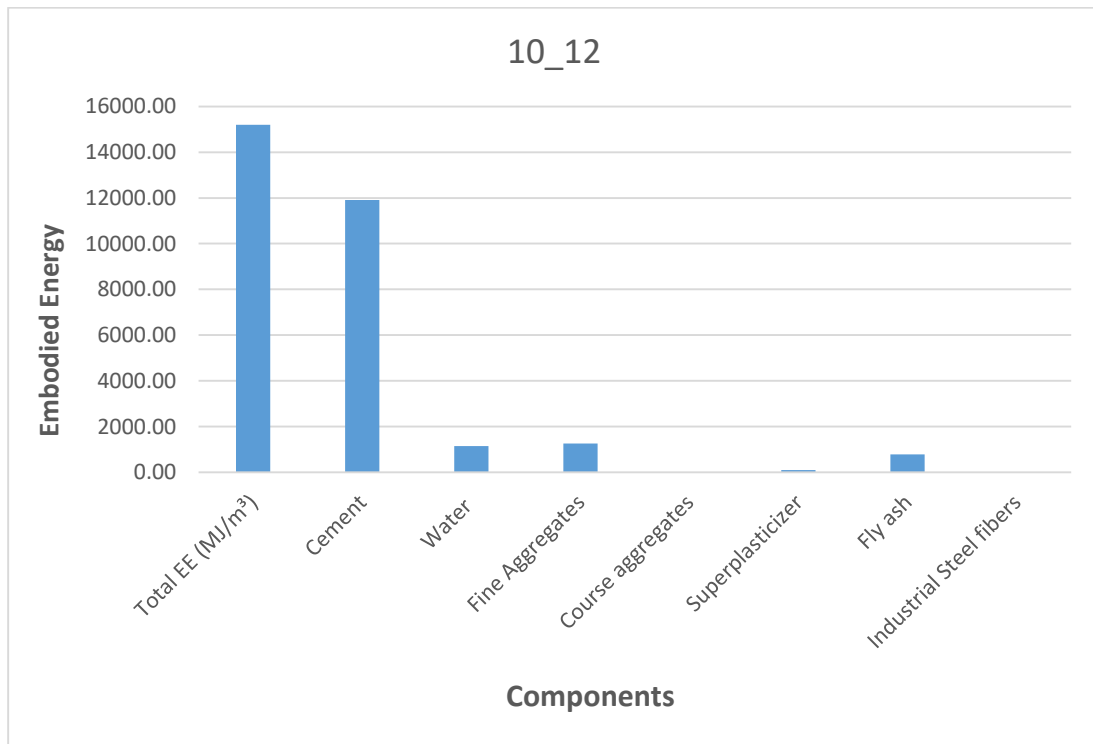
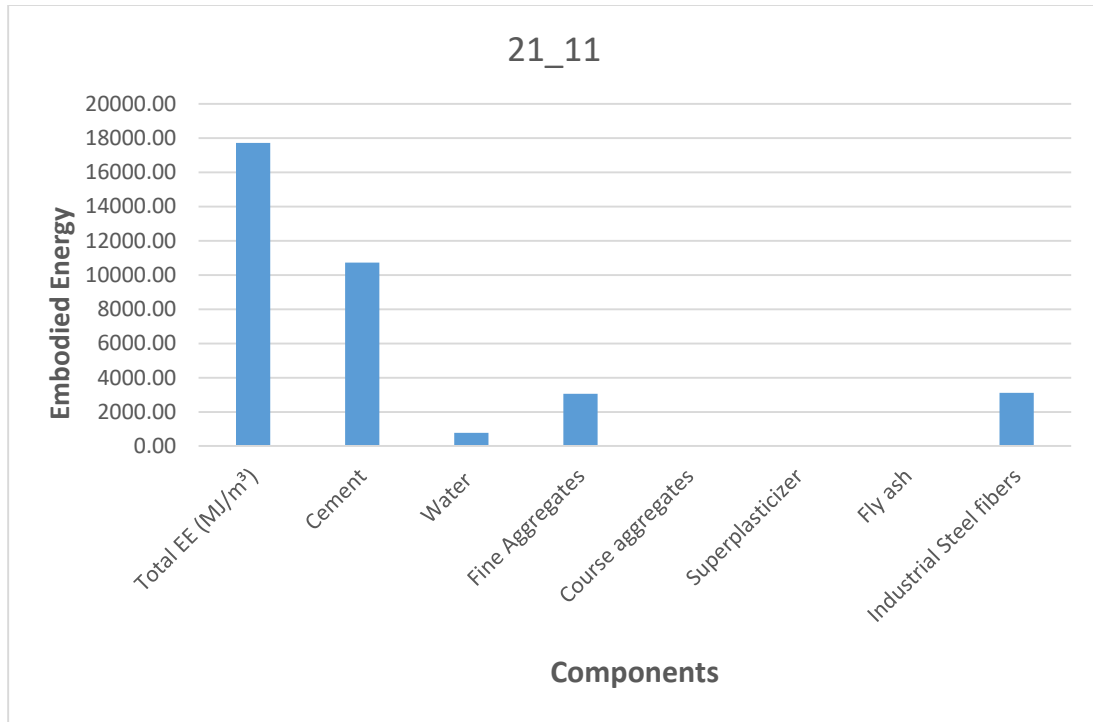
Mixes	Density	Total EE (MJ/m ³)
23_09	6242.71	14888.84
15_10	6623.44	18710.66
29_10	6766.12	18427.45
06_11	6218.47	15201.55
21_11	6158.24	17724.72
10_12	6080.93	15201.55
18-02	6180.28	15201.55
25-06-A	5890.10	14519.91
25-06-B	5462.88	14519.91

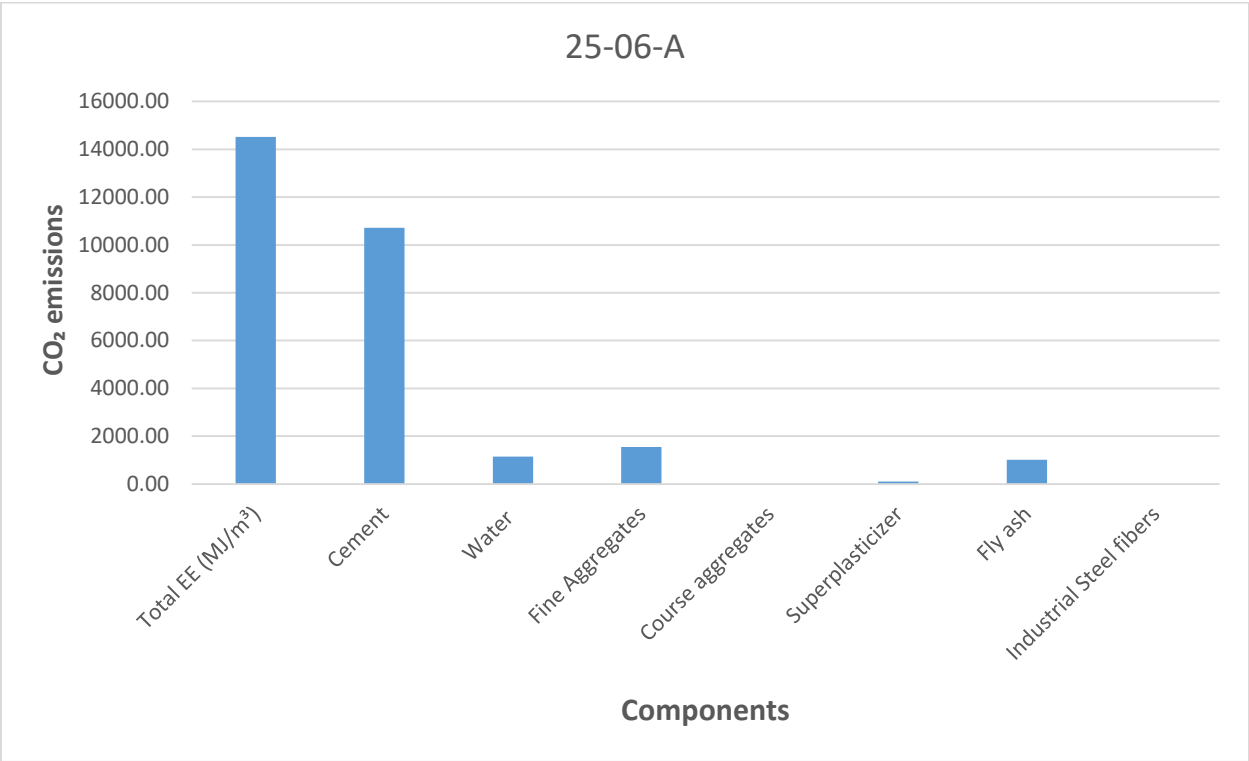
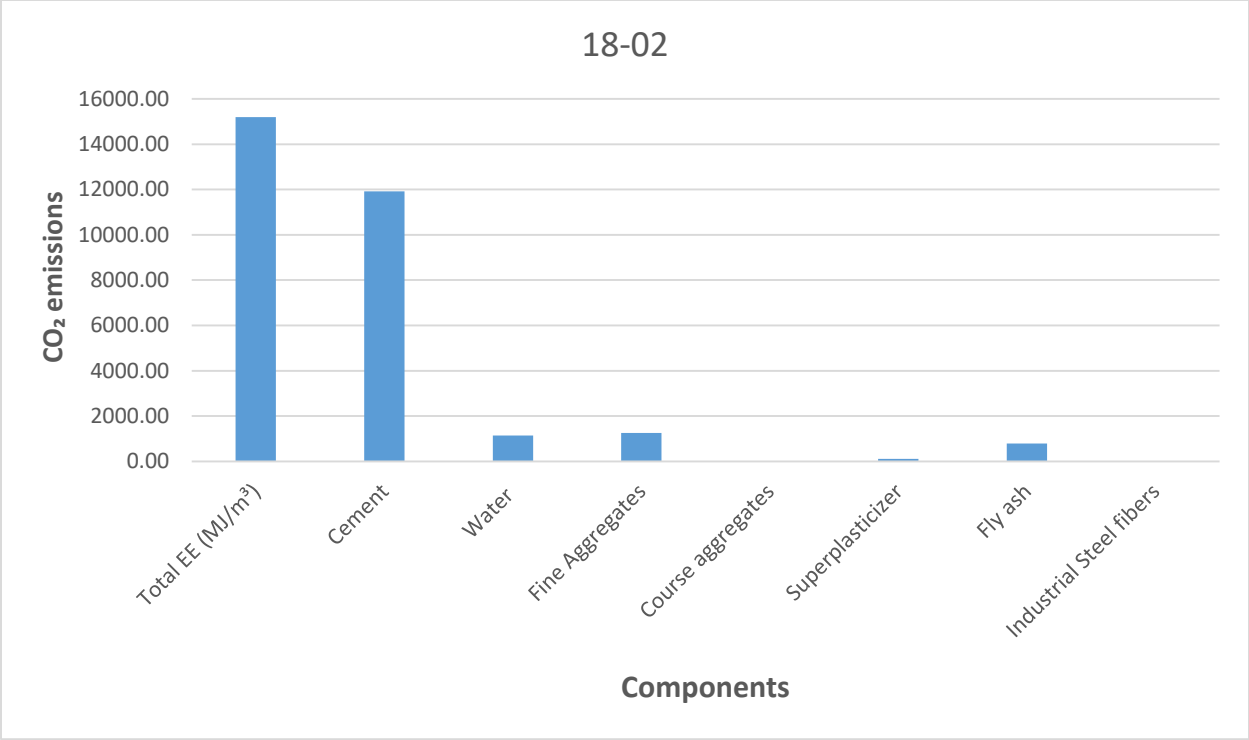
Table 6.5: Total Embodied Energy value

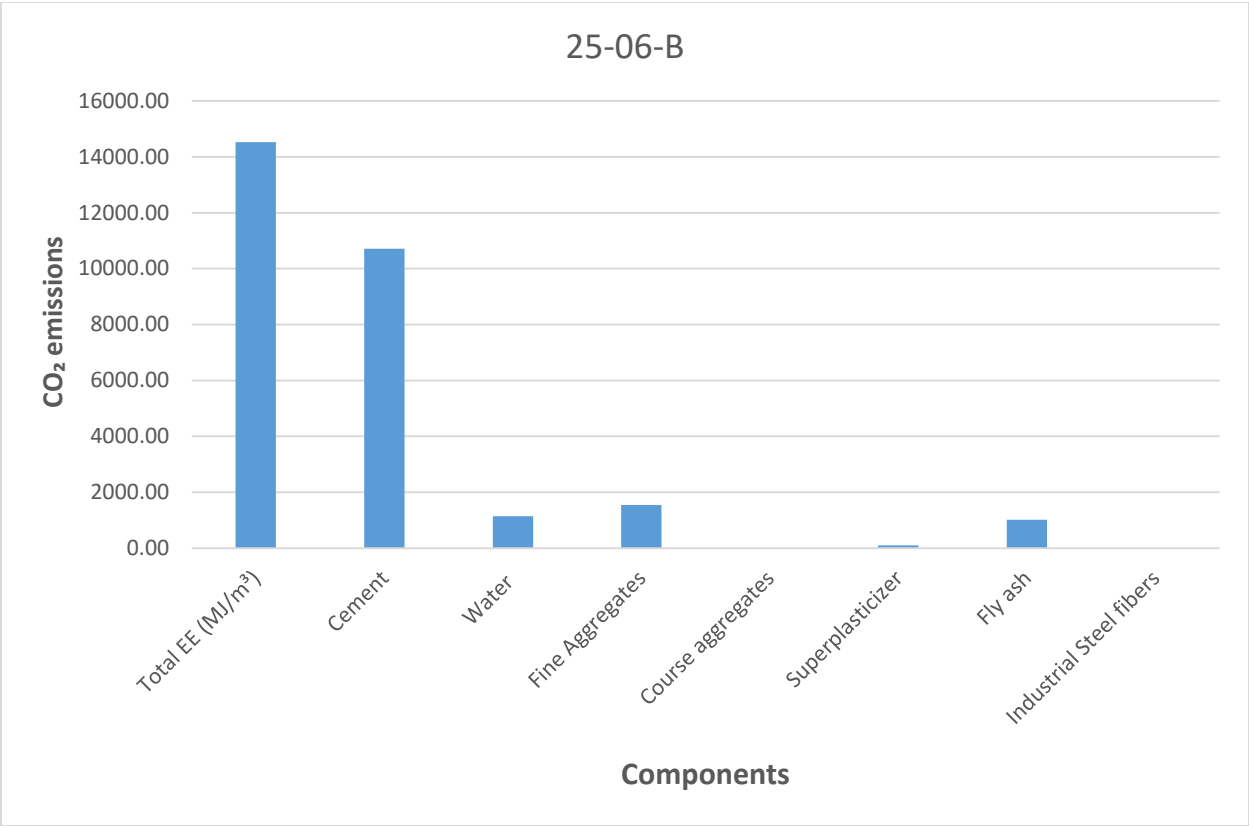
These values were used to conduct the eco-mechanical assessment, which will be described in the next section, to find a balance point between mechanical and environmental performance.











6.4: Eco-mechanical Analysis

All estimated values in previous sections were used to conduct the Eco-mechanical assessment, which will be described in the next chapter, to find a balance point between mechanical and environmental performance. We are looking for the mixture that lower the environmental impacts while compensating the mechanical parameters.

In this section, simultaneously analyzed the mechanical and environmental efficiency of HPFRCC mixes that were evaluated separately in Sections 5.1 and 5.3, to assess which solutions can provide low environmental impact without sacrificing the mechanical response.

This eco-mechanical evaluation is carried out using the chart presented by Fantilli and Chiaia and described already in Section 1.7. Maximum compressive stress and ductility were considered mechanical parameters (MI), instead the ecological impact with CO₂ emissions (EI) was assessed.

For the ecological part we considered two different concept for the evaluation of the EI. In the first part we just considered the total impact which is closely connected with the CO₂ emission of different mixes, while in the second section we mixed this concept with embodied energy and we evaluated a new EI value. Regarding the mechanical part, we considered three different aspects from tensile test, compressive test and ductility of our specimens.

Mixes	α (Kg CO ₂)	β (MJ/m ³)	EI (Kg CO ₂ MJ/m ³)= $\alpha*\beta$
23_09	2376.90	23080.86	54860786.46
15_10	1826.67	18710.66	34178156.45
29_10	1818.90	18427.45	33517683.69
06_11	1374.14	15201.55	20889048.28
21_11	1287.87	17724.72	22827203.00
10_12	1374.14	15201.55	20889048.28
18_2	1374.14	15201.55	20889067.28
25-06-A	1247.87	14519.91	18118994.12
25-06-B	1247.87	14519.91	18118994.12

Table 6.6: Ecological data for the preparing chart

Mixes	MI (MPa)	sigma (MPa)	(Pmax-Pcr)/Pcr
23_09	12.28	31.23	2.26
15_10	13.47	54.96	0.90
29_10	13.96	42.68	0.95
06_11	12.44	36.52	0.75
21_11	10.04	49.9	0.41
10_12	9.44	39.64	0.85
18-02	9.23	43.28	1.10
25-06-A	10.05	51.83	0.90
25-06-B	17.79	54.97	1.28

Table 6.7: Mechanical data for preparing chart

The MI and EI values within the diagram shown in previous table. According to a definition, MI_{inf} is the lower limit value of concrete mechanical results in this diagram, since code rules generally require minimum strength and ductility values to guarantee a pre-established safety format. Whereas EI_{sup} , which should be the maximum environmental impact of concrete to satisfy ecological policies, represents the upper bound value of environmental impact. In other words, both of these boundaries can be prescribed by code rules, or imposed by requirements for bidding. But in our case since we need to compare the mixes with the one produced from industrial fibers, we assume these values equal to the ones from 21-11 mix.

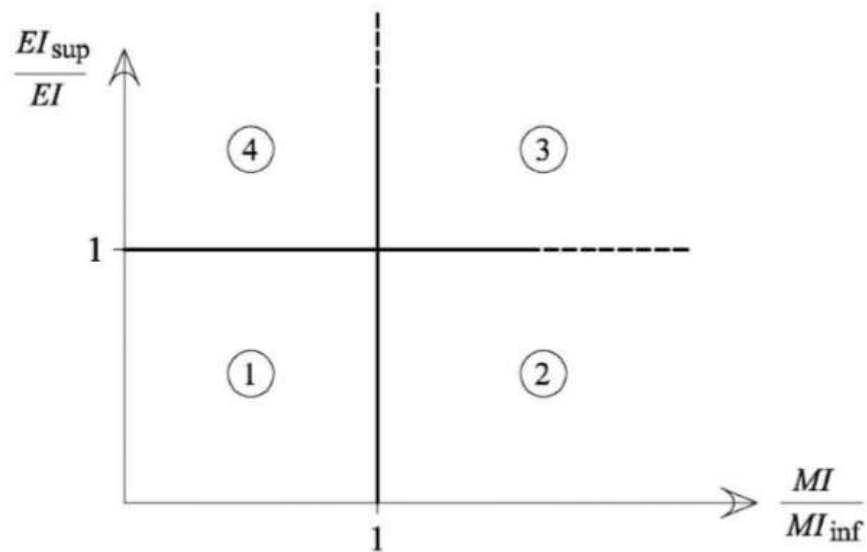
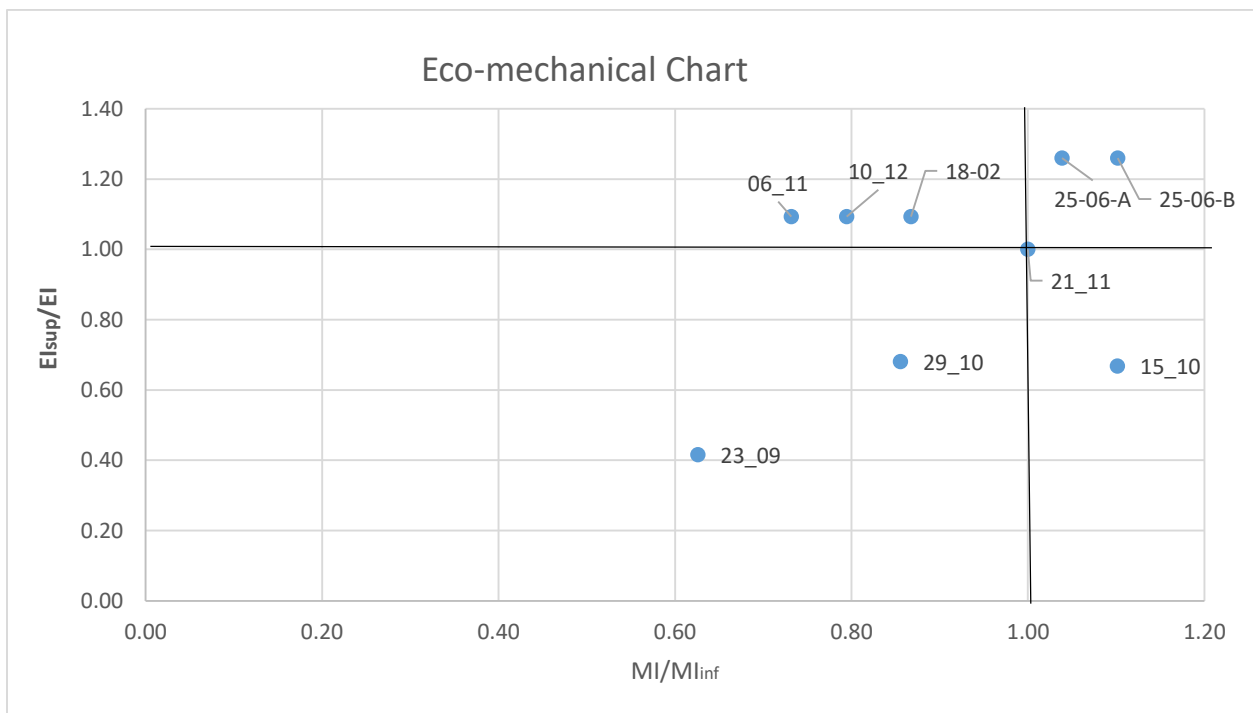
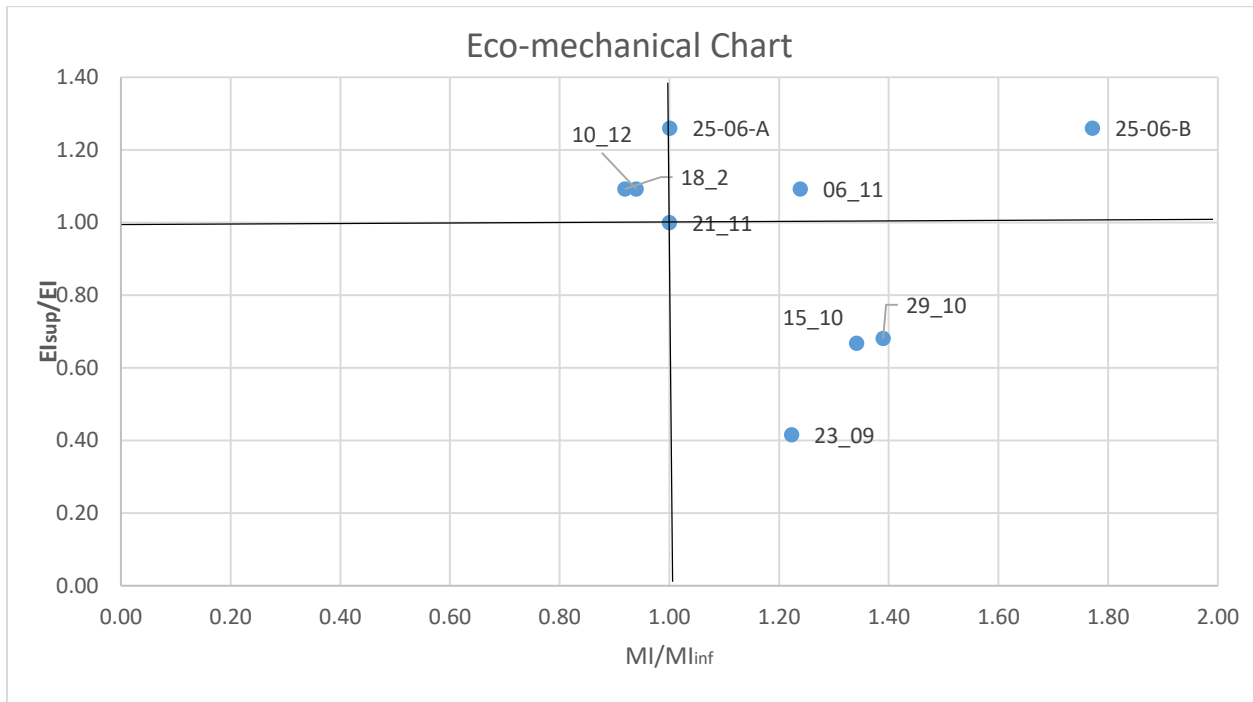
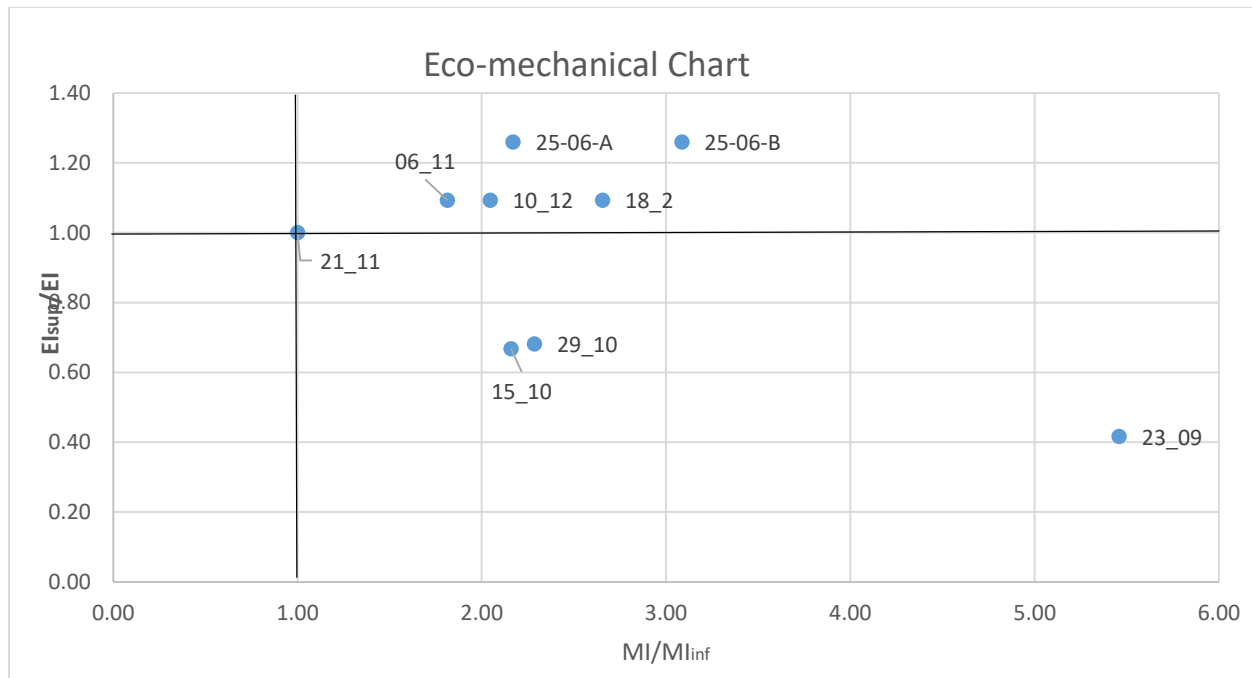


Table 6.8: Eco-mechanical chart

6.5: Eco-mechanical chart





The main focus of this chart is to find the mixes which represent simultaneously acceptable mechanical performances and comparable ecological properties. These mixes are the ones on the top right side of this chart.

As mentioned previously, we considered three different parameter for comparing the mechanical performance of our mixes. Regarding the Ecological aspect, considering simultaneously embodied energy and CO₂ gives us a better perspective. It is also clear that the enhancement of steel fiber volume will not always lead to improvement of mechanical properties.

From these provided charts we can observe that both of the mixes which were tested on 25th June are ecologically and mechanically acceptable compare to the industrial mix, which was tested on 21st of November. We can also figure out that by increasing the amount of steel fibers from 3% to 6%, we have better mechanical performance of our mix.

Chapter 7 Conclusion and Recommendations

7.1: Conclusions

Due to the high mechanical properties such as high compressive strength, high ductility, durability and energy absorption capacity, HPFRCC is often used recently for the repair, reinforcement and seismic retrofitting of old constructions. In particular, a widespread application is to 'harden' those parts of the structure that are exposed to high environmental and mechanical loading, such as columns and beams, especially in the most stressed sections and vital structural locations.

Nevertheless, while these cement composites boost the mechanical responses, their ecological effect is very strong due to both the amount of cement used in the mixtures of HPFRCC and the steel fibers. In fact, during cement production, a large amount of CO₂ is released, particularly for calcination of chalkstone and for manufacturing. In this study, chemical by-products, such as fly ash, are included in the binder in place of different percentages of cement to address the strong environmental effects. The replacement of part of the cement content with fly ash could therefore be an effective way to improve the ecological properties of HPFRCC composites as well.

An eco-mechanical analysis has enabled the identification of solutions that can ensure a low environmental impact, without compromising the mechanical response. The eco-mechanical study was carried out according to the non-dimensional graph suggested by Fantilli and Chiaia, in which ecological and mechanical results is merged by the Ecological Index (EI) and the Mechanical Index (MI), respectively.

The mechanical properties considered are the maximum compressive stress and the ductility, estimated by the energy of the absorption. Instead the CO₂ emission released by the production of 1 m² of HPFRCC mixture was considered instead of the ecological parameter.

The eco-mechanical study showed that partial replacement of cement with fly ash ensures improved mechanical and ecological performance:

This thesis demonstrates that vast technological issues persist, particularly when it comes to dealing with Methods of concrete mix preparation and fiber counting, to be studied in more profundity. Often promoting a more organized and structured approach to research Comparisons of experiments performed by various researchers which allow for the creation of more precise methods for predicting the efficiency of reinforced concrete elements Different fiber forms.

Some important points are listed below:

- The big influence of the fibers in fiber reinforced concrete was regarding the post cracking case, where the fibers bridge across the cracked matrix. Waste tires modified concrete represents a ductile failure rather than a brittle one.
- The non-dimensional diagram depicted in eco-mechanical section can be effectively used to tailor concrete mixtures with the best ecological and mechanical performances.
- When mineral additives and fiber reinforcement are correctly mixed, a new generation of cement-based composites can be developed, with the functional strength of a conventional concrete but with decreased environmental effect and increased durability;
- Recycled tire-fibers decrease the crack width of concrete systems at the serviceability level, and may thus remove the fabricated fibers without penalizing the structural efficiency.

7.2: Recommendation for Further Study

A whole range of Interesting issues remain unanswered, fresh work areas opened up Validation is needed for investigation and many propositions. SFRC is very much a subject broad and this research contributed a contractive part of information thinking that it will proceed investigations for a deeper understanding of the issue should proceed. This is assumed to be the more progress is expected hereafter.

1. The used eco-mechanical approach, is only based on the evaluation SFRC specimens under three-point bending load and compressive tests. Thus, further research should be developed in order to assess the eco-mechanical performances of more complex structures, such as RC frames and bridges. It is clear that regarding the more complex structures the material can represent a different behavior.
2. A huge amount of flexural tests of various beam dimensions must be carried out; Concrete strength and fiber content to include additional form and fiber data magnitude of the profiles for strain-crack distance.
3. A computer controlled process to clean, sort and chop the recycled fibers should be developed for any length needed. Improving the recycling process and increase the fiber quality.

REFERENCES

1. A.P. FANTILLI(1), R. FURNARI(2), M. GUADAGNINI(3), B. CHIAIA(4), K. PILAKOUTAS(5), AND P. PAPASTERGIOU(6), ECO-MECHANICAL ANALYSIS OF TYRE-FIBER-REINFORCED CEMENT-BASED COMPOSITES
2. Ana Baričević, Marija Jelčić Rukavina, Martina Pezer, Nina Štirmer, influence of recycled tire polymer fibers on concrete properties
3. M.A. Aiello, F. Leuzzi, G. Centonze, A. Maffezzoli, Use of steel fibres recovered from waste tyres as reinforcement in concrete: Pull-out behaviour, compressive and flexural strength
4. Giuseppe CENTONZE^{1,a}, Marianovella LEONE^b, Francesco MICELLI^c, Daniele COLONNA^d and Maria Antonietta AIELLO, Concrete Reinforced with Recycled Steel Fibers from End of Life Tires: Mix-Design and Application
5. M. Leone, G. Centonze, D. Colonna, F. Micelli, M.A. Aiello, Fiber-reinforced concrete with low content of recycled steel fiber: Shear behavior
6. Akkaya Y., Picka J., Shah S.P., 2000, Spatial distribution of aligned short fibers in cement composites, Mater. in Civil Engng.
7. Bayasi MZ, Soroushian P., 1992, Effect of steel fiber reinforcement on fresh mix properties of concrete, ACI Materials Journal.
8. BS EN 12390, 2009, Testing hardened concrete - Part 3: Compressive strength of test specimens.
9. BS EN 14651, 2005, Test method for metallic fibered concrete - Measuring the flexural tensile strength (limit of proportionality (LOP), residual).
10. BS EN 14721+A1, 2007, Test method for metallic fibre concrete - Measuring the fibre content in fresh and hardened concrete.
11. Balaguru P., Ramesh N., Patel M., 1992, Flexural Toughness of Steel Fibre Reinforced Concrete, ACI Material Journal.
12. Chen L., Mindess S., and Morgan D.R. (1994) Specimen geometry and toughness of steel fibre reinforced concrete. Journal of Materials in Civil Engineering.
13. di Prisco, M., Colombo, M., Dozio, D. 2013: Fibre-reinforced concrete in fib Model Code 2010: principles, models and test validation. Structural Concrete, 14.
14. di Prisco M., Plizzari G., Vandewalle L., 2009, Fibre reinforced concrete: new design perspectives. Materials and Structures, 42.
15. Dupont D., Vandewalle L., 2004, Distribution of steel fibres in rectangular sections, www.elsevier.com/locate/cemconcomp.

16. Dupont D., Vandewalle L., 2002, A practical proposal to drive a stress-strain relation with residual tensile strengths. Brite-EuRam Project BRPR-CT98- 0813.
17. Environment Agency, 2003, Tyres in the environment. Environment Agency's.
<http://www.environment-agency.gov.uk>.
18. Fantilli A.P., Vallini P, 2003, a cohesive model for fiber-reinforced composites. In: Bontempi F (ed) Second international structural engineering and construction conference ISEC-02 Swets and Zeitlinger, Lisse
19. Fantilli A.P., Vallini P., 2003, Bond-slip relationship for smooth steel reinforcement. In: Euro-C Conference, Proceeding: Computational Modelling of Concrete Structures, St. Johann im Pongau, Austria.
20. Manouselis I., 2002, Use of Recyled Steel Fibres from Tyres in Concrete. MSc. Thesis, University of Sheffield, UK.
21. Papastergiou P. et al., 2012, Technical Report, 3rd series of SFRC prism tests for Twintec Ltd, United Kingdom
22. Papastergiou P. et al., 2013, Technical Report, 4th series of SFRC prism tests for Twintec Ltd, United Kingdom
23. Papastergiou P. et al., 2015, Technical Report, 5th series of SFRC prism tests for Twintec Ltd, United Kingdom.
24. Parviz S., Cha-Don L., 1990, Distribution and Orintation of Fibres in Steel Fibre Reinforced Concrete. ACI Materials Journal.
25. Pilakoutas K., Strube R, 2001, Re-use of tyre's fibres in concrete. Proceedings of the international symposium on recycling and reuse of used tyres, Thomas Telford, Dundee Scotland.
26. RILEM TC 162-TDF, 2002, Test and design methods for steel fibre reinforced concrete: bending test. Materials and Structures
27. T. Nishiwaki, K. Suzuki, A. Fantilli, G. Igarashi e S. Kwon, «Ecological and Mechanical Properties of Ultra High Performance – Fiber Reinforced Cementitious Composites containing High Volume of Fly Ash,» 2017.
28. A. Fantilli, F. Tondolo, B. Chiaia e G. Habert, «A sustainable approach to the design of reinforced concrete beams».
29. J. Dragas, S. Marinković, I. Ignjatovic e N. Tomic, «Properties of high-volume fly ash concrete and its role in sustainable development,» Journal of Faculty of Civil Engineering Conference, pp. 849-858, 2014.
30. P. Mehta e P. Monteiro, Concrete - microstructure, properties, and materials, vol. 4, New York: McGraw-Hill, 2014.

31. «High-Volume Fly Ash System: concrete solution for sustainable Development,» ACI Materials Journal, vol. 97, n. 1, pp. 41-48, 2000.
32. K. Holman, J. Volz e J. Myers, «Comparative Study on the Mechanical and Durability Behaviour of High-Volume Fly Ash Concrete versus Conventional Concrete,» in First International Conference on Concrete Sustainability (ICCS 2013), 2013.
33. A. Fantilli e B. Chiaia, «The work of fracture in the eco-mechanical performances of structural concrete,» Journal of Advanced Concrete Technology, vol. 11, pp. 282-290, 2013.
34. M. Longo, «The behavior of concrete confined by Ultra High Performance - Fiber Reinforced Cementitious Composite,» Tohoku University, Sendai, 2017.
35. A. E. Naaman, «High Performance Fiber Reinforced Cement Composites,» in High Performance Construction Materials - Science and Applications, World Scientific Publishing Co. Pte. Ltd, 2007, p. 68.
36. A. E. Naaman e H. Reinhardt, High Performance Fiber Reinforced Cement Composites, London: E & FN Spon, 1996, p. 505.
37. A. E. Naaman, «Properties and applications in repair and rehabilitation,» in High Performance Fiber-Reinforced Concrete in Infrastructural Repair and Retrofit, Detroit: ACI, 2000.
38. R. Bergamante, P. De Donato, P. Manetta e S. Maringoni, «Intervento di miglioramento sismico di un edificio in c.a. a Coppito (AQ) classificato con esito E a seguito del sisma del 06.04.2009,» Progettazione Sismica, n. 02-2013, pp. 125-130, 2013.
39. E. Denarié e E. Brühwiler, «Cast-on site UHPFRC for improvement of existing structures - Achievements over the last 10 years in practice and research,» in HPFRCC7: 7th workshop on High Performance Fiber Reinforced Cement Composites, Stuttgart, Germany, 2015.
40. V. Lisi, «Ecological and mechanical properties of Ultra High Performance Fiber Reinforced Cementitious Composites containing fly ash,» 2018.
41. E. 1992-1-1, Eurocode 2: Design of concrete structures - Part 1-1: General rules and rules for building, Brussels: E. for Standardization, 2005.
42. ASTM C 143/C 143M-00: "Standard Test Method for Slump of Hydraulic Cement Concrete".
43. ASTM C231-03: "Standard Test Method for Air Content Of Freshly Mixed Concrete by the Pressure Method".
44. ASTM C 1437-01: "Standard Test Method for Flow of Hydraulic Cement Mortar".

45. [H. El-Enein, H. Azimi, K. Sennah e F. Ghrib, «Flexural strengthening of reinforced concrete slab-column connection using CFRP sheets,» Construction and Building Materials, vol. 57, pp. 126-137, 2014.
46. J. A. 1149:2017, Method of test for static modulus of elasticity of concrete, Japanese Industrial Standard/Japanes Standards Association, 2017